TECHNISCHE
UNIVERSITÄT
MÜNCHEN

Annual Report 2002
ZWE FRM-II

Contents

Directors' Report

The new German Neutron Source FRM-II is ready to start its nuclear operation. As a consequence the project for the construction of FRM-II has changed its legal character and since 1st January 2002 the FRM-II is operated as Central Scientific Unit (Zentrale Wissenschaftliche Einrichtung ZWE) of the Technische Universität München. The project manager for the construction, Dr. Anton Axmann has retired in April 2002. The ZWE FRM-II is now directed by the Scientific Director Prof. Dr. Winfried Petry, the Technical Director Prof. Dr. Klaus Schreckenbach, and the Administrative Director Guido Engelke. For the coming administrative tasks a small but efficient administration within FRM-II has been built up. During the last year the project team of the construction of FRM-II, the former FRM reactor group and the groups of building up the scientific instruments merged to one operational unit. Today about 160 people are working on site. While entering new staff at FRM-II the task of integration will certainly continue in the next year.

Advice for both, science and operation will come from two advisory boards. The TUM-Advisory Board with members from different faculties of the university gives advice with particular intention on the integration of FRM-II within the TU-München.

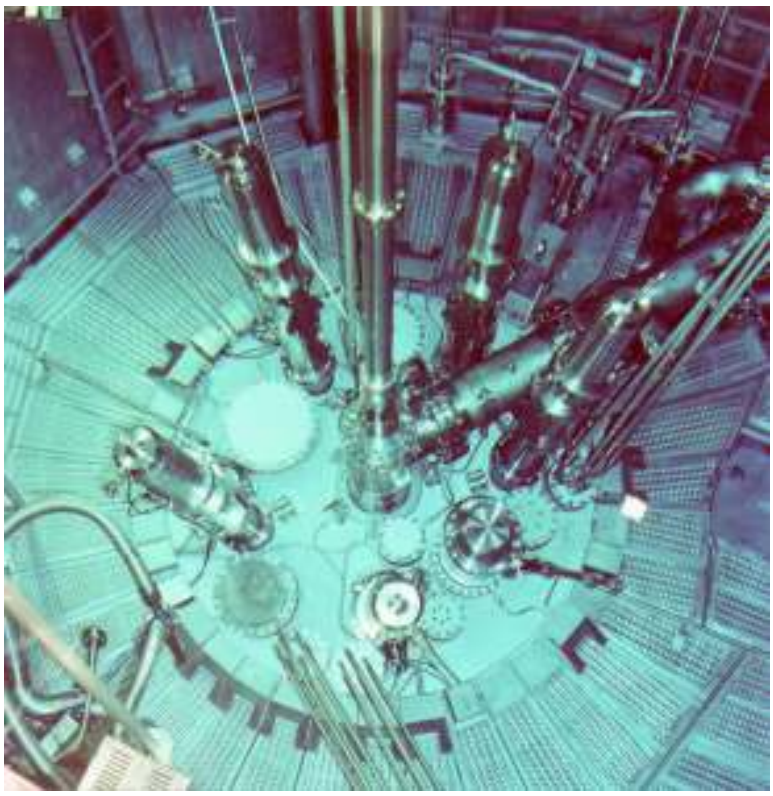

The Strategic Advisory Board with members from the national and international scientific community and representatives from the funding bodies (agencies) of the State of Bavaria and the Federal Republic of Germany gives us advice for an effective use of the neutron facility.

Nuclear licensing of the FRM-II has progressed considerably. In October and December 2001 the committees for evaluating nuclear safety and radiation protection confirmed the safety of FRM-II, its accomplishment according to the state of science and technology and recommended the permission for the nuclear operation. In January 2002 the Federal Minister for Environment requested additional evaluations, going far beyond the recommendations of his own committees, thereby partly neglecting their advice. In June a revised draft of the license for nuclear operation

of FRM-II has been submitted with considerable effort of our main constructor Siemens, the staff of FRM-II and the Bavarian Safety Authority. End of October 2002 after the election for the German Parliament the Federal Minister for Environment commented this resubmission and asked for a few further evaluations. Mid January 2003 Siemens and TUM replied to these requirements. After this exhaustive and careful revaluation of safety aspects of the FRM-II we are looking forward to receive the final nuclear license early 2003. The FRM-II is ready for the nuclear start up.

The waiting period of the year 2002 has been used to accomplish the instrumentation of FRM-II. Today the construction of most of the instruments has progressed so much, that five irradiation facilities and 14 beam hole instruments will be operational with the start of routine operation of FRM-II, which is foreseen some nine month after the nuclear start up. For the user service considerable investments have been put into sample environment. An innovative highlight will be the low temperature equipment free of cryogenic liquids. Large effort has been taken to provide services for the instruments concerning computer network, electronics and software.

In October 2002 funding was provided for the realization of an industrial application center on the site of the FRM-II, providing offices and laboratories for the industrial use of neutrons. The building will be ready for use in 2004.

In October 2001, Prof. Dr. Wolfgang Gläser, former director of the FRM and the project FRM-II retired. In honor of his long lasting engagement for the realization of the FRM-II a colloquium was held on 18th February 2002. Highlights were the talk by Prof. Dr. K. Böning "The stony way to FRM-II" and by Prof. Dr. P. Egelstaff reviewing Gläser's scientific work.

On behalf of many other instruments the three axis spectrometer for polarized neutrons build by the Max Planck Society (Prof. B. Keimer, MPI für Festkörperforschung, Stuttgart) has been officially inaugurated on 5th November 2002 by the vice president of the Max-Planck Society Prof. K. Mehlhorn.

In commemoration of the importance of the work of Prof. Heinz Meier-Leibnitz for the science with neutrons and his particular engagement at the Technische Universität München a statue has been unveiled the 16th December 2002.

We would like to thank our friends at the different European neutron sources which gave us advice and helped us by providing neutrons in a painful time of missing neutrons at Garching. With the hope of becoming operational soon we are looking forward to welcome users from all over the world.

Guido Engelke Winfried Petry Klaus Schreckenbach

Events at FRM-II

Highlights in 2002

16.12.02 Technical University of Munich commemorates his great savant - unveiling the statue of Heinz Maier-Leibnitz.
4.12.02 Visit from the "research reactors"-committee.

28.11.02 Mr. Maurel - head of Framatome - is visiting the FRM-II.
24.11.02 TUM live - open day - record attendance beats all expectations - more than 20.000 visitors take interest in technology, natural and medical science at the Technical University of Munich, 500 visitors at the FRM-II

5.11.02 Official inauguration of the NRSE-TAS spectrometer - scientists from the Max-Planck-Institute present their instrument at FRM-II.

23.10.02 Visit from the state parliament party (CSU).
21.10.02 80th birthday of Prof. Dr. Lothar Koester, former technical director of the FRM - celebration at the physics department.

19.07.02 Special guided tour through the FRM-II for the "Friends of TUM" with festive talks and lectures.
6.06.02 Visit from the Chinese NSFC-research centre.

4.06.02 Successful transport of used fuel rods from the FRM.

29.04.2002 Visit of states secretary Mrs. Görlitz (Landwirtschaftsministerium Bayern)

24.04.2002 Visit of Members of the Federal parliament and Bavarian State Minister of Science, Research and the Arts.

19.04.02 Official retirement of Dr. Anton Axmann.
18.02.02 Conferment of emeritus status on Prof. Dr. Wolfgang Gläser.

Diffractometers

3.1 *STRESS-SPEC* – Materials Science Diffractometer

M. Hofmann[(1)], G.A. Seidl[(1)], R. Schneider[(2)]
[(1)]ZWE FRM-II, Technische Universität München
[(2)]BENSC, Hahn-Meitner-Insitut, Berlin

Introduction

The measurement and analysis of residual stresses has gained significant importance over the past couple of years due to the increasing demand in improving the properties of new engineering materials and components. Latest trends in the field of residual stress analysis show that texture evolution has to be considered in conjunction with internal strains.

Experimentally, non-destructive analysis of phase specific residual stresses is only possible by means of diffraction methods. While x-rays scattering is essentially a surface method, the high penetration depth of neutrons into matter (e.g. 20 mm into steel or 100 mm into aluminium) allows to extract reliable information within the bulk of components. In addition, these measurements can be performed utilising a scattering angle $2\theta \approx 90^\circ$. In this case large vertical divergences due to focusing monochromators do not affect the spatial resolution and the gauge volume is cubic. The tensor character of residual stress requires strain measurements in different sample orientations in order to analyse a local stress state. The possibility to define such a regular shaped (e.g. cubic) gauge volume is extremely helpful in residual stress analysis.

In future, neutron scattering will gain further importance for strain measurements as new diffractometers built for this purpose become available. These instruments will allow to utilize the full potential of the technique and will help to establish neutron stress analysis as a routine method.

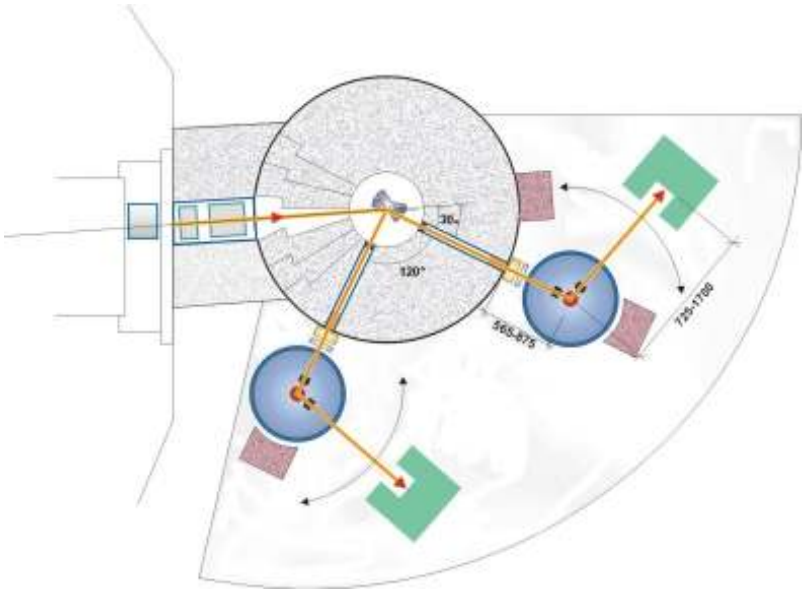

Figure 3.1: General layout of the materials science diffractometer STRESS-SPEC

Description

The materials science diffractometer STRESS-SPEC (fig-

ure 3.1), which is currently being installed at the new intense neutron source FRM-II in cooperation with the Hahn-Meitner-Institut (Berlin), is such an optimized instrument. It will offer high resolution strain measurements as well as facilitate investigation of the texture of materials and components. The main components and the current status of the instrument will be reviewed briefly below.

Figure 3.2: Front view of the Si-monochromator used in STRESS-SPEC

The diffractometer is installed at the thermal beam tube SR3. The incoming beam divergence can be defined by Soller type collimators with horizontal divergencies of 15' and 25', respectively. For further control of the primary beam shape and to reduce background a vertical and horizontal adjustable slit system is installed in front of the monochromator housing.

A large and continuously variable monochromator take-off angle ranging from $2\theta_M$=30° up to 120° together with up to three different monochromators allow to find a good compromise between resolution and intensity for each measuring problem. Generally a scattering angle of $2\theta_S$ = 90° can be chosen, which is a favourable configuration for strain measurements due to the resulting cubic gauge volume (see above). The actual monochromator options comprise a vertical focusing Ge(511) and an elastically bent Si(400) monochromator. A vertical focusing device for the Ge(511) crystals will be available in spring 2003, whereas the Si monochromator is complete (figure 3.2). The monochromators can be exchanged by remote control using a vertical translation device. Rotating the monochromators around θ_M by only a few degrees gives access to further reflections, e.g. in case of Ge monochromator the (311) and (711) reflections. The performance of both monochromators, respectively the crystals, has been tested by neutron diffraction. Since the space allows for another monochromator, it is planned to add a Cu(220) or similar in the future, giving even greater flexibility in choosing optimal conditions for the particular experiment.

Between monochromator and sample the beam can be defined by combination of slits just after the monochromator and in front of the sample. It is also possible to place Soller collimators (15' and 30') in the beam path between monochromator and sample. These can be easily mounted and exchanged. The gauge volume for strain scanning is defined by remotely adjustable vertical slits in the scattered beam and Cd-masks coated with Gd_2O_3 just in front of the sample. A series of such masks ranging in size from 0.5x0.5 mm^2 to 10x10mm^2 are available. Currently design work is undertaken to replace this fixed Cd-masks by a motorised slit system adjusting the horizontal and vertical apertures to define

the gauge volume.

A two dimensional position sensitive ^{3}He detector (PSD) is installed as the primary detection option. This detector, developed by EMBL (Grenoble, France), is a multiwire detector with a delay time encoding. It has an active area of 200x200 mm^2 with a resolution of about 1.5x1.5 mm^2. The measured efficiency for neutrons of a wavelength λ = 1.8 Å is 73 %. By using such a detector, the measurement time can be drastically reduced since part of the Debye-Scherrer ring is available in vertical direction. For $2\theta_S \neq 90^\circ$ appropriate corrections have to be made with respect to the shape of the Debye-Scherrer ring. This PSD-detector can be exchanged for a second detector system based on 5 vertically mounted ^{3}He tube detectors. The additional detector has been manufactured and delivered by the Forschungszentrum Karlsuhe, Germany.

The sample stages comprise a xyz-sample stage for heavy components up to 200 kg with a positional accuracy better than 50 μm. For smaller components and texture measurements a combined rotation (ϕ, χ) and translation (x, y, z) device has been delivered by Fa. Huber (Rimsting, Germany). The lifting capacity of this device is 30 kg.

Status

The primary diffractometer is installed at the thermal beam port SR3. Most of the remaining work consists of aligning and testing the components with neutrons once the reactor FRM-II starts operation. The secondary diffractometer including sample table and electronics has been transfered to the beam port E7 of the neutron source (BENSC) of the Hahn-Meitner-Institut in order to be used in the time FRM-II is waiting for starting routine operation. The instrument is available for routine measurements since January 2003.

3.2 *MatSci-R* – Materials Science Reflectometer

J. Major[(1)], J. Franke[(1)], U. Wildgruber[(1)], H. Dosch[(1)]
[(1)]Max-Planck-Institut für Metallforschung, Stuttgart

Within the framework of the FRM-II initiative of the Max-Planck-Gesellschaft the Max-Planck-Institut für Metallforschung is designing and building a neutron reflectometer, which is optimized for the study of magnetic phenomena, at the neutron guide NL-1 in the guide hall of the FRM-II. A continuous – optionally polarized – monochromatic neutron beam illuminates horizontal or vertical samples. The primary beam covers a wavelength range from 2 Å to 6 Å. Special design features of the instrument are:

- a two-dimensional ^{3}He detector
- two-dimensional polarization analysis with ^{3}He gas neutron spin filter
- insitu x-ray reflectometry
- reflectometry using the neutron-spin echo method

After the "Tanzboden" was installed in 2001, in the year 2002 the monochromator shielding was finalized (P. Jüttner, FRM-II design group), constructed (Pantolsky, Neuried) and delivered. Due to spatial limitations the monochromator shield design concept (cf. fig. 3.3) is a slim tunnel with a sliding wall which carries a small off-center drum instead of a large shield drum centered with respect to the monochromator axis. This approach maximizes the available energy range without compromising the instrument background and allows a short distance between monochromator and sample if desired. Easy ac-

cess to the monochromator for maintenance is possible through a “backdoor”.

The design of the Monochromator(-axis) (P. Jüttner) is basically completed.

Figure 3.3: Monochromator shielding without sliding front wall during construction

During the year 2002 the second (of four) beam defining slit systems (design P. Jüttner) was build at the main shop of the TUM Physics Department and sucessfully tested. Each slit system has six translational degrees of freedom and all but the one inside the monochromator shield have two built-in rotations to accomodate both primary beam orientations. Miniature stepping motors (Type Arsape, Faulhaber, Schönaich) are controlled by compact, fieldbus-ready stepper control module (Type Monopack and Sixpack, Trinamic, Hamburg).

Currently Monte Carlo simulations (McStas) are in progress to optimize the mosaicity and the geometrical arrangement of the HOPG monochromator (a focussing array of eleven crystal plates).

The design of the “diffractometer” part of the Materials Science Reflectometer became a main effort in 2002 (P. Jüttner, K. Lichtenstein, J. Franke). The “diffractometer” consists of two optical benches (between monochromator and sample table and sample table and detector) and the sample table itself. For several reasons the sample table is quite demanding:

1) A maximum load of 4000 N for the sample environment is needed
2) Sample and sample environment have to be tilted by up to 10° with respect to a horizontal axis (“rocking sample mode”).
3) Sample and sample environment need to be translated by up to 200 mm vertically (“liquid mode”).
4) An in situ x-ray reflectometer as an optional sample environment. (A preliminary design study indicates that a high precision x-ray source can be integrated (EFG, Berlin)).
5) The low height of the primary neutron beam as given by the neutron guide NL-1 requires a very compact structure.
6) Active vibration dampening for a total load of 9000 N on a small foot print.

The detector, a two dimensional position sensitive ^{3}He wire chamber (“Gabriel detector”, ESRF design) is already available and currently tested at the EVA beamline (ILL, Grenoble). For detector readout and histogramming, an adapted version of the “standard” Geesthacht hardware and software (J. Burmester, GKSS) is in preparation.

3.3 *REFSANS* – Reflectometer for Investigating the Air/Liquid Interface

R. Kampmann[(1)], M. Haese-Seiller[(1)], V. Kudryashov[(1,3)], M. Tristl[(2)], V. Deriglazov[(3)], A. Schreyer[(1)], E. Sackmann[(2)]
[(1)]GKSS-Forschungszentrum Geesthacht GmbH
[(2)]Technische Universität München, Physik Department E22
[(3)]Petersburg Nuclear Physics Institute, Russian Federation

The reflectometer REFSANS is dedicated to the comprehensive analysis of surfaces, interfaces and phase boundaries at the air-water interface of liquid or soft matter samples.

Design of REFSANS

REFSANS is being built at the end of the cold neutron guide NL-2b at ≈48 m from the reactor. NL-2b starts with a height of 170 mm and a width of 12 mm close to the cold source and is twisted by 90° over a length of 36 m within a novel NL-section in order to achieve a 12 mm high and 170 mm wide beam cross-section at the junction of REFSANS.

REFSANS is a time-of-flight (TOF) instrument, its chopper system consists of three double discs. Each of them represents effectively one single disc. Their opening angle γ as well as their phases can electronically be set according to experimental requirements $(0 < \gamma < 120°)$. The Master Chopper (MC) is located at a fixed position at the junction of REFSANS with NL-2b in the chopper chamber (CC) whereas Slave Chopper 1 (SC_1) can be moved on a x-y-table in the CC to various distances between 50 mm and 2340 mm from the MC to adjust the wavelength resolution $(0.25\% < \Delta\lambda/\lambda < 15\%)$ (Fig. 3.4). SC_2 is located in the beam guide chamber (BGC) at a distance of ≈600 mm or ≈3000 mm from the sample and allows to operate the chopper system with high transmission and almost constant resolution $\Delta\lambda/\lambda$ [2]. Novel TOF-design and neutron optics have been developed to make REFSANS a most flexible device which allows to perform comprehensive analyses of samples with horizontally aligned surfaces at different reflection geometries: The conventional one employs a horizontally slit-smeared beam with a small vertical and large horizontal divergence. It is used to derive the concentration profile perpendicular to the sample surface from the specular reflectivity and to measure off-specular scattering if strong smearing of lateral momentum transfer can be tolerated.

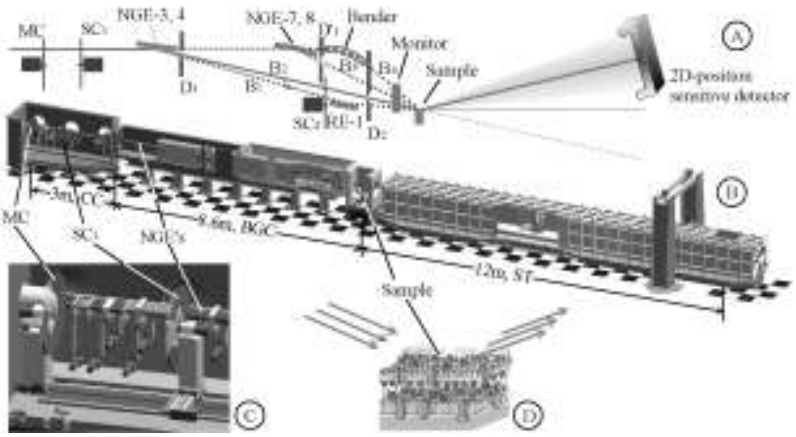

Figure 3.4: Schematic view of REFSANS, its chopper system and its beam guides. SC_1 can be moved on a x-y-table to distances between 50 mm and 2340 mm from the MC.

More sophisticated analysis of evanescent SANS can be performed by setting a point collimating geometry. In this case the intensity is optimised by means of a low wavelength resolution ($\Delta\lambda/\lambda > 10\%$) and by focusing 13 point collimated beams in the detector plane at a distance of ≈10 m from the sample. This geometry together with the low wave length resolution is further the key for measuring extremely small specular reflectivity at REFSANS from substrates with strong incoherent scattering such as H_2O.

A third geometry is used for measuring the tails of diffuse surface scattering patterns at large momentum transfer for which the intensity is increased beyond the point collimating one by means of slit-height smearing the primary beam parallel to the reflection plane. These in parts novel scattering geometries require a rather long beam guide chamber equipped with specific neutron optical components (Fig. 3.4).

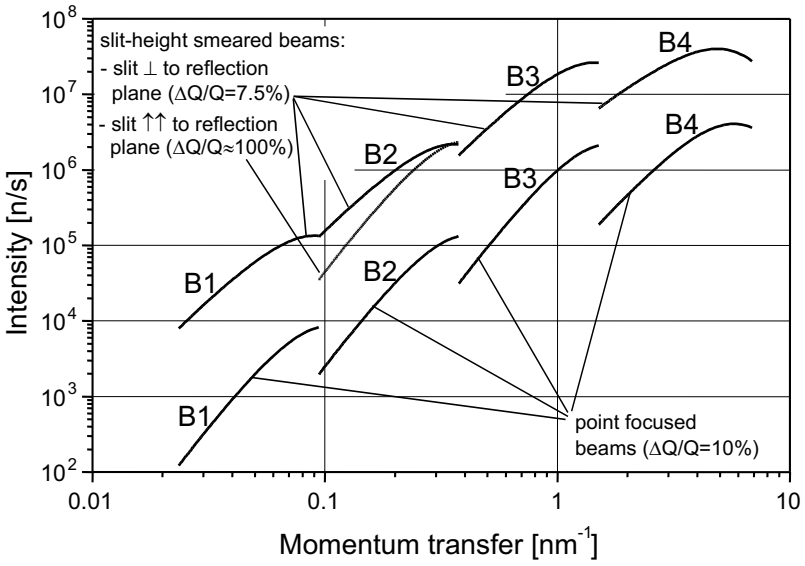

Figure 3.5: Calculated peak intensity I_{peak}. The beams B_1 to B_4 hit the sample at angles of 3, 12, 48 and 180 mrad to cover the broad range of momentum transfer. The 3-disc chopper is operated with a resolution of $\Delta\lambda/\lambda = 5\%$ and minimum and maximum wavelengths of $\lambda_{min} = 0.4$ nm and $\lambda_{max} = \lambda_0 = 1.6$ nm, respectively. The conventional geometry (beam slit-height smeared perpendicular to the reflection plane) leads to the highest intensity. The rather high intensities in point collimation geometry as well as for the case of beam B_2 slit-height smeared parallel to the reflection plane result from focussing 13 beams in the detector plane.

The sample environment is well protected against vibrations, the sample temperature is controlled and different Langmuir troughs equipped with a Wilhelmi system to control the surface tension online are available. Samples with sizes up to ≈80 mm in width and ≈100 mm in length can be investigated at a resolution of the incidence angle in the range $\approx 0.25\% < \Delta q/q < 10\%$.

In the scattering tube, a 2D-position-sensitive ^{3}He-area detector with an active area of 500 × 500 mm^2 and a resolution of ≈3 mm × 2 mm can be positioned at distances from ≈2 m to 12 m from the sample. The detector tube can be raised by up to 1 m at its back to adjust the height of the detector according to the incidence angle. Data are stored by means of a 3D-data acquisition system.

In the chopper chamber, a polarizer can be inserted into the REFSANS beam. Electrical coils in the CC and the BGC keep the polarization of the beam and gradient resonance flippers in the BGC and closely behind the sample allow the spin to be flipped with high efficiency over an extended wavelength range. This design allows to use polarized neutrons in all of the above mentioned scattering geometries. A ^{3}He filter will be made available for polarization analysis of both

specular and off-specular reflected neutrons.

Performance of REFSANS

REFSANS is a novel reflectometer which allows to measure:

1) reflectivity curves at the air/liquid interface over extreme ranges of momentum transfer and resolution of $0.024\ \mathrm{nm}^{-1} < q < 7\ \mathrm{nm}^{-1}$ and $0.25\% < \Delta q/q < 15\%$, respectively (Fig. 3.5),
2) minimum reflectivities of $R < 10^{-8}$ (at low q-resolution) within a few hours,
3) minimum specular reflectivity of $R \approx 10^{-7}$ in the case of a strong incoherently scattering substrate such as a thick layer of H_2O, and
4) evanescent SANS with a primary beam intensity surpassing those at the world-best SANS instruments by more than one order of magnitude.

The different scattering geometries can optionally be set at REFSANS in short times, and all investigations can be performed on the air/water interface with optimized beam intensity. To our knowledge there is worldwide no other instrument with this broad potential of different investigations on horizontal surfaces. Therefore REFSANS is expected to become a unique device for future investigations especially in soft matter and biological research fields.

Acknowledgements

The development of REFSANS has been supported by the German Federal Ministry of Education, Research, and Technology (BMBF) under Contracts Nos. 03-KA5FRM-1 and 03-KAE8X-3.

[1] R. Kampmann, M. Haese-Seiller, M. Marmotti, J. Burmester, V. Deriglazov, V. Syromiatnikov, A. Okorokov, F. Frisius, M. Tristl, E. Sackmann: The Novel Reflectometer REFSANS for Analyses of Liquid and Soft Surfaces at the New Research Reactor FRM-II in Munich / Germany, Applied Physics A **75** (2002)

[2] R. Kampmann, M. Haese-Seiller, V. Kudryashov, V. Deriglazov, M. Tristl, A. Schreyer, E. Sackmann: Design and Potential of the Reflectometer REFSANS at FRM-II for Investigations on the Air/Liquid Interface, submitted to Langmuir

3.4 *RESI* – The Reciprocal Space Investigator

B. Pedersen[(1)], G. Seidl[(1)], W. Scherer[(2)], F. Frey[(3)]
[(1)]FRM-II, TU München
[(2)]Inst. f. Physik, Universität Augsburg
[(3)]Inst. f. Kristallographie, LMU München

Scientific design

Structure analysis using thermal neutrons (λ = 0.8-2Å) complements structural studies with X-ray diffraction methods. The single-crystal diffractometer *RESI*[1], designed as a high-resolution instrument using thermal neutrons at the high-flux neutron source FRM-II provides optimal measurement condition for weak diffraction phenomena in a large portion of the reciprocal space. Furthermore, *RESI* can be employed to investigate scientific questions

in chemistry, physics and materials science.

Main research fields:
Electronic structure, bond activation in catalysis, exploration of functionality of advanced materials: The instrument is optimized for the following main focal areas:

- Combined X-ray and neutron scattering experiments to analyze and visualize electronic structures of materials and catalysts
- Characterization and identification of bond activation in catalysts
- Establishment of relationships between structure and functionality in advanced materials.

Analysis of diffuse diffraction patterns, by highly-resolved mapping of large areas of the reciprocal space:

- Partially crystalline compounds, fibers
- Aperiodic crystals (“quasi crystals”)
- Structural phase transitions
- Modulated structures

In-situ diffraction experiments are crucial for chemists and material scientists to trace and analyze reaction pathways or to discover intermediate reaction products. These experiments require both special sample environments and fast reciprocal space mapping techniques. Application examples are:

- Hydrothermal synthesis
- Heterogeneous catalysis
- Combinatoric chemistry

This list of examples shows, that *RESI* offers a wide range of application in chemistry, physics, crystallography, mineralogy, materials science and biology.

Current status

Neutron guide and shielding

To achieve a low background at the instrument, *RESI* is installed at a 12 m focusing super-mirror neutron guide[2]. This guide is shielded by a specially designed concrete shielding and aims at a background well below 5μSv/h at the detector position. During the last year, the assembly and adjustment of the neutron guide have been finished, and the shielding is completed.

Monochromator

Designed as a single crystal diffractometer for thermal neutrons *RESI* will operate in the wavelength range of 0.8 Å - 1.5 Å. However, in its standard configuration, *RESI* will use neutrons of wavelength of *ca.* 1 Å to cover a large area of the reciprocal space. The design of the monochromator allows the usage of high monochromator take-off angles since most of the planned studies will depend on good resolution conditions at high diffraction angles ($\sin\Theta/\lambda > 1.0$) simultaneously. In

Figure 3.6: View of the secondary diffractometer. This image shows three different configurations of the goniometer.

the standard configuration a copper 422 monochromator allows take-off angles of 90° or 70° providing wavelengths of 1.04 Å and 0.85 Å, respectively. Our Cu-monochromator consists of 8 independent, horizontally arranged single crystals. A specially designed mechanics allows adjusting of the focusing angle, adjusting of the tilting angle to correct the scattering angle and a translational movement of each crystal independently. The vertical divergence at the sample can be adjusted up to a maximum value of 1.8° while the corresponding horizontal divergence values below 0.5°.

The copper crystals have been cut to size, and were measured at T3C (ILL, Grenoble). They show high reflectivity and the required mosaic spread of about 12'.

As a second option a germanium monochromator will be installed which covers the wavelength area up to 1.5 Å to allow diffraction studies on compounds displaying large lattice parameters (>15 Å). For this option the germanium wafers have been cut. They are currently soldered and deformed to the desired mosaic spread at Risø.

Secondary diffractometer

In contrast to the standard eulerian goniometer geometry which is commonly employed for most neutron diffraction experiments, *RESI* makes use of a four-circle diffractometer with κ-geometry (MACH3, Nonius). In this case the known advantages of this geometry *e.g.* reduced obscuration and larger mobility can be used for the first time in the field of neutron diffractometry. Furthermore, after some necessary adaption we can provide user friendly and advanced data collection software for area detectors which has been developed during the past few years for X-ray diffraction studies.

For special measurements such as *in-situ* diffraction studies which demand special sample environments, we will, however, use a robust goniometer as an alternative to the κ-goniometer. This is currently under construction, and expected to be fully operational by end of 2003.

Imaging plate detector

Parallel to the fast development of area detectors in the field of X-ray single crystal diffractometry during the past decade there has been several attempts to develop neutron sensitive area detectors. Although IP detectors for X-rays are established, a clear trend towards the usage of these detectors in neutron research is evident. Especially, due to the large dynamic range and an unsurpassed spatial resolution NIPs are possibly the best choice for diffraction experiments. Also an upgrade of the detector by more advanced NIPs in the future is easily done by simple replacement of the plate. *RESI* is therefore equipped with an on-line IP scanner (MAR-research) and neutron sensitive plates (diameter of 35 cm, FUJI). The detector can be moved on a translational stage which allows the adjustment of the sample-to-detector distance. The minimal sample-to-detector-plane distance is about 280 mm and the maximal 2Θ-angle for the detector offset will be about 135°.

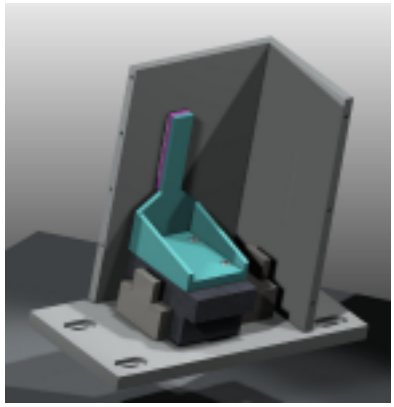

Figure 3.7: Sketch of the fast shutter, parts of the housing are not shown.

The fast shutter

To allow for short and reproducible exposures times, a fast shutter system is needed. A pneumatical supported linear motor, combined with a programmable stepper controller is employed in our design.

The specified reproducibility of the motor is $\pm 2\mu m$, with 75 m/s^2 maximum acceleration. This allows us to get 100 ms transition time for 20 mm beam path. LiF in a polymer matrix is used as neutron absorber, supported by a aluminum carrier. Lead or boron-containing materials can be added as additional absorbers.

[1] G. R. J. Artus, F. Frey and W. Scherer, Physica B, **276-278**, 77(2000) .

[2] G. R. J. Artus, R. Gilles, F. Frey and W. Scherer, Physica B, **283**, 436(2000).

3.5 *SPODI* – Structure Powder Diffractometer

R. Gilles[(1)], B. Krimmer[(1)], H. Boysen[(2)], H. Fuess[(1)]
[(1)]Technische Universität Darmstadt, Petersenstrasse 23, 64287 Darmstadt
[(2)]Ludwig-Maximilians-Universität München, Theresienstrasse 41, 80333 München

The new **S**tructure **PO**wder **DI**ffractometer (SPODI), a project of the Technische Universität Darmstadt and the Ludwig-Maximilians-Universität München is currently built up at the new FRM-II reactor.

This article describes the concept, the new technical features and the status of the instrument. To optimise all optical components Monte Carlo simulations have been carried out of the whole beam path beginning at the core via the neutron guide system, monochromator, sample collimator, standard sample, detector collimator, up to the detector [1,2]. Detailed comparisons of various physical parameters like coating and shape of supermirror guides, different detector heights or monochromator angles were performed [3]. The installation of a detector system with 80 single ^{3}He detectors which are position sensitive in vertical direction opens further applications for data evaluation. The neutron guide system effectively increases the intensity, but results in a complicated divergence profile at the monochromator. It requires a positioning unit of the monochromator crystals with very high accuracy. The higher monochromator take-off angle of 155° in comparison to other instruments significantly improves the resolution at higher 2θ angles. Improvements of the detector collimators allow a reduction of the sidewall thickness to increase the number of collima-

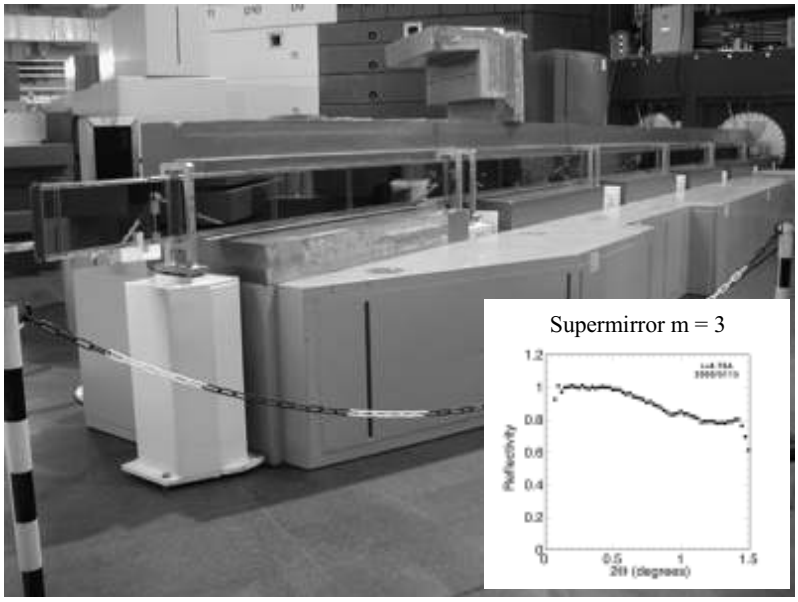

Figure 3.8: Neutronguide at beamline SR8a

tors by 25 % while keeping a height of 300 mm. This concept aims at an optimum compromise of improved resolution, higher intensity, better profile shape and lower background. First test measurements of single components at other neutron facilities promise many new applications of SPODI. Apart from classical powder samples (average particle size a few mm), nanoparticles, polycrystalline sintered compacts or textured materials can be investigated. Typical examples are high temperature superconducting oxides, ceramics, combustibles, Li batteries, materials with giant magnetic resistance, zeolites, metal-hydrogen-storage materials, etc..

Neutron guide

Recently the set-up of the supermirror neutron guide has been finished (Fig. 3.8). The cross-section of the neutron guide is constant (25 mm x 100 mm) up to the biological shield. Here the vertical extension starts to increase up to the monochromator in a so-called trumpet shape. Supermirrors with m_h = 2 (horizontal) and m_v = 3 (vertical) are used for this guide. Reflectivity measurements of m = 3 supermirrors showed values above 74 % (Fig. 3.8).

Monochromator

In cooperation with RisøNational Laboratory we have developed a germanium composite monochromator with orientation (551).

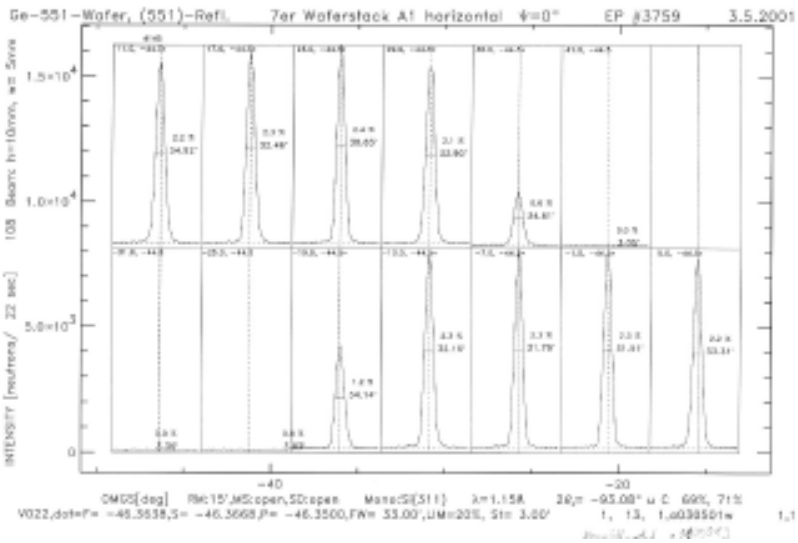

Figure 3.9: Raw data of rocking curves measured with neutrons at HMI Berlin

The neutron guide leads to an effective horizontal divergence of $\alpha_1 \approx 20'$ for the standard wavelength λ = 1.5469 Å. The germanium monochromator with the high take-off angle (155.4° in 2θ) has a mosaicity of $\beta \approx 20'$ [4]. The mosaicity was checked by rocking curve measurements (Fig. 3.9). A special positioning unit is necessary to focus the beam on different sample heights. This unit allows to independently align each germanium crystal in three directions (two rotations and one translation). The concept was developed at the Ludwig-Maximilians-Universität München. The long beam path from monochromator to sample will be evacuated to minimise the thermal neutron absorption.

Detector Bank

The detector bank (Fig. 3.10) is equipped with an array of 80 ^{3}He position sensitive detectors. Active length is 300 mm to cover an enlarged part of Debye-Scherrer rings. The tubes have a diameter of 1 inch. Test measurements revealed a position resolution better than 5 mm [5]. Collimators with an $\alpha_3 = 10'$ will be positioned in front of each detector. Currently a first version of the software to treat detector data and especially evaluate the Debye-Scherrer rings is in development [6].

At present the shutter system and the slit system will be installed. Afterwards it is planned to insert the detector collimators together with the single ^{3}He tubes into the bank to test the movements of the whole instrument in a scanning mode.

Figure 3.10: Current status of the detector bank (left) and detector collimators (right)

[1] R. Gilles, G. Artus, J. Saroun, H. Boysen, H. Fuess, Physica B, **276-278**, 87-88 (2000).

[2] R. Gilles, B. Krimmer, J. Saroun, H. Boysen, H. Fuess, Materials Science Forum, **378-381**, 282-287 (2001).

[3] R. Gilles, J. Saroun, H. Boysen, H. Fuess, Proceedings of the HERCULES X EuroConference, **NT09** (2000).

[4] R. Gilles, B. Krimmer, H. Boysen, H. Fuess, Applied Physics A, (2003), in print.

[5] B. Krimmer, R. Gilles, K. Zeitelhack, R. Schneider, G. Montermann, H. Boysen, H. Fuess, Applied Physics A, (2003), in print.

[6] F. Elf, R. Gilles, G.R.J. Artus, S. Roth, Applied Physics A, (2003), in print.

3.6 *HEiDi* – Single Crystal Diffractometer at the Hot Source

M. Meven[(1)], M. Misera[(1)], G. Heger[(2)]
[(1)]Technische Universität München, ZWE FRM-II
[(2)]RWTH Aachen, Institut für Kristallographie

The TU München and the RWTH Aachen build a single crystal diffractometer at the hot source of the FRM-II. The instrument will use the beam tube SR-9B. The hot source yields a neutron flux distribution which is shifted to shorter wavelengths. The large available Q-space ($|Q| = \sin\Theta_{max}/\lambda$) increases the amount of observable Bragg reflections significantly. Therefore, the main applications for this instrument will be detailed structural investigations on single crystals using the different Q dependences of different structural parameters, e.g. mean square displacements in the region of structural phase transitions and magnetic structures. Further applications are investigations on hydrogen bonds, extinction effects and heavy ion (e.g. Gd,

Sm) compounds with reduced absorption at shorter wavelengths.

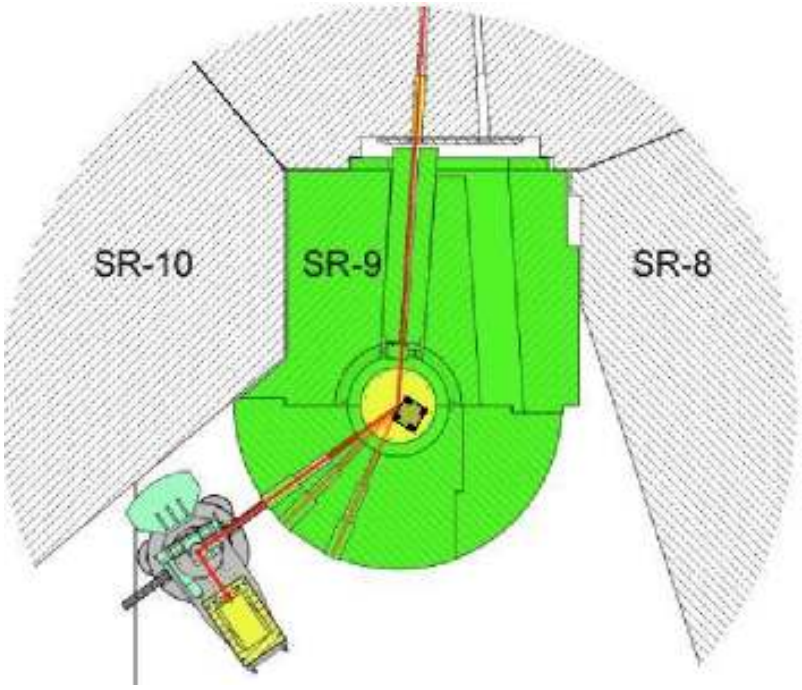

Figure 3.11: Overview

This report describes the progress of several components of HEiDi in 2002. An overview of the instrument is shown in figure 3.11.

Primary Collimator

The horizontal divergence of the primary beam entering the biological shielding can be defined by three selectable soller collimators (15', 30', 60'). This year the 30' and 60' collimators were manufactured by the HMI/Berlin. They were tested at the SV28 at the FZ Jülich. The transition behavior and the homogenity of the collimators were found to be very good. The 15' collimator will be ready in January 2003. All three collimators will be mounted in the shutter in February 2003.

Biological Shielding

The biological shielding was delivered at the end of 2001. In 2002 it was optically aligned to the primary beam of SR-9B. The beam channel between the main shutter of SR-9B and the monochromator pit was surrounded by a 150 mm thick boronized PE tube to optimize radiation protection. For the same reason the monochromator pit itself was covered with 100 mm lead and 100 mm boronized PE on the level of the primary beam. Monte-Carlo simulations (FZ Rossendorf) show a significant reduction of radiation of about a factor of 3 was estimated using the additional shielding. Two shutters were integrated in the shielding, one at the transition from the the PE-channel to the monochromator pit and one at the end of the outgoing beam tube to the sample. The manufactuing of these shutters is in progress. At the beginning of 2003 all parts will be assembled and mounted in the shielding.

Monochromator Unit

A small and cheap motor controller for this device was developed and manufactured by our group. Furthermore, in 2002 the extention with a third monochromator (Ge-(311)) was granted. The focussing device for this crystal was bought from AZ-Systemes. The selection of suitable crystals is in progress and will be settled at the beginning of 2003.

Diffractometer Unit

In 2002 the air cussions of the unit were successfully tested. The mechanical guidance system that connects the diffractometer with the biological shielding was manufactured and assembled.

Figure 3.12: Overview with open shielding

Detector Unit

In dependence on the different instrument configurations - e.g. in combination with the analyser unit - the distance and the angle of the detector to the sample need to be changed. Therefore, in 2002 the base of the detector unit was manufactured which consists of a carriage (max. range 250 mm) and a turntable. A box-like case of Al covers the PE detector compartment itself. Recently the the detector unit was mounted on the diffractometer unit as shown in figure 3.12.

Analyser Unit

Not only elastically ($\Delta E = 0$) scattered neutrons from the sample reach the detector window during measurement. There are also contributions from inelastically scattered neutrons ($\Delta E = 0$) and from neutrons scattered at the sample environment, e.g. the cryostat or furnace.

These contributions reduce the quality of Bragg data collections by worsening the signal to background ratio. The quality of data collection can be improved by using an analyser crystal in front of the detector which accepts only those neutrons which are elastically scattered at the sample. In 2002 a set of three pyrolytical graphite crystals was bought to create the analyser device. Each crystal has a height of 30 mm, a width of 50 mm and a thickness of 2 mm. This yields a reflecting area of 30*150 mm^2. The length of 150 mm is necessary because of the small diffraction angle ($2\Theta_{\text{Analyser}} \approx 14.86^\circ$ at $\lambda = 0.87$ Å). The crystals were tested at the UNIDAS three axes spectrometer at the FZ Jülich with a wavelength of $\lambda = 2.663$ Å. All crystals show the same reflectivity, the same FWHM of 0.5° and well defined Gauss-like profiles. The analyser unit can be mounted directly on the detector shielding.

2D Detector

In collaboration with the detector group (K. Zeitelhack) a very detailed list of specifications for area detectors acceptable for our needs was developed. Discussions with several manufacturers yielded that two methods of measuring are suitable for short wavelengths. One is a position sensitive photomultiplier with a neutron sensitive scintillation plate. Another one is a position sensitive ^{3}He gas chamber with a high pressure of about 8 bar. The solicitation of quotations is nearly settled.

Therefore we expect that we can make our decision for a certain device at the beginning of the next year.

3.7 *MIRA* – Very cold neutrons for new methods

R. Georgii[(1)], N. Arend [(1),(2)], P. Böni [(2)], H. Fußstetter[(1)], T. Hils [(2)], G. Langenstück[(1)]
[(1)] Technische Universität München
[(2)] Technische Universität München, Physik-Department, E21

A beam line for VCN has being built at the new neutron source FRM-II. Situated in the neutron guide hall at the end of a curved neutron guide looking to the cold source, MIRA will operate between 7.7 Å and 30 Å. The beam line is designed to develop, test and demonstrate new methods to use very cold neutrons, therefore the instrument will be equipped with different instrument options. The instrument consists of a neutron guide (1 cm×12 cm) with a shutter in the neutron guide casemate. The monochromator mechanics is situated at the end of a 7 m long curved neutron guide (R=84 m) inside the shielding. The differential flux will reach a maximum at the wavelength $\lambda = 8.5$Å and will be around $4 \cdot 10^7$ neutrons /(Å cm^2). A mica (Phlogopite) monochromator with d_{200} = 9.9 Å and a mosasicity of 0.9° will be used in the wavelength range from 7.7 Å, the cut-off of the curved neutron guide, up to 14 Å. A $\Delta\lambda/\lambda$ in the range of 2 - 8% will be obtained, depending on the choice of the beam divergence before and after the monochromator. For wavelengths of 15 Å, 20 Å and 30 Å multilayer

Figure 3.13: The shielding for the monochromator of MIRA.

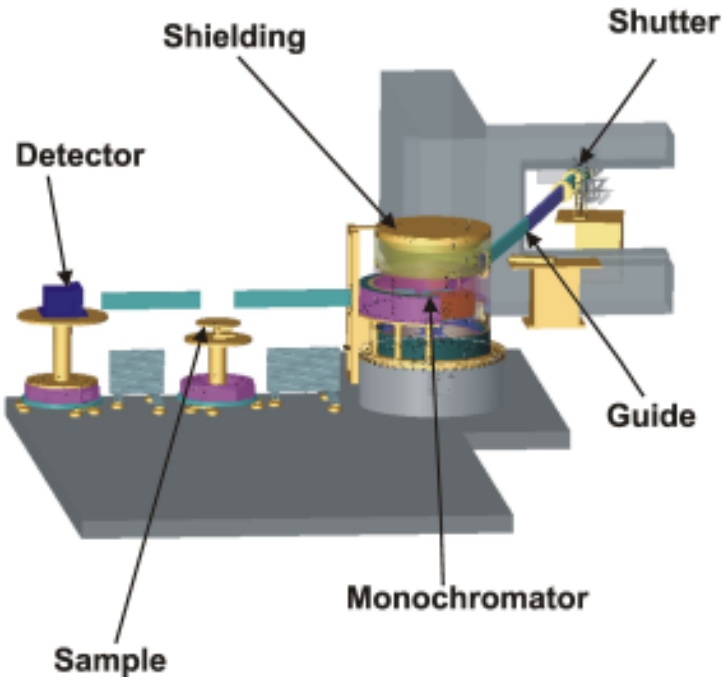

Figure 3.14: MIRA in the reflectometer option with its neutron guide.

monochromators on glass or silicon substrates are foreseen. The multilayer monochromatise the neutrons with a $\Delta\lambda/\lambda$ of about 2 - 10% depending on the bandwidth of the multilayer sequence. A low-band pass mirror in front of the monochromators can be brought into the beam for suppressing the long wavelength contributions (from the regime of total reflection) which would otherwise contaminate the beam after monochromatisation with a multilayer monochromator.

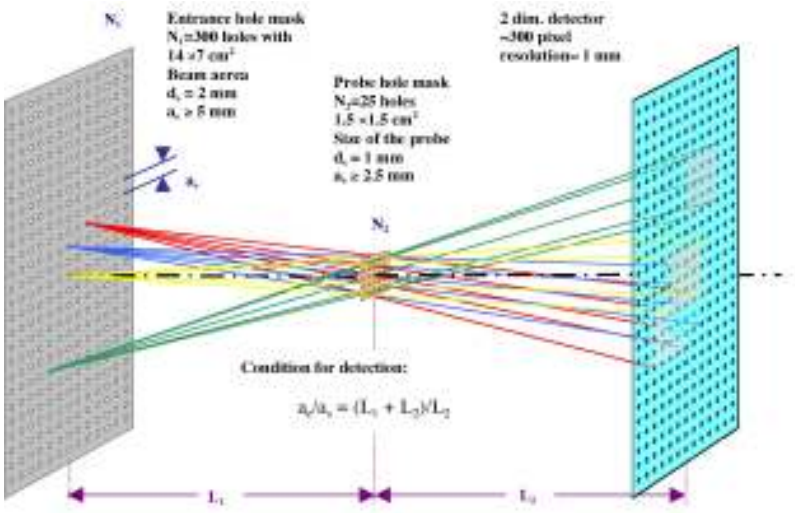

Figure 3.15: The multi-SANS option.

The 4 monochromators can be individually rotated into the beam. The whole monochromator unit, with different tables for rotation and x-y-z translation, an aperture for the incoming neutrons and a monitor counter is surrounded by the shielding. It consists of 10 cm lead and 25 cm concrete (ρ = 4.7 g/cm^3) with a 10 mm neutron absorbing layer of B_4C (see figure 3.13).

During 2002 the design of the instrument was finished. The neutron guide with the shutter in the casemate was installed and is now ready for routine operation. The shielding was designed and manufactured at Swiss Neutronics. The shielding is now installed at its final position in the neutron guide hall. The mechanics and control electronics for the monochromator is waiting for the installation into the shielding. The mica monochromator is finished and was characterised with neutrons of 5 Å at PSI in Switzerland. The data evaluation is proceeding.

The very cold neutron reflectometer option of MIRA

One of the instrument options is a classical reflectometer in horizontal geometry (see figure 3.14). Such a reflectometer for very cold neutrons has the advantage over most existing reflectometers that the angles of reflection are larger and alignment errors near to the critical edge are less critical, yet the accessibility of the phase space is comparable to reflectometers with cold or thermal neutrons.

After monochromatisation in the shielding the neutrons will enter a vacuum tube and hit a sample. Neutron mirrors above and below the beam for the transport of the vertical divergence from the monochromator to the sample are foreseen to be installed in this tube. In the beginning the instrument will mainly operate as a classical reflectometer, with a $\theta - 2\theta$-scan for a vertical sample geometry. It will reach a q-transfer of $7.0 \cdot 10^{-4}$ Å$^{-1} < q < 1.1$ Å^{-1} within the wavelength range of the instrument. Apertures will be used to adapt the wavelength spread of the beam to the beam divergences from the different monochromators. The reflected radiation from the sample will be detected in the detector unit, which will be a ^{3}He-counter. Later the use of a 2-dimensional

position sensitive detector is planned.

For using the reflectometer with polarised neutrons a multilayer polarisation filter shortly after the monochromator can be brought into the beam. After the sample there will be a supermirror-based analyser. There will be also spin-flippers before and after the sample. The idea is to perform specular and non-specular polarised neutron reflectometry in the classical way, i.e. measurement of the four moduli of the reflection matrix [1]. For this only 4 reflectivities need to be measured, namely R_{++}, R_{+-}, R_{-+} and R_{--}, where the + and - refers to the polarisation of the beam before and after the sample.

In 2002 the design for the reflectometer option was finished and a performance analysis of the option was performed. First components, especially of the sample table have been ordered and are expected to be installed in summer 2003.

The Multiple SANS Option

Normal SANS machines are, due to the small angles being measured, relative long and need therefore long measurement times since the sample is seen from the detector only under a very small solid angle. Using a set-up as shown in figure 3.15 two-dimensional small angle scattering with several beams can be performed. This would allow to measure with higher intensities and smaller machines as standard SANS. The working principle of such a device will be tested at MIRA. In 2002 the design for this option was finalised and 2 prototypes of the apertures were manufactured.

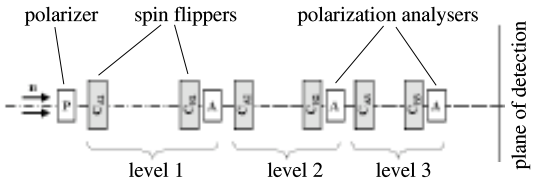

Figure 3.16: Scheme of a multi level-MIEZE.

Multi level-MIEZE setup

This option of MIRA will be used for the investigation of longitudinal coherence properties of neutron beams. This can be achieved by using the multi level-MIEZE variant of the Neutron Resonance Spin Echo (NRSE) technique [2] with VCN. The longitudinal coherence properties of the two neutron spin states can be studied by a very short temporal modulation of the polarisation of the neutron beam. Stacking of several MIEZE setups with a common detector position results in a signal which is the product of the sinusoidal signals from all individual setups. A time resolution of 10^{-7} is possible and the respective coherence length would be of the order of cm. It should be mentioned that the multi level-MIEZE principle has not been verified so far and shall be verified with this setup of MIRA. Crucial parts of the instrument are the spin flippers, which must be suitable for VCNs. Since the neutron beam has to penetrate the coils, interaction (scattering, absorption) with the coil windings is a serious problem, especially in the cold neutron range. Therefore material test measurements to find new adequate material combinations have been performed at the SANS machines at PSI. Furthermore the coil design is under optimisation using finite element simulations.

[1] G.P. Felcher, Physica B, **198**, 1595 (1981)

[2] Scattering and Inverse Scattering in Pure and Applied Science, edited by Roy Pike, Pierre Sabatier. pp. 1264-1286, San Diego, CA, Academic Press (2002)

Spectrometers

4.1 *PANDA* – Three Axis Spectrometer with Cold Neutrons

N.M. Pyka[(1)], D. Etzdorf[(1)], M. Rotter[(2)], M. Loewenhaupt[(2)], R. Schedler[(2)], R. Sprungk[(2)], E. Kaiser[(2)], B. Fuchs[(2)], C. Wetzig[(2)]
[(1)] Technische Universität München, ZWE FRM-II
[(2)] Technische Universität Dresden, IAPD

The Institute of Applied Physics of the TU Dresden (IAPD) and the ZWE FRM-II of the TU-Munich have built a three-axis-spectrometer at the cold source of the FRM-II [1]. This high neutron flux instrument is equipped with elaborate focusing optics and exploits a particular wide range of incident wavelengths due to its position close to the reactor. Moreover, the spectrometer is equipped with Heusler crystals for a full polarization analysis. Details of the spectrometer can be found in [2, 3] and www.frm2.tu-muenchen.de/panda.

Figure 4.1: Neutron guide and monochromator shielding.

Examples of **scientific applications** are:
Analysis of the dynamics in crystal and magnetic lattices, non-harmonic effects and magnon-phonon interaction; the high Q-ω resolution will permit the study of the dynamics of phase transitions and modulated phases, critical scattering of soft modes, central peaks, and spin relaxation effects. Current examples of projects are the examination of magnetic phase diagrams comprising field and temperature dependent spin reorientations, e.g. in RCu_2 (R=Ce, Pr, Dy, Tb); the measurement of phonons and magnetic correlations of high-T_C superconductors; investigations of heavy Fermion systems like inter-metallic Ce-, Yb-, U-compounds and of non Fermi liquid states close to a magnetic instability; the analysis of the interplay between superconductivity and magnetically ordered states in heavy Fermion metals.

Primary Spectrometer

The primary spectrometer was optimized by Monte Carlo simulation [4] and has been manufactured by MOWO Ltd, Berlin, see figure 4.1. A composite structure of the n/γ ra-

diation shielding was used for the first time. Different types of heavy concretes, partly non-magnetic, were used with densities up to 6.3 g/cm^3. This year the mechanics inside the shielding was completed: an exchanger of the primary collimator, a neutron guide, a horizontal diaphragm acting as virtual cold source, a monochromator exchanger, and the mechanics to move the monochromator. For the first time a super-mirror neutron guide, M=3, was installed in the shutter section in order to maximize the phase space element, see figure 4.2.

Figure 4.2: View inside the neutron guide in shutter section.

Secondary Spectrometer

The sample table, the base-, and the rotational modules of the secondary spectrometer were built by AZ-Systemes, Grenoble. The analyzer and detector modules were built by the central workshop of the TU-Dresden. The assembly and the equipment with the electronics took place at a specially prepared laboratory at the IAPD. The sample table and the environment are fully non-magnetic in order to permit the use of highest magnetic fields (15 Tesla cryomagnet) as sample environment. The sample environment is best complemented by a possible load of the sample table of 10 kN, positioning precessions of some 10^{-3} deg, an x-y goniometer and x-y translation table.

Monochromators

This year a novel x-z bending mechanism as PG monochromator mechanics was built and tested, see figure 4.3. It shows excellent focusing properties. The active surface of 460 cm^2 is composed of 121 single crystals. The bending mechanism is based on an idea of the Neutron Optics Service of the ILL, Grenoble, and was constructed and manufactured by AZ-Systemes. Our demand of a precise focusing (<0.03 degree) and reproducibility was successfully implemented in combination with only sparse material, which may be activated. Thereby the signal-to-noise ratio was optimized. The chassis is made of titanium in order to best assimilate the mechanical forces due to the bending. A frame made of aluminum around the chassis serves an automatic monochromator exchanger. Plugs and a mechanical interlock to the goniometer are incorporated. The x-z bending device is controlled by two piezo motors and two capacitive measuring devices. A Heusler monochromator and analyzer were built this year, too. Owing to their monochromatic vertical and horizontal focusing a very high flux of polarized neutrons is expected with coeval excellent energy- and momentum resolution.

Figure 4.3: Double focussing monochromator.

In order to align the PANDA spectrometer next year, neutrons are needed urgently. The 15 Tesla cryomagnet, ordered by the IAPD, will be delivered. A commissioning period of several months is planned. User operation will be possible in autumn 2003.

[1] N.M. Pyka, M. Loewenhaupt, and M. Rotter, Chapter 4.1 in "Experimental facilities at FRM-II", Publisher: Technical University of Munich (2001)

[2] M. Loewenhaupt and N.M. Pyka, Physica B **267-268**, 336 (1999)

[3] M. Loewenhaupt and N.M. Pyka, Journal of Applied Physics, **85,8**, 5145 (1999)

[4] N.M. Pyka, K. Noack, and A. Rogov, Journal of Applied Physics A **74**, 277-279 (2002)

4.2 *NRSE-TAS* – A novel high resolution spectrometer

T. Keller[(1,3)], K. Habicht[(2)], H. Klann[(1)], M. Ohl [(1)] and B. Keimer[(1)]
[(1)] Max-Planck-Institut für Festkörperforschung, Stuttgart
[(2)] BENSC, HMI Berlin
[(3)] Technische Universität München, FRM-II

A novel neutron spectrometer combining the resonance spin echo (NRSE) and the three axis spectroscopy (TAS) techniques has been constructed at the FRM-2 [1]. The instrument will allow the determination of energies and linewidths of dispersing excitations, including both phonons and magnons, over the entire Brillouin zone. This is not possible with conventional neutron or optical spectrometers, which either lack in resolution or in the accessible Q-range. In a combined NRSE-TAS instrument, the spin echo technique provides the energy resolution in the μeV range, while the TAS background spectrometer defines the momentum resolution. The instrument applies a focussing technique first proposed by Mezei in the 1970's: by tilting the boundaries of the spin

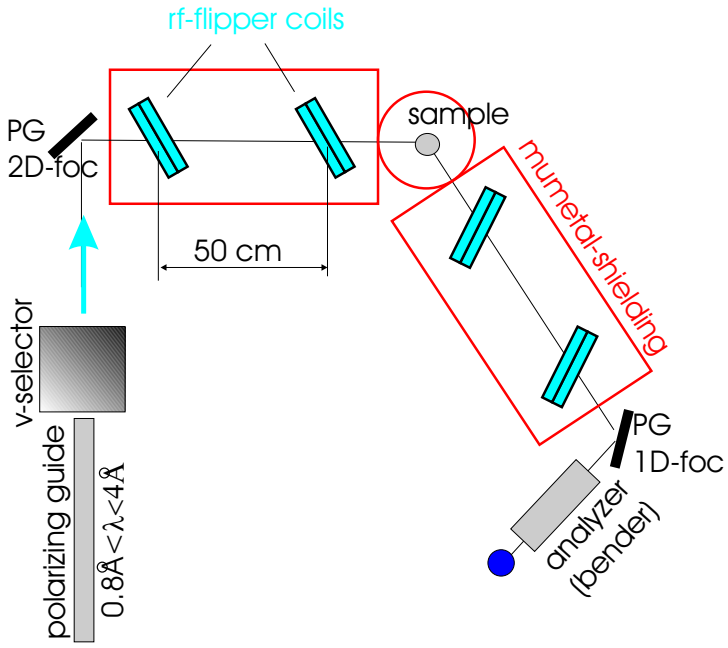

Figure 4.4: Sketch of the NRSE-TAS spectrometer at the FRM-2. The polarizing neutron guide with supermirror coating located at a thermal beam tube provides a polarized neutron flux $d\phi/d\lambda \simeq 3 \times 10^9 \mathrm{cm}^{-1}\mathrm{s}^{-1}\mathrm{\AA}^{-1}$. A carbon fibre Fermi velocity selector removes second order contamination. Monochromator and analyzer crystals (pyrolytic graphite) with variable curvature allow to adjust the momentum resolution. The radio frequency coils and the sample are housed inside a mu-metal magnetic shield to reduce the sensitivity against external fields.

echo precession fields relative to the neutron beam the spin echo resolution function is tuned to the slope of the dispersion curve.

Figure 4.5: Photograph of the current setup at the FRM-2.

Spin echo phonon focussing was successfully demonstrated at a prototype NRSE spectrometer installed at the three axis spectrometer V2 at Berlin Neutron Scattering Center (BENSC) [2]. The NRSE technique uses precisely flat radio frequency spin flippers instead of the large DC solenoids of conventional neutron spin echo spectroscopy to define the precession field boundaries. Field inclination is achieved by rotating the RF flipper coils. From experiments conducted at this prototype spectrometer, we have obtained important parameters for the design of a new instrument at the FRM-2 (Fig. 4.4). As the expected interest for the new instrument is predominantly in the area of excitations with high energies ($1 - 100$meV, resolution $1 - 100\mu$eV), the spectrometer is placed on a thermal beam tube at the end of a polarizing neutron guide with a very high flux for neutron wavelengths between 0.8Å and 4Å.

In combination with a conventional graphite monochromator, the polarizing guide clearly outperforms Heusler monochromators (by a factor of 3 at 2Å) and ^{3}He spin filters. At the time of this writing, construction of the spectrometer at the FRM-2 is almost complete. All major components are in place (Fig. 4.5), and the instrument will be ready for commissioning as soon as the reactor obtains its final operating license.

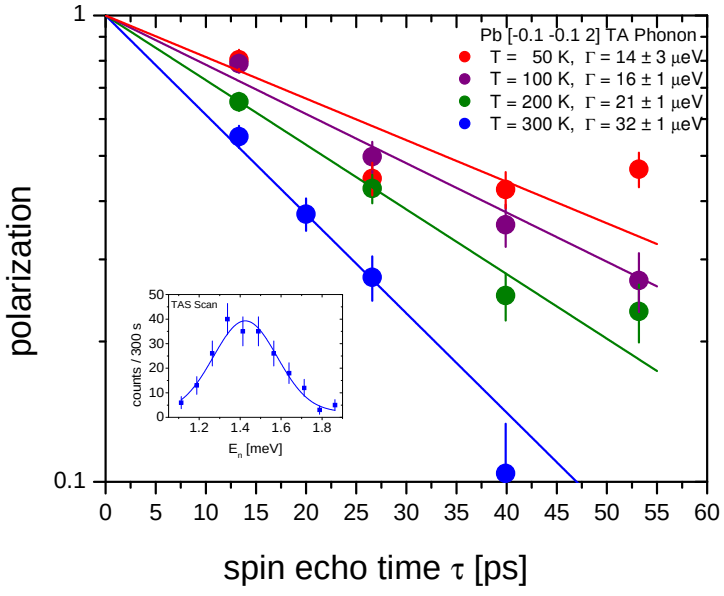

Figure 4.6: NRSE-TAS linewidth measurement obtained for a TA phonon in Pb at the prototype spectrometer at BENSC. The inset shows a TAS energy scan on the same phonon with spin echo switched off.

In the meantime, experiments have been performed on the prototype spectrometer at the BENSC in order to explore the capabilities of the technique. One of the motivations for building the spectrometer is derived from the electron-phonon interaction which plays a crucial role for most transport phenomena in metals. In particular, it has been demonstrated by tunneling spectroscopy a number of years ago that it is responsible for superconductivity in elemental metals. Modern ab-initio band structure calculations for simple metals predict the electron-phonon coupling of every phonon over the entire Brillouin zone, as well as its contribution to the superconducting condensation energy. The phonon line broadening due to the electron-phonon interaction is typically of the order of 10 μeV. It is possible to achieve an energy resolution in this range by optical methods, but these are limited to $Q = 0$. Figs. 4.6 and 4.7 demonstrate that the NRSE-TAS technique is capable of resolving the instrinsic linewidth of a transverse acoustic phonon in Pb away from $Q = 0$.

The beam polarisation at the detector *versus* spin echo time τ (proportional to the frequency applied to the RF flipper coils) is the Fourier transform of the phonon line shape. A Lorentzian line transforms to an exponential with slope proportional to the line width Γ (Fig. 4.6). As the NRSE instrumental resolution is $\simeq 0.5$ μeV (corresponding to $\tau_{max} = 1000$ ps), the measured phonon width is not resolution limited. (For comparison, the inset in Fig. 4.6 shows a TAS energy scan of the same phonon, with the spin echo coils switched off, whose peak width, $\sim 200\mu$eV, is given by the TAS instrumental resolution.)

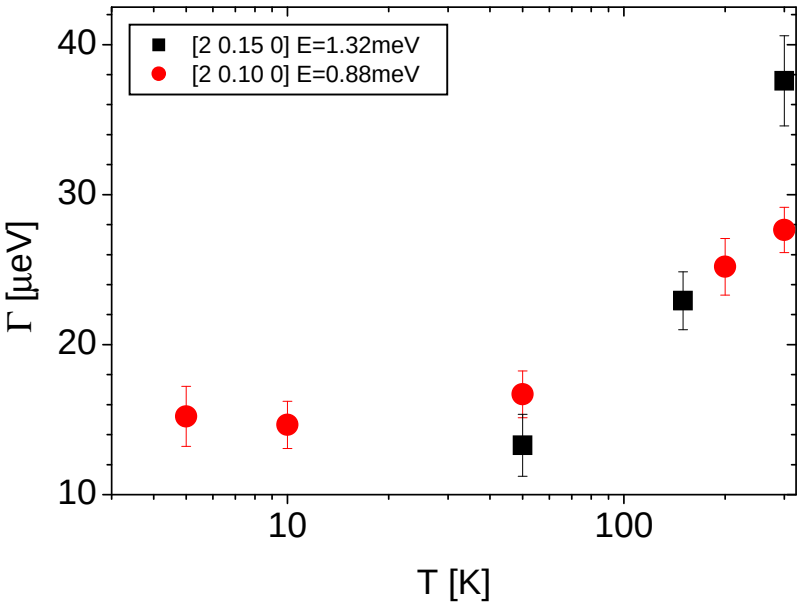

Figure 4.7: Temperature dependence of the line width of the TA phonon in Pb extracted from the profiles of Fig. 4.6, showing temperature dependent and temperature independent contributions.

Fig. 4.7 shows the line width extracted from the spin echo profiles as a function of temperature. As the Pb sample is cooled, the phonon line width Γ decreases before saturating at a temperature independent value of 15 μeV. Whereas the temperature dependent part is due to phonon anharmonicity, the temperature independent contribution can be attributed at least in part to the electron-phonon interaction. At the moment, the low neutron flux at the prototype spectrometer limits these studies to acoustic phonons at low energy. Once it is fully operational, the new spectrometer at the FRM-2 will allow quantitative tests of the band structure calculations for Pb over the entire Brillouin zone as well as detailed studies of the effect of superconductivity on the phonon line widths. This will be a starting point for analogous investigations of more complex systems such as high temperature superconductors.

Finally, the NRSE technique also has a high potential for other new applications. For instance, Rekveldt recently proposed to use the setup for high resolution diffraction (*Larmor diffraction*). The basic idea is to mark each neutron trajectory by a Larmor precession angle, thus obtaining very high resolution ($\Delta d/d \leq 10^{-6}$ where d is the lattice spacing) independent of beam divergence (up to several degrees) and monochromaticity [3].

[1] T. Keller, K. Habicht, H. Klann, M. Ohl, H. Schneider, B. Keimer, Appl. Phys. **A74[Suppl.],**332 (2002).

[2] T. Keller, R. Golub, R. Gähler, F.Mezei, Physica **B241-243**, 101 (1998)]

[3] M. Th. Rekveldt, W. Kraan, T. Keller, J. Appl. Cryst. **35**, 28 (2002).

4.3 *PUMA* – The thermal three-axis spectrometer at SR7

P. Link[(1,2)], G. Eckold[(1)], K. Hradil[(1)], J. Neuhaus[(2)], W. Petry[(2,3)]
[(1)]Institut für Physikalische Chemie, Georg-August Universität Göttingen
[(2)]Technische Universität München, ZWE FRM-II
[(3)]Technische Universität München, Physik Department E13

Within a cooperation of the Physical Chemistry Department of the Georg-August University of Göttingen and the Physical Department of the Technical University of Munich (E13) a thermal three axis spectrometer is under construction at the beam tube SR7 of the FRM-II.

The main concept of the instrument is an optimal utilisation of the beam using focusing techniques, reduction of background and higher-order contamination using a velocity selector. An optional multianalyser/multidetector system is intended. Thus the instrument is designed to be well adapted with regard to resolution, intensity and background for the planned experiments. Therefore, beside the study of phonon and magnon dispersion curves on complex solid solutions a wide application range is covered like the study of diffuse scattering, the analysis of anharmonic effects, the study of systems under extreme conditions or time resolved studies on non-equilibrium systems [1].

In the course of this year all components of the primary and secondary spectrometer were completed, assembled and proven with regard to their mechanical functionality. The individual components are connected to the electronic control system and tested. The electronic control of the instrument is fully operational, including the specially designed counter modules of the FRM-II detector group allowing stroboscopic data acquisition.

Figure 4.8 shows a view of the spectrometer in the standard configuration for the experiments. Inside the monochromator shielding, which is shown on the left hand side, a velocity selector can be automatically placed in the primary beam via computer control and used as higher order filter and as a tool for the reduction of the background. All components for adjusting this device including the electronic control are completed.

In the following a description of the status of the individual components from left

to right is given. The fully automated primary/secondary Soller collimator changer and the monochromator crystal changer equipment for four different monochromator crystals constructed by the mechanical workshop of the University of Göttingen can be seen on the monochromator shielding.

Figure 4.8: Current view of the spectrometer at SR7, from left to right: monochromator shielding with the holders of the secondary collimators seen on the top, sample table and analyser/detector shielding.

All these components are aligned and proven concerning their functionality and can be computer controlled. Four different monochromator/analyser crystals (PG (002), Cu (220), Cu (111), Si (311)) can be provided for the measurements with the possibility of a continuous vertical and horizontal bending (PG (002), Cu (220), Cu (111)) and a continuous horizontal and a fixed vertical bend for the Si (311) crystal. The focussing device for the monochromator/analyser crystals has been developed in close cooperation between the FRM-II and the University of Göttingen. The focussing Si (311) monochromator will be built by Swiss Neutronics and expected to be delivered mid of next year. For the $Cu(111)$ monochromator it is considered to make use of the so-called "onion peel" method, originally developed at ILL.

The sample table, here viewed in the standard configuration, is fully operational. It consists of a 430 mm high base module on air-pads with a ω and ϕ turning table and a manual length adjustment of the distance monochromator to sample table. On top of it a double goniometer with a tilt possibility of $\pm$ 20° for a load of 150 kg, $\pm$ 2° for a load of 1000 kg and a xyz-stage is provided. The high flexibility concerning the usable distance to the beam of 300 mm allows complex sample environments as cryomagnets, furnaces, etc. to be placed. Optionally to these sample environments also an Eulerian cradle can be mounted. Beside the FRM-II standard equipment, PUMA provides an 4K cryocooler and a high temperature furnace for the Eulerian cradle. Due to the use of completely amagnetic materials the work with high field magnets is possible.

The analyser/detector unit, seen on the right hand side of figure 4.8, is also fully operational. The analyser and the detector is placed in one common shielding box, which can be moved around the sample table on air pads. The detector itself is movable around the analyser by use of air pads on a polished stone plate within the shielding box. The concept to choose a common shielding for both the analyser and detector considers beside the standard operation with a single analyser also straightforward mounting of a multianalyser/-detector system. In addition, also the con-

tamination by spurious background scattering towards the detector is expected to be reduced. Currently, the design study and mechanical construction for a multianalyser/-detector system, allowing for a most flexible arrangement of 11 independent analyser blades, is underway.

The control software of the spectrometer is based on the TACO server/client concept provided by the software group of the FRM-II. The development of the user interface in combining the provided modules is ongoing.

After adjustment and characterisation with neutrons, the spectrometer will be fully operational and available for external users.

[1] P. Link, G. Eckold, J. Neuhaus, Physica B, **276-278**, 122 (2000)

4.4 *TOF-TOF* – High resolution time-of-flight spectrometer

T. Unruh[(1)], J. Ringe[(1)], J. Neuhaus[(1)], W. Petry[(1,2)]
[(1)]Technische Universität München, ZWE FRM-II
[(2)]Technische Universität München, Physik Department E13

The high resolution time of flight spectrometer TOFTOF is located in the neutron guide hall of the FRM–II. The instrument is being built by the Physics Department E13 of the Technische Universität München. The multichopper instrument is best suited for the investigation of e.g.:

- local motions in polymers, proteins and biological membranes,
- dynamics in emulsions, suspensions and other liquids,
- diffusion mechanisms of atoms and molecules, respectively, in condensed matter,
- magnetic excitations and fluctuations and
- dynamics of glass transitions.

The technological concept of the instrument described in detail elsewhere [1,2] has been developed on the basis of the results of Monte–Carlo simulations including the calculation of the elastic and inelastic resolution functions. In the following the progress of the construction of the instrument is summarized.

Primary spectrometer

The chopper system

Main component of the primary spectrometer is a system of seven chopper discs used to produce an intense pulsed neutron beam with widely configurable intensity / energy resolution ratios. For this spectrometer special carbon fibre discs with a diameter of 600 mm were developed in cooperation with the Lehrstuhl für Leichtbau. The discs have two and four slits respectively and are coated with elementary ^{10}B as neutron absorbing material.

Presently five of the discs are produced, tested and being mounted into the chopper vessels. Another two discs are under construction. For a first instrument version the chopper discs were tested at a rotation speed of 23000 rpm. An upgrade with discs that work on 26000 rpm or higher speeds is planned and pushed by recent successful tries with speeds up to 29000 rpm. The increase of the angular frequency of the discs leads to a significant improvement of the energy resolution of the spectrometer.

The chopper driving and control system has been completed by ASTRIUM, Friedrichshafen, including the communication software. The whole system with the mounted discs will be de-

livered in spring 2003. The vacuum system for the vessels and the neutron guides and the supports for the vessels and the guide tubes are completed. Thus the chopper system should be operational in April 2003.

Figure 4.9: Flight chamber of the TOFTOF spectrometer

The neutron guide

For neutron flux amplification at the sample position the neutron guide between the chopper vessels and the sample is constructed in an anti–trumpet–like configuration. The reflecting multilayer of the elements of the neutron guide which compresses the beam must have enlarged critical angles. Therefore neutron guides with critical angles of $m = 2$, $m = 3$ and $m = 3.6$, respectively, were ordered from the company S-DH in Heidelberg, Germany. The coating of the glass elements has recently been completed and the assembling of the guides will be finished in 2002. The most of the glass elements surpass the demanded specification significantly. The whole guide is expected to be deliverd and adjusted in the first quarter of 2003.

Secondary spectrometer

Flight chamber and sample chamber

The flight chamber was built up in 2002. Fig. 4.9 gives an impression of the construction which is shielded from the outside with more than 11 t of B_4C coated polyethylene. This shield will reduce the background signal of the detectors produced by cosmic radiation and parasitic scattering of neutrons from other experiments. The inner side of the flight chamber is coated with cadmium sheets which serves as absorption material for neutrons scattered to directions where no detectors are installed. For fire protection the whole flight chamber has to be covered by a 1 mm Al-sheet. This work will be completed in January of 2003.

The last part of the neutron guide, which can be replaced by a collimator to achieve higher Q–resolution, is integrated into the sample chamber. A thin aluminium sheet separates the gas volumes of the sample and the flight chamber. The installation of the sample chamber will be completed when the Al fire protection sheets are mounted.

Detectors, Electronics and Software

In 2002 500 ^{3}He–detectors were delivered by Canberra Eurisys. The detectors are squashed counting tubes with an active length of 400 mm and a depth of about 15 mm. The gas pressure is 10 bar (9.7 bar ^{3}He and 0.3 bar CF_4). The geometry of all detectors was measured using a specially constructed semi automatic apparatus in order to check the agreement with

the demanded specifications. Presently for all detectors the pulse height spectra are measured using a Californium–252 spontaneous fission neutron source (cf. Fig. 4.10).

The final test version for the pre–amplifires of the detectors has been delivered from Leyser electronic. The complete set of preamplifiers will be deliverd in the beginning of 2003.

The time of flight electronics is running and the control and readout software, which is being developed from the FRM-II software group, will be available in 2002.

For instrument control the TACO system is used in conjunction with the NICOS user interface. The TACO system including the required TACO servers as well as the basic NICOS methods are available. Some special devices and operations for the TOFTOF instrument still have to be implemented.

Figure 4.10: Experimental arrangement for recording pulse height spectra of the ^{3}He detector tubes.

Concerning the detectors and other electronic components we got excellent service and further support from the central FRM–II detector and electronics laboratory. We greatly acknowledge the members of the mechanical workshop (E13), Reinhold Funer and Joachim Dörbecker, for their engaged support in the building up of the flight chamber. We also thank the central workshop of the Physics Department where several components of the spectrometer were produced.

[1] A. Zirkel, W. Schneider, J. Neuhaus, W. Petry, Physica B, **128**, 123 (2000)

[2] S.V. Roth, thesis, Technische Universität München (2001)

4.5 Backscattering spectrometer

P. Rottländer, O. Kirstein, M. Prager, T. Kozielewski, D. Richter

Forschungszentrum Jülich, Institut für Festkörperforschung, Institut 5 – Neutronenstreuung

A multitude of studies on slow processes in matter, such as dynamics of polymers, require a high energy resolution. In neutron scattering this can be achieved by refraction of neutrons at the monochromator as well as at the analyzer with the highest possible Bragg angle of 90°. The variety of possible applications of such a backscattering spectrometer convinced the community of neutron scatterers to add a backscattering spectrometer to the range of first generation instruments to be built at the European Spallation Source ESS. The spectrometer RSSM of the FRM-II which will be presented in the following implements all currently known optimizations.

The essential components are a phase-space transformation chopper (PST) as well as a fast Doppler monochromator. By means of reflection at a moving crystal, the PST achieves an intensity gain of 4 in the entire useful energy range of 2.08 ± 0.032meV of the spectrometer at the expense of an increased beam divergence (“from white to wide”). The monochroma-

tor, according to its Doppler speed, selects from the incident band a small energy range of $\approx 1\mu$eV width. The physical and technical layout offers a dynamical range of $\pm 32\,\mu$eV.

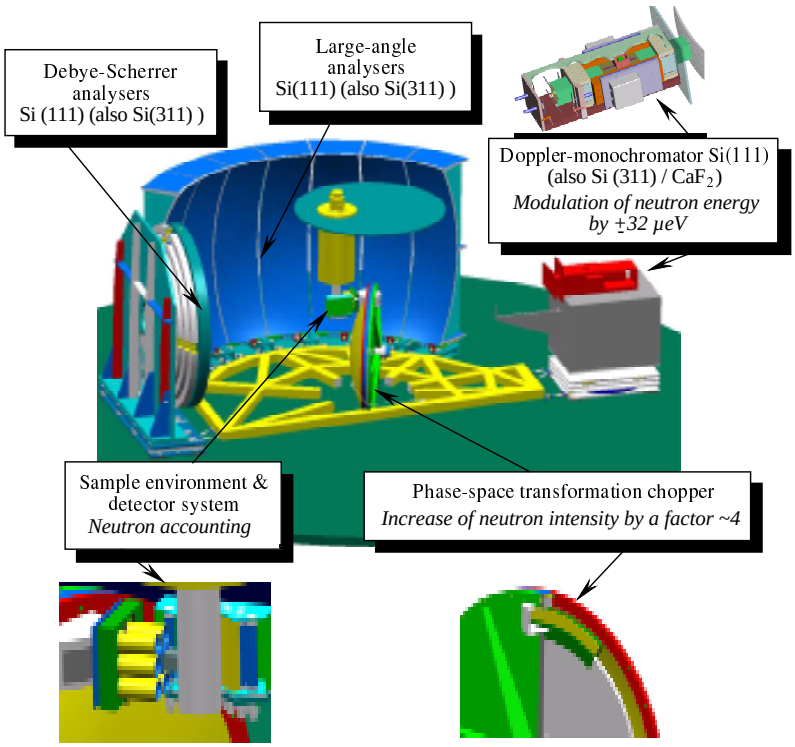

Figure 4.11: Schematical display of the backscattering spectrometer.

In 2002, we achieved the following goals:

- Construction of the element replacement box ELREBO (Neutron guide, Be filter, beam stop).
- Construction of the rotor of the MgLi neutron selector.
- Manufacturing of the vacuum chamber of the instrument specific neutron guide.
- Two PST chopper wheels were manufactured of carbon-fibre reinforced plastic (CFRP). The first one has been balanced and will be spinned at 1.1 times the final speed. Another wheel made of Al is in construction (backup position).
- PG(002) crystals were delivered by the manufacturer and afterwards treated. There is now a sufficient number of crystals to finish the chopper.
- Magnetic bearing and drive for chopper are in assembly.
- Si(111) wafers were glued onto Debye-Scherrer rings, on the large angle analyzers, and the monochromator support.
- More large angle analyzers cast from Al, for polished Si(111) and Si(311) (see Fig.4.12), and crystals were ordered.
- The bases for the large angle analyzers and Debye-Scherrer rings have been manufactured. Air cushions were successfully tested.
- The construction of the rotatable base frame is finished, the manufacturing is commissioned.
- The electronic data acquisition is delivered and will be integrated in 2003.
- Concepts of gas supply and vacuum systems are prepared.

ELREBO, selector, and neutron guide

The first component the neutron beam traverses is the ELREBO (element replacement box). It serves as an alternative beam stop and as support for a beryllium filter which transmits low energy neutrons only. Additionally, a plain piece of neutron guide may be inserted. To achieve an optimal transmission of thermal neutrons, the Be filter will be cooled down to 77K with liquid nitrogen. As a thermal insulation — and in order to avoid dam-

ages through condensed water —, a vacuum of 10^{-6}mbar is provided. The following selector and neutron guide will have a vacuum of about 10^{-3}mbar. The manufacturing of ELREBO and instrument specific neutron guide has been awarded to S-DH in Heidelberg. The chamber of the neutron guide is already delivered, the ELREBO will follow in January.

Figure 4.12: left: Detector bank (finished in 2001). Centre: Chopper wheel with crystal support dummies. Right: Casting of large angle analyzers at Mittelrheinische Gießerei, Andernach.

The selector confines the neutron energies to a comparably small energy band, avoiding higher order reflections at the Doppler monochromator and a related background from unused neutrons. Due to financial constraints, the development and manufacturing of the selector is performed at the IFF. A modified turbomolecular pump serves as drive. The rotor will be made of a Mg^6Li alloy, because ^6Li absorbs neutrons quite well and does not emit gamma radiation. The alloy will be casted at the Hannover university. The blades will be milled at the central workshop of the research centre in Jülich. A preparing milling experiment was successful.

PST Chopper

The phase-space transformation chopper has two purposes: The geometry is designed to enable us to fulfill the 90° Bragg scattering condition at the monochromator, which reflects the neutron beam into itself. The chopper has to reflect the incident neutron beam in the direction of the monochromator.

Neutrons coming from the monochromator, however, have to pass the chopper unhampered. In order to achieve this, the chopper wheel is divided in six 60° segments, three of which carry the reflecting graphite crystals. The other three are empty. Thus, the primary beam is chopped in pulses. During the time such a pulse needs to propagate to the monochromator and back, the chopper wheel turns by 60° and the monochromatized neutron pulse passes.

According to an idea of J. Schelten and B. Alefeld [1], the chopper also may be used to increase the neutron beam intensity in the desired range. This is the already mentioned phase space transformation. The chopper wheel is equipped with pyrolytic graphite (PG002) crystals with a mosaic width of $\eta = 7.5°$. Thus, the reflected beam has a divergence of $\approx 2\eta$. Neutrons of the desired energy of ≈2.08 meV are reflected at a Bragg angle of 69°. At a crystal speed of 300 m/s the energy dispersive, parallel beam is transformed into an angle dispersive, but better monochromatized beam. As a result, we expect a four times higher neutron beam intensity in the exploited energy range.

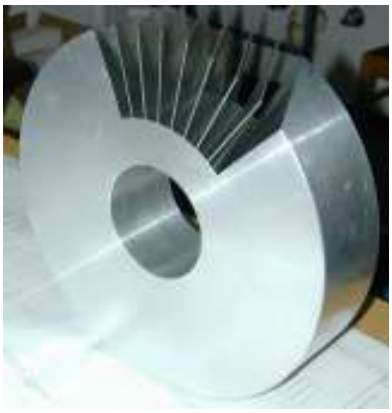

Figure 4.13: Successful milling test for the rotor blades.

The wheel has been designed and manufactured by the RWTH Aachen in collaboration with the Central Department of Technology (ZAT) at the Research Centre in Jülich. The fabrication of the crystal holders and the final assembly of the wheel was performed in the central workshop of the Research Centre. At the moment, the wheel with dummies for the crystal holders is being balanced and subsequently hurled at 1.1 times the operating speed. As the Research Centre does not have the necessary equipment to do so, this has been awarded to MAN in Oberhausen.

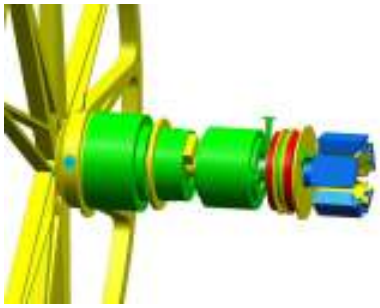

Figure 4.14: Rotor of the chopper drive.

The pyrolytic graphite(002) crystals were made by Advanced Ceramics (USA). Due to difficulties in the production process, it was necessary to determine the mosaic width as seen by neutrons at the Research Centre, and to perform a subsequent treatment if required. After that, it was possible to select from the initially 340 crystals about 200 usable crystals with a mosaic width in the regime of $2.5^\circ \pm 0.5^\circ$. In packets of three, these provide the required mosaic width of 7.5°.

The chopper wheel is mounted on a shaft in a magnetic bearing. Both bearing and the driving motor will be manufactured by Chemnitz based EAAT after a design of the ZAT.

Doppler monochromator

After being reflected at the chopper, the neutrons fall upon the Doppler monochromator after a flight of about 2 m. The monochromator panel is covered with Si(111) crystals. As the 90° backscattering condition is fulfilled by a crystal curvature of approximately the distance to the PST crystals, the panel reflects neutrons in a very sharp energy band only. The analyzers are also Si(111) crystals, which are statically mounted in the spectrometer. To achieve a spectrometer function, we therefore need to modulate the energy of the incident neutrons. This is done by a rapid movement of the monochromator panel exploiting the Doppler effect.

The monochromator panel has to be rather large to catch the divergent neutron beam reflected by the PST chopper. In order to work closely to the backscattering condition, it is also important to have a stroke as small as possible. In order to still achieve the high speed of 4.7 m/s, the monochromator panel and the arbor have to be as lightweight as possible. This is why both are made of carbon-fibre reinforced plastic (CFRP). Due to foreseeable problems with the stability of the material, Aerolas (Munich) prepared a testing model with an aluminium arbor which runs lower speed. At the moment the Al version is subject to an endurance test.

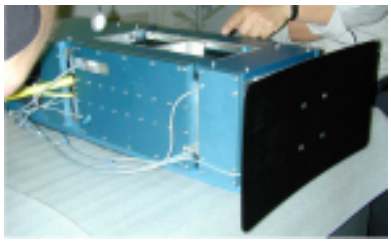

Figure 4.15: The Doppler drive with Al arbor and monochromator panel of CFRP as a test model.

Based on these experiences, the air bearings were modified to allow the use of a CFRP arbor. (The testing model later will be used in a different instrument.)

Analyzers

After being reflected at the monochromator, the neutrons will be scattered by the sample, then they hit the analyzers. For small scattering angles, these are mounted on the Debye-Scherrer rings, other-

wise on the large angle analyzers. Here too, the 90° Bragg condition is observed. Neutrons which are reflected by the analyzers eventually will arrive at the detectors which are 10 cm behind the sample, and thus in the immediate neighbourhood of the chopper wheel. In the basic version of the spectrometer, un-polished Si(111) crystals will be used. Extensions with polished Si(111) for a better energy resolution, and with Si(311) crystals to increase the energy and momentum regime are in preparation.

Figure 4.16: Debye-Scherrer rings before glueing of the Si(111) crystals.

To glue the crystals to the various elements, namely monochromator panel, Debye-Scherrer rings, and large angle analyzers, a glueing device has been constructed which allows to glue up to six crystals at a time.

Figure 4.17: Fixing of Si(111) crystals on a large angle analyzer.

The required pressure is applied by means of radially guided pressure plates. The Debye-Scherrer rings and large angle analyzers for unpolished Si(111) are already equipped with their crystals.

Figure 4.18: Base for a large angle analyzer.

As Si(111) and Si(311) require different reflection angles at the graphite, the chopper wheel, monochromator, and analyzers are mounted to a turnable rigid frame, which allows to position them to the respective angles, and at the same time to facilitate the adjustment. All components have air cushions which can be vented during repositioning.

The air cushions for the large angle analyzers are already successfully tested. The air flow for the Debye-Scherrer rings was not sufficient, new, larger fittings are already ordered (Fig. 4.18). In summary, we expect an air consumption of 3500 l/min for about 10 min. during repositioning, which has to be provided by the infrastructure of FRM-II.

Electronic data acquisition

A measurement at the spectrometer requires to assign an energy transfer at the sample to each detected neutron. All neutrons reflected at the analyzer have the same energy, and so the energy transfer is determined by the speed of the monochromator panel at the time when the particular neutron was reflected. Moreover, the primary neutron beam creates a higher background dur-

ing the time when it is not reflected by the chopper wheel. To account for these effects, a fast electronic is necessary which computes the necessary information for each detected neutron from the position information given by the chopper wheel and the monochromator. We have chosen a system provided by SIS GmbH, Hamburg, which has a processing time of 10 μs and which is already in use at the NIST in Washington, USA.

Figure 4.19: Electronic data acquisition.

Our system is already delivered and awaits being integrated with the rest of the system beginning in the second half of 2003.

Shielding

As a protection of persons and experiments in the neighbourhood the spectrometer has a case which is coated with a cadmium shield. This shield absorbs the thermal neutrons which are used in our experiment (fast neutrons are already absorbed in the Be filter and the selector). Moreover, the reactor and experiments in the vicinity may generate neutrons which would increase our background, some of which are fast. To assure the efficiency of the Cd shield, a 10 cm layer of polyethylene is posed between the chamber wall and the Cd foil. This way, fast neutrons are moderated to thermal energies. The chamber is designed gas-proof which allows to fill it with argon. In comparison to nitrogen, argon has a much lower scattering cross section. Therefore, less neutrons will be scattered out of the beam, which doubles the yield of the apparatus. Additionally, the background through uncontrolled neutrons will be reduced.

The construction of the chamber by the ZAT is finished, and after an invitation to bid the manufacturer will be found before end of 2002.

Energy supply

The backscattering spectrometer features two sensitive major components, the PST chopper and the Doppler monochromator. Because they include rapidly moving parts, they and the data acquisition will be buffered by uninterruptable power supplies – also in view of a CE certificate (safety of operation in case of a mains failure). The total energy consumption of the instrument is estimated to 60kW at 400 Vac, and 16kW at 230 Vac.

[1] J. Schelten, B. Alefeld, in: R. Scherm, H. H. Stiller (Hrsg.), Proceedings of the Workshop on Neutron Scattering Instrumentation for SNQ, Report Jül-1954, FZ Jülich, 1984

4.6 *RESEDA* – Neutron resonance spin-echo spectrometer

Markus Bleuel[(1)], Roland Gähler[(2)]
[(1)] Technische Universität München, ZWE FRM-II and Physik Department E21
[(2)] Institut Laue Langevin, Grenoble, France

The main parts of the spectrometer RESEDA are already at the final position in the north-west corner of the neutron guide hall (fig. 4.20).

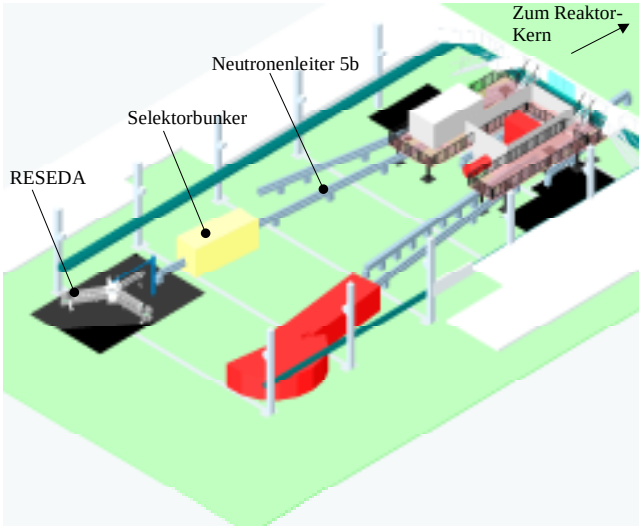

Figure 4.20: Position of Reseda in the Neutron Guide Hall.

The main activities in the year 2002 were the testing and installation of missing components. Also the cabling of the instrument (motors, air cushions, air sensors, water, DC- and HF-supply for the Bootstrapcoils) was continued and the instrument-control-programme was continuously improved (component-test-panels, automated adjustment of the coils and the spectrometer, testing of parameters before execution was added). The three-dimensional modeling of RESEDA (fig. 4.21, 4.22) and surrounding installations with the construction programme "Solid Works" was a great improvement, because the interfaces with other instruments could be defined easier. For example the position of the working cabin and the design of the selector protection need to be chosen carefully, without disturbing other instruments. It was then possible to construct the working cabin and the selector protection and include these drawings in the "Solid Works" file.

A detailed simulation of the neutron beam with the programme "Mcstas-1.6" showed a very good polarization of at least 96% for the used wave length spectrum 2.5-15 Å. The set-up of the neutron guide 5b to RESEDA was started in the end of 2002. For a good polarization of the super-mirror surface it is important, that the

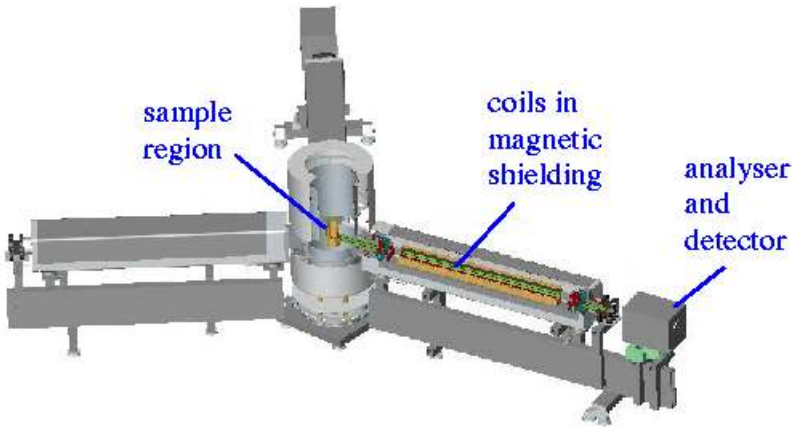

Figure 4.21: 3D-model of the instrument.

neutron guide and the magnetic guide field is built simultaneously. Then it is possible to achieve a high magnetization of the super-mirrors in a higher magnetic field (about 400 Gauß). The following magnetic guide field (180 Gauß) at the final position of the neutron guide sustains the high polarization of the super-mirror.

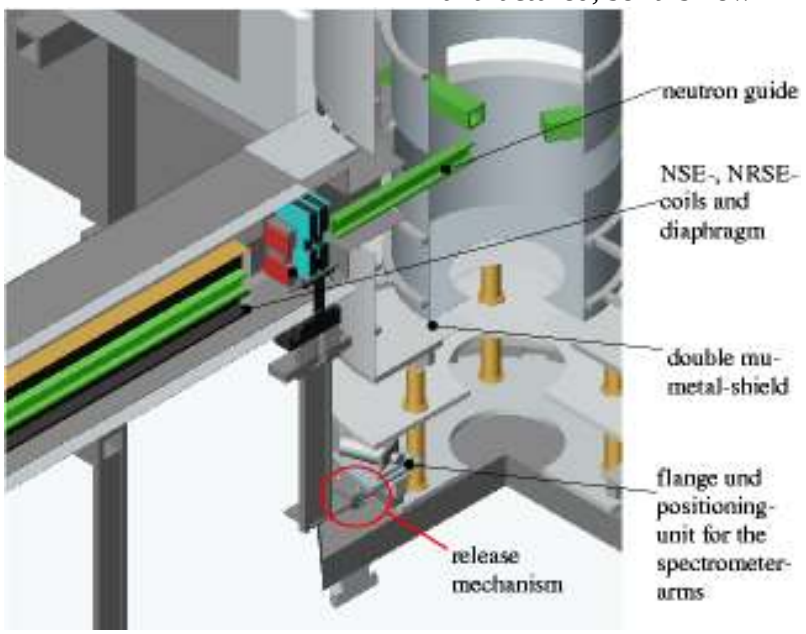

Figure 4.22: Sample position.

The coils are the most vital parts of the spectrometer. Therefore we make a great effort in improving them. The Resonance-HF-Circuit was tested in an alternative configuration with a ceramic-ring ferrite. The ferrite prevents the output of the HF-amplifier from a burnout, due to an always present load, which makes up the primary winding. The first NSE-Z-Coil was tested in the correct position inside the spectrometer. Additional B0-Coils were manufactured, so it is now possible to test them and use only the best ones. In actual fact we are now in possession of some spare parts of this most important component of the spectrometer.

The MIEZE-Option needs a time resolving detector. So a new detector box is under construction, which has a larger inner volume, that gives enough room for a time resolving scintillation glass with a following photo multiplier.

As an alternative set-up we will use a crystal for inelastic measurements. In collaboration with the electronic laboratory the multiplexer circuit boards for the diaphragm are under development. The connection scheme is lined out; a first circuit board is under construction. The Mu-Metal-shielding stands at its final position making it now possible to measure the shielding factor and comparing it with model calculations. The measurements show, that the double shield is by far good enough to prevent depolarization of the neutrons inside of RESEDA. But it is important to demagnetize all parts of Mu-Metal from time to time. To do so, we constructed an automated demagnetizing switching mechanism, which is presently being tested.

Particle Physics

5.1 *MEPHISTO* – a MEasuring facility for particle PHysIcS with cold neutrons

Oliver Zimmer[(1)]

[(1)]Technische Universität München, Physik Department E18

"In jeden Quark begräbt er seine Nase" says Mephistopheles in Goethes Faust to characterize man as created by the Lord. MEPHISTO at FRM-II will provide man a new facility to learn more about the forces, which keep Earth together. Quarks and their basic interactions are usually studied at accelerators. At the energy scale accessible with cold neutrons, quarks manifest their nature less directly than at high energy. However, one can perform plenty of complementary investigations relevant to particle physics, many of them with very high accuracy.

The limitation of available neutron flux often necessitates a long time of event accumulation to get the physics answer. At the Institut Laue-Langevin in Grenoble, only a single cold beam is scheduled for particle physics. Experiments typically extend over one or two complete reactor cycles, i.e. 50 to 100 days. Research groups from all over the world thus feel a severe limitation of beam time at this still most intense neutron source. MEPHISTO will provide a cold neutron beam of comparable if not even higher flux density, thus giving opportunities for new experiments to the nuclear and particle physics community. The facility is located in the neutron guide hall, at the end of the neutron beam NL3a with size 112×50 mm^2. It shall be ready for users once FRM-II has been brought into normal operation. A large size supermirror polariser is already available. MEPHISTO will be a user instrument, and thus the following selection of possible applications does not intend to fix a program at this new facility.

In a somewhat arbitrary manner, we can define effects studied with cold neutrons belonging to a first class as those, which are rather directly related to fundamental interactions and basic symmetries of Nature. Among other things, observables in neutron decay, the electric dipole moment of the neutron, its electric polarisability and neutron-antineutron oscillations belong to this class. In neutron decay for example, the weak axial-vector and vector coupling constants of the neutron are deduced from measurements of the neutron lifetime and the value of an angular correlation coefficient appearing in the differential decay rate. Accurate values are needed to calculate cross sections of weak processes, which cannot be measured in laboratory, like e.g. the fusion of two protons in the sun. Moreover, the combination of these values with the muon lifetime provides an experimental value of the element V_{ud} of the weak quark mixing CKM matrix. It is an interesting test of the standard model of particle physics to see if this value coincides with the value

deduced from the requirement of CKM unitarity, including data from kaon and B-meson decays. At present this test seems to fail [1]. Further efforts are needed to clarify the situation and new experiments are in preparation. A second test of the standard model in neutron decay searches for a breaking of time reversal invariance beyond the mechanism induced by the CKM matrix. Presently at least two groups are performing new experiments [2,3].

In a second class of effects, experiments primarily provide data about effective degrees of freedom. A well-known example is the neutron-nucleus weak interaction, about which only little is known experimentally. Due to the repulsive hard core of the strong nucleon-nucleon interaction, it cannot be described by a direct exchange of W and Z bosons between nucleons. The task of theory to describe such processes in terms of the relevant degrees of freedom, which respect the symmetries found valid at a more fundamental level, led to a picture of meson exchange with one strong and one weak vertex [4]. Studies of selected weak neutron-nucleus interactions can provide the weak pion-nucleon coupling constant. One possible way is via the γ-asymmetry in n(p,γ)d, induced by polarized neutrons in a para-hydrogen target. So far, all attempts to measure its value failed due to insufficient beam intensity. A second, promising way are studies of α- and γ-asymmetries in polarised neutron induced reactions with light clustering nuclei [5].

The nuclear few-body problem also belongs to the latter class, where theory has to provide the relevant effective degrees of freedom, and where slow neutrons can contribute significantly, e.g. to determine the effective couplings. In recent years, starting with a qualitative description by Steven Weinberg [6], a very promising new strategy has been developed to describe nuclear forces at low energy. Compared to traditional models based on phenomenological potentials, chiral perturbation theory requires no parameter fitting and only little experimental input. Nucleon-nucleon interactions are described by pion exchange and contact interactions. Only a few so-called low-energy constants have to be fixed by experiment. It is particularly appealing that, for the first time, the uncertainty of a theory of nuclear interaction can be estimated. Although the range of applicability of this new approach is limited to energies below about 100 MeV, many important quantities can thus be reliably calculated, like e.g. ground state properties of bound systems and cross sections relevant for big-bang and stellar nucleosynthesis. A recent calculation has demonstrated an impressive predictive power in the description of various scattering observables at low energy [7]. Also the correct binding energy of the α particle thus follows from a completely parameter free Hamiltonian! In order to extend the limits of this theory, neutron scattering length measurements at highest possible accuracy, in particular that of the deuteron, are presently of outstanding importance. The theory can be further tested with complementary measurements of other observables. Very interesting but also challenging for both theory and experiment are spin-dependent observables, like the circular polarisation of γ-quanta emitted in the reaction n(p,γ)d, induced by polarised neutrons in para-hydrogen. The value of -1.5(3)$\times 10^{-3}$ measured by a Russian group [8] needs to be improved by a factor 4-5 to make this test sensitive to modern theoretical predictions [9].

More information about some of the projects and proposals mentioned can also be found in the Proceedings of the workshop Particle Physics with slow Neutrons, held at the ILL, 22 - 24 October 1998 [10].

[1] H. Abele, M. Astruc Hoffmann, S. Baeßler, D. Dubbers et al., Phys. Rev. Lett. 88 (2002) 211801.

[2] T. Soldner, C. Plonka, L. Beck, K. Schreckenbach et al., Proceedings of the IX International Seminar on Interaction of Neutrons with Nuclei, Dubna 2001.

[3] L.J. Lising, S.R. Hwang, J.M. Adams, T.J. Bowles et al., Phys. Rev. C 62 055501 (2000).

[4] B. Desplanques, Phys. Rep. 297 (1998) 1.

[5] V.A. Vesna, Yu.M. Gledenov, P.V. Lebedev-Stepanov et al., nucl-th/0004028 (2000).

[6] S. Weinberg, Nucl. Phys. B 363 (1991) 3.

[7] E. Epelbaum, A. Nogga, W. Glöckle et al., nucl-th/0208023, accepted for Phys. Rev. C.

[8] A.N. Bazhenov, L.A. Grigor'eva, V.V. Ivanov et al., Phys. Lett. B 289 (1992) 17.

[9] T. Park, K. Kubodera, D. Min, M. Rho, Phys. Lett. B 472 (2000) 232.

[10] O. Zimmer, J. Butterworth, V. Nesvizhevsky, E. Korobkina (Ed.), Nucl. Inst. Meth. A 440 (2000).

5.2 *MAFF* — Munich Accelerator for Fission Fragments

D. Habs[(1,3)], R. Krücken[(2,3)], M. Groß[(1,3)], W. Assmann[(1,3)], H. Bongers[(1,3)], T. Faestermann[(2,3)], O. Kester[(1,3)], H.-J. Maier[(1,3)], P. Maier-Komor[(2,3)], F. Ospald[(1,3)], M. Schumann[(1,3)], J. Szerypo[(1,3)], P. Thirolf[(1,3)]
[(1)] Ludwig-Maximilians-Universität, Am Coulombwall 1, D-85748 Garching
[(2)] Technische Universität München, Physik-Department E12, D-85747 Garching
[(3)] Maier-Leibnitz-Labor f. Kern- und Teilchenphysik, Am Coulombwall 6, D-85748 Garching

The **M**unich **A**ccelerator for **F**ission **F**ragments (MAFF) is a reactor-based Radioactive Ion Beam (RIB) facility which is being planned and set-up at the FRM-II mainly by the group for experimental nuclear physics (Prof. Habs, LMU) and the physics department E12 (Prof. Krücken, TUM).

The goal of this installation is the production of very intense beams of neutron-rich isotopes that will be available for a broad range of nuclear physics experiments as well as applied physics and nuclear medicine.

In a first step the beam will have an energy of 30 keV (low-energy beam). In a second step also a high-energy beamline will be set up where the ions are post-accelerated to energies adjustable in the range 3.7–5.9 MeV/u. An overview of the project can be found, e. g. in [1,2]. Here we will summarize mainly the progress within the last year.

Authorization procedure

MAFF is at present still in the design and planning stage, as a dedicated authorization procedure will be necessary to set up and run the instrument. This procedure will commence only after FRM-II

has received its final authorization.

Apart from preparing documents, the safety barrier concept of MAFF with respect to loss of pool water and release of radioactivity has been revised and agreed by TÜV Süd.

Figure 5.1: The opened (i. e. without heat shields) MAFF ion source prototype.

Preparatory work

The construction of the eastern experimental hall is a necessary prerequisite of the second expansion stage (high-energy beamline) of MAFF. This hall will house the LINAC and experimental areas at the high-energy beam as well as non-MAFF related experiments in its northern part. As there will be some delay in the construction of this hall and the cryosystem being an essential part for running MAFF already in the first stage, the compressor will be placed at the UTA building. The arrangement of pipelines is being planned by KAM.

Moreover, provisions are made to place lead-throughs in the wall between neutron guide tunnel and casemate which are necessary for operating the source trolley manually.

Development of components

The target / ion source system

Central part of MAFF is the target/ion source unit where radioactive nuclei are produced by fissioning ^{235}U homogeneously dispersed in porous graphite. The fission fragments diffusing out of the target are ionized, then mass-separated and transported towards the experiment.

Different graphite grades have been tested with respect to their uranium doping characteristics, i. e. which amount of uranium can be introduced into the material and whether it is homogenously dispersed. The uranium distribution has been determined by REM. Among the tested samples UCAR PG 100 proved to be of superior quality.

Within the framework of a diploma thesis [3], a prototype of the ion source has been built and its mechanical and thermal characteristics have been investigated as well as its performance as surface ionization source. The target was heated up to 1500° C in a controlled way by electron bombardment.

At the MLL ion source test facility, ion beam currents in the order of 1–10 μA (10^{13} – 10^{14} ions/s) could be extracted which correspond to the expected MAFF beam currents.

A transverse emittance between 14 and 25 π mm mrad has been measured which exceeds the value given by IGUN simulations (10 π mm mrad) by a factor of two. This discrepancy can be explained assuming the actual beam to be composed of several components originating from a larger surface than taken into account in the simulation. On the whole, the concept for the MAFF ion source could be confirmed, but some useful modifications for an advanced prototype became also evident.

The in-pile cryopanel

About one third of the fission product activity produced

in the target are radioactive gases. The in-pile cryopump of MAFF is designed to provide good vacuum conditions in the reactor beam tube and to localize the dominant part of this volatile component onto its cryopanels so that only a small amount will escape to the outer beamline. Volatile uranium fission products typically exhibit short-lived β decay halflives in the order of minutes with only a few exceptions of longer-lived activity. It is the purpose of the cryopump to freeze out gaseous activity in order to localize it onto the cold surfaces until the dominant fraction of volatile activity decays into non-volatile species.

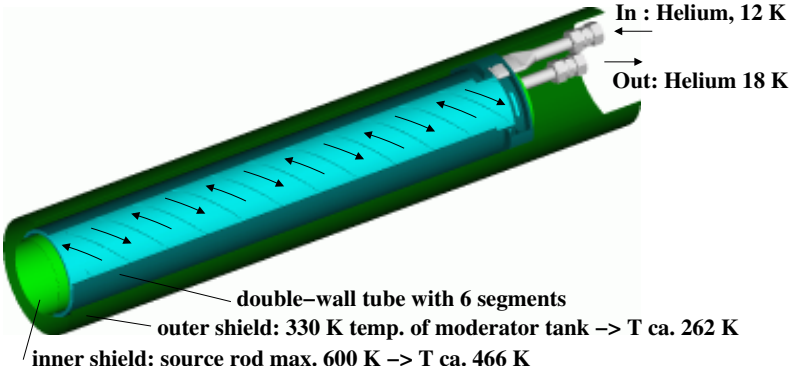

Figure 5.2: Schematic view of the double-tube cryopanel designed to freeze out volatile radioactivity near the MAFF fission source.

The cryopanel has to provide a homogeneous temperature of about 15 K over a large area within a very limited space available in the MAFF beam tube. As a solution a double-wall tube design was chosen, where six spiral-type segments allow for a circulation of cold He gas (cf. fig. 5.2). Since the limited space does not allow for actively cooled lN_2-shields, passive floating inner and outer shields will be installed to reduce the thermal radiation heat load from the outside beam tube and the inner hot titanium rod of the source trolley.

Since many aspects of the cryosystem performance can only quantitatively characterized via experimental studies, extensive prototype tests are foreseen. A test beamline has been set up at the MLL, simulating the inner part of the MAFF beamline. A prototype of the cryopanel has been successfully manufactured by the company Accel and will be installed into this test beamline. It will be connected to an existing He refrigerator in order to determine the pumping capacity of the cryopanel, considering also long-term tests, where we have to take into account a buildup of condensate from the residual gas on the cold surfaces. The homogeneity of the temperature distribution along the panel will be measured, with and without a prototype of the hot ion source installed in the center of the beamline. Safety tests will also simulate the effect of leakages into the beamline.

Finally the attenuation factor for the confinement of volatile fission products will be measured with a mass spectrometer by introducing defined amounts of tracer isotopes from Kr, Xe, Br, and I.

Within the 6^{th} framework EU programme a European network SAFERIB (coordinated by LMU Munich) will be started, dealing with safety aspects at RIB facilities in general. Part of the subject of this network is radioactivity handling, where techniques like freezing out of gaseous activity or intercepting it by circulating the gases in storage tanks through pumping oil are discussed and investigated in a more general context.

Ion beam cooler

For efficient cooling of intense low-energy ion beams a new cooler concept is under investigation. The cooler is a 450 mm long stack of 223 single stainless steel ring electrodes. The thickness of each electrode is 1 mm and

the gap between adjacent electrodes is 1 mm as well. The series of rings forms a channel with varying inner diameter which is filled with He buffer gas in the pressure range around 0.1 mbar for stopping and cooling the ions. Each electrode is supplied by an oscillating electric field in the Radio Frequency range ($\sim$ 5 MHz) where the phase shift between adjacent electrodes is π. The RF fields with amplitudes up to 150 V generate an average repelling force perpendicular to the electrode surfaces causing the reflection and focusing of the ions around the length axis of the channel. Additionally a DC electric field gradient is applied along the electrodes for compensating friction and dragging the ions towards the exit.

Since in such ring electrode structures the RF forces are mainly acting close to the electrode surfaces the created pseudo potential well is box shaped and screening effects due to space charges are less significant than in the quadratic pseudo potentials of the conventional RFQ coolers. Hence, higher currents can be held. A further advantage is the high flexibility in shape since rings can easily be exchanged independently from each other. In detailed Monte Carlo simulations we found that we can expect transmissions close to 100 % by choosing a proper shape and parameter settings for the ring electrode structure. Moreover, these predictions have been verified in first experimental investigations of a 45 mm long miniature prototype with 40 ring electrodes working as an RF ion guide. Experimental investigations of the 450 mm long cooler will start early in 2003.

Figure 5.3: Interior view of the 7-gap resonator.

IH 7-gap resonator

The MAFF postaccelerator is a LINAC consisting of a series of highly efficient resonators of different types: A radiofrequency quadrupole (RFQ), an IH-RFQ booster section with three resonator tanks and an third section of two identical 7-gap resonators which will be used to vary the final beam energy. By switching off or on the third IH resonator, fission fragments will enter the 7-gap section with energies of 4.15 and 5.40 MeV/u, resp. Subsequent acceleration or deceleration yields energies in the range 3.7–5.9 MeV/u. The IH-RFQ and the 7-gap structures are new developments.

The latter has been developed and tested in the framework of a PhD thesis [4]. This very compact component has been designed for a mean particle velocity of $\beta = 0.10$ and a mass-to-charge ratio of $A/q \leq 6.3$. The resonator is operated at a frequency of 202.56 MHz (CERN standard) and a pulsed power of up to 100 kW at 10 % duty factor. The MAFIA code has been used to simulate the RF structure and to determine

its dimensions. By varying its geometries, resonator characteristics have been derived experimentally from a real-size model. The codes LINAC and LORASR have been used to investigate beam dynamics. They show a rather low emittance growth of $< 5\,\%$ even for the most extreme acceleration or deceleration szenarios. Subsequently power tests have been performed at different levels in order to verify calculations and to demonstrate that the required design voltages and beam energies can be achieved.

A test beamline was set up at the MLL where a bunched 4.15 MeV/u $^{16}O^{5+}$ ion beam has been injected into the resonator and successfully accelerated and decelerated. The measured shunt impedance of 120 MΩ/m at nominal RF power results in a total resonator voltage of up to 2.4 MV which corresponds to a final beam energy between 3.6 and 6.0 MeV/u. The quality factor amounts to 9833.

MAFF-Trap

A Penning trap system similar to REXTRAP at ISOLDE (CERN) or JYFLTRAP at Jyväskylä is currently under design to measure nuclear masses with high precision and/or to do nuclear spectroscopy at trapped ions. This device can be installed either at the low-energy beamline or at the high-energy beam.

[1] *MAFF — Physics Case and Technical Description,* ed. by D. Habs et al., http://www.ha.physik.uni-muenchen.de/maff/

[2] D. Habs et al., *The Munich Accelerator for Fission Fragments MAFF,* Proc. EMIS-14, to be published in NIM B

[3] F. Ospald, *Aufbau und Test eines Ionenquellen-Prototypen für den Münchner Spaltfragmentbeschleuniger (MAFF),* LMU diploma thesis, January 2003

[4] H. Bongers, *Entwicklung der 7-Spalt-Struktur für den Münchner Spaltfragmentbeschleuniger MAFF,* LMU PhD thesis, January 2003

5.3 Ultracold Neutron Source Mini-D_2

I. Altarev, A. Frei, E. Gutsmiedl, F.-J. Hartmann, S. Paul, G. Petzold, W. Schott, D. Tortorella, U. Trinks, O. Zimmer
Technische Universität München, Physik Department E18

The Mini-D_2 source for ultracold neutrons will be installed in the beam tube SR-4a. This source is dedicated for storage experiments to measure elementary properties of the free neutron with high precision, especially the electric dipole moment, the lifetime, and the angular correlation coefficients of the decay.

A double-walled cryogenic tube - containing 200 cm^3 of solid deuterium at 5 K as converter - shall be installed in the beam tube SR-4a inside an inpile-cryostat. In this converter slow neutrons from the cold source will be scattered down to become ultracold neutrons with a kinetic energy less than ≈ 250 neV, corresponding to the Fermi potential of Be. The solid deuterium is frozen directly into the converter cup, positioned at the very inner end of the cryogenic tube. The inside surface of the this cryo-

genic tube will be covered with Be in order to transport the ultracold neutrons - escaping from the converter- by total reflection to the storage experiments in the experimental hall. Because these storage volumes need to be refilled every few minutes only, the ultracold neutrons, produced continuously, will be accumulated during the intermediate periods in the cryogenic tube.

In the past year the development of Mini-D_2 was continued: - The safety concept was completed. The barriers against water loss from the reactor pool as well as those to protect the deuterium from oxygen input from the air were fixed in agreement with the safety experts from TÜV. The protection against overpressure of all subsystems was matched, and the nuclear classification scheme was designed. This design work caused some changes in the details of the source.

- Calculations of the radiation shielding based on the original curved shape of the cryogenic tube and its cryostat did not give satisfactory results. Therefore a vertical bypass was introduced behind the in-pile part, lifting the axis of the tube by 40 cm for the following horizontal tube (length: 1.6 m), then lowering the tube axis again to the original level and ending after another horizontal part of 1.5 m length into the end cryostat with the exit windows for the ultracold neutrons. The new design is shown in Fig. 5.4. The bypass allows a very effective shielding of the radiation from the direct beam. Preliminary results from new shielding calculations gave sufficiently low radiation levels at the final cryostat.

- Together with the redesign of the cryogenic tube and its cryostat in the experimental hall a buffer was introduced at the descending part of the cryogenic tube. Its volume should be matched to the storage volume of the experiment to obtain optimum filling. This was confirmed by calculations based on neutron transport theory.

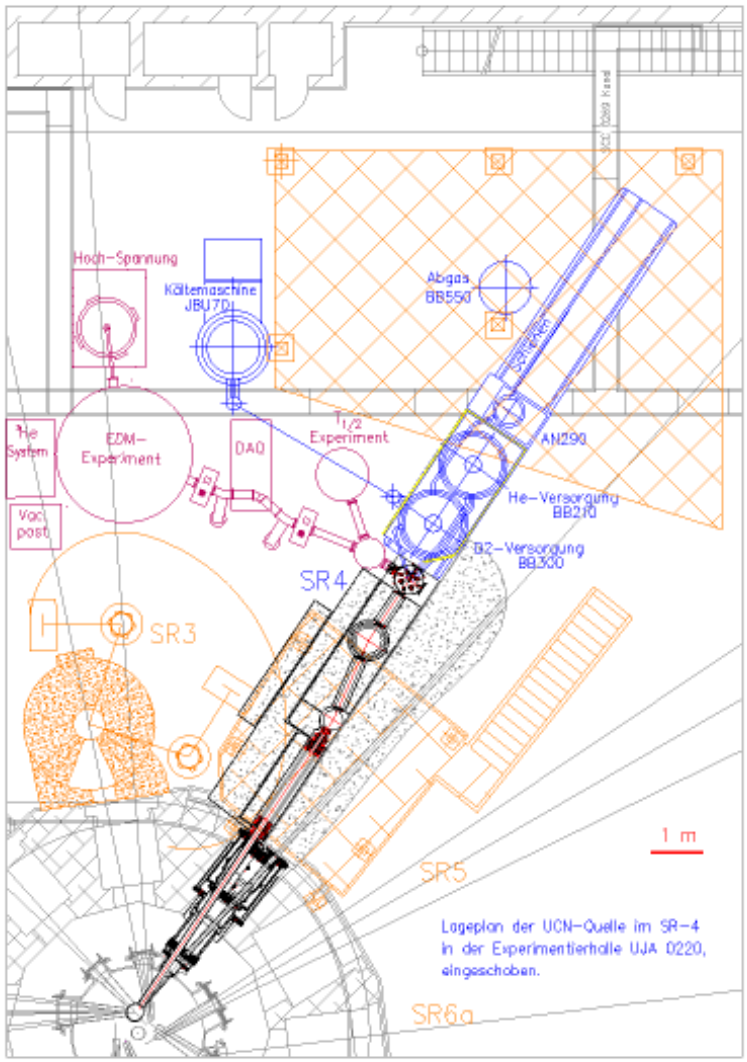

Figure 5.4: The experimental hall at SR-4a with Mini-D_2

Figure 5.5: Inner and outer part of the converter cup

- Several thin-walled converter-cups (Al6061) were produced (see Fig.5.5). They will be used for investigations of the optimum conditions for creating the solid deuterium converter in the near future, and of the ultracold-neutron yield at the pulsed TRIGA reactor in Mainz next year.

- The final cryogenic tube with thin double walls and spacers in between was produced by extrusion. Presently the TÜV is working on the certificates for the tubes.

- The inpile-cryostat has to obey special safety regulations. In order to demonstrate that all technical requirements can be fulfilled, the material and tools for the production of a prototype (of half length) were ordered.

- Of similar importance with respect to the safety are the double-wall bellows, connecting the end of the inpile-cryostat to the end plate of beam tube SR-4a. Three out of in total 30 of this double bellows were bought and tested under realistic conditions with very satisfying results.

- The deuterium gas handling system in a vessel with helium gas protection is almost ready for being used.

- A test cryostat for the investigations of the ultracold-neutron yield in deuterium converters at the TRIGA reactor in Mainz is in an advanced state.

- A new device for sputtering beryllium on the inside surfaces of the long cryogenic tube is under construction. With this device the tube can be cleaned and sputtered with different materials without exposing the sensitive surfaces to air in between.

- Planning for the incorporation of the cooling system for Mini-D_2 into the infrastructure of FRMII has been brought on its way.

- Last but not least, progress has been made in the preparation of the first experiments at the UCN source, the measurements of the lifetime and of the electric dipole moment of the neutron.

Radiography and Tomography

6.1 ANTARES

B. Schillinger[(1,2)], E. Calzada[(1)], F. Grünauer[(1)]
[(1)] Technische Universität München, ZWE FRM-II
[(1)] Technische Universität München, Physik Department E21

The neutron tomography facility ANTARES will have an unprecedented combination of high flux and high beam collimation with two selectable beam-adjusted collimators. The space for the installation was assigned very late during the planning of the new reactor FRM-II. This lead to several harsh constraints due to surrounding experiments, e.g. the site is not accessible by crane. We describe the engineering solutions as well as the current progress in the construction.

The Facility

In the early planning stage of the reactor, the tomography facility was foreseen at a neutron guide leading out of the reactor hall to an external building. When it became clear that the beam geometry of a neutron guide was unsuited for tomography, a classical flight tube design hat to be fitted into the remaining space in the reactor hall. The tomography facility at FRM-II shares the beam port (with two channels) with the UCN source and is surrounded by a spin-echo spectrometer and the platforms of the positron source at the inclined beam tube above its beams tube (Fig. 6.1). The UCN source will insert a nozzle through the second channel of the drum shutter in the biological shielding, so an additional secondary shutter outside the reactor wall is required.

Shutter and Collimator

The beam geometry resembles a classical pinhole camera imaging the square source area onto the sample area. A special beam-adjusted collimator with a cross section with varying shape follows exactly the contours of the pinhole imaging of the source area. This collimator also limits the penumbra region of the beam. The first part of this collimator is integrated into the drum shutter in the biolog-

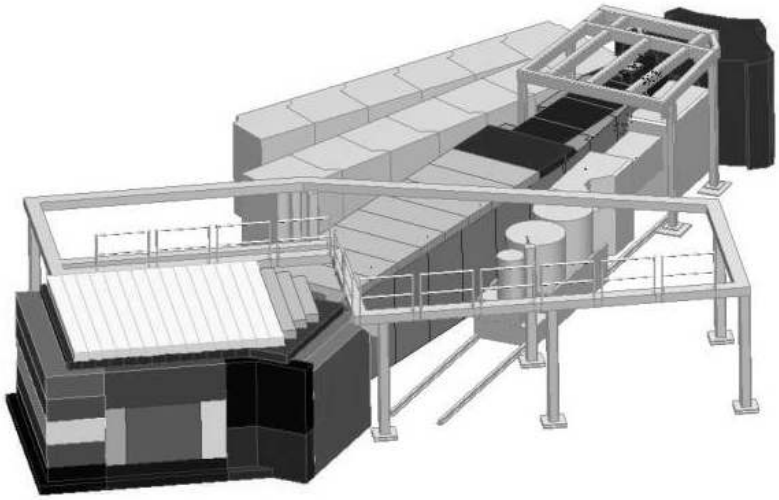

Figure 6.1: Tomography facility surrounded by other experiments.

ical shielding, the second part consists of two separate channels above each other inside the vertical secondary shutter (Fig.6.2). With these two collimators, the beam can be adjusted for high resolution (L/D=800, 3×10^7 n/cm^{2}s) or high flux (L/D=400, 1.2×10^8 n/cm^{2}s). The secondary shutter is driven by a regulated hydraulic positioning system with a pressure storage and fail-safe mechanism that shuts the beam off even in case of power failure.

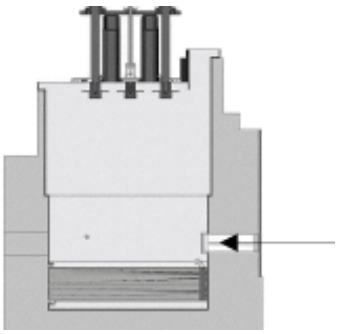

Figure 6.2: Cross section of the vertical beam shutter.

Flight tube and shielding

The collimator feeds a divergent 12 m long flight tube. It consists of six sections made of aluminum with square cross section (Fig.6.3) . Each section can be removed in order to install instruments, for example a velocity selector. The tube size and geometry are adapted to the beam generated by the collimator, therefore the penumbra region of the beam does not touch the beam tube wall, avoiding excessive gamma generation in the aluminum walls.

Figure 6.3: The flight tube.

The flight tube is shielded by L-shaped walls and a roof made of heavy concrete-filled steel containers. As the access by crane is blocked by the positron source platform, the wall elements have to be positioned by air cushions, the roof components will be positioned onto the walls in the small accessible space between the platforms and will be rolled on ball bearings into their final position. The neutron beam enters the measurement cabin through a square hole of 400 mm$\times$400 mm, the penumbra being absorbed by the wall. The walls consist of several segments with a thickness of 800 mm and less than 10 t weight which will be stacked vertically in the crane accessible area. The walls will

Figure 6.5: Variable beam size limiter.

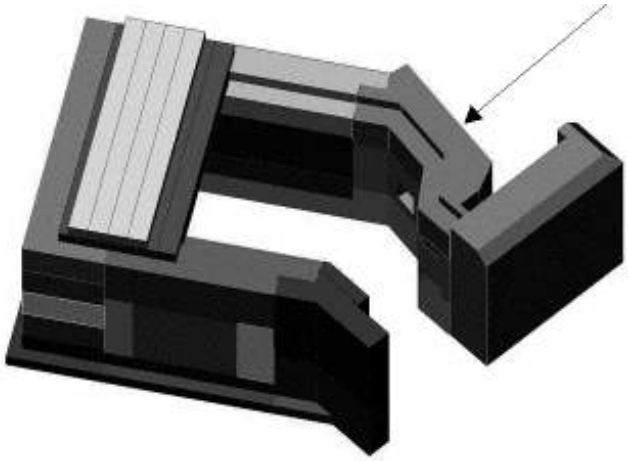

Figure 6.4: Measurement cabin.

then be positioned by air cushions. As there is no space for a conventional door to swing open, a whole 20 t wall section will be moved on rails parallel to the UCN experiment (Fig. 6.4).

Figure 6.6: The collimators.

Manipulator and beam size limiter The motor driven sample manipulator allows for samples of up to 500 kg and 1 m diameter to be rotated and translated in height and width across the neutron beam.

The maximum beam cross section is 400 mm×400 mm. It can be reduced by a variable beam size limiter (Fig.6.5), installed at the end of the flight tube outside the cabin. It consists of a aluminum frame with four sliding plates covered with BorAl layers. A fast pneumatic beam shutter with B_4C, situated at the beginning of the flight tube, captures the thermal flux in intermissions between measurements (e.g. for data transfer time) to keep the activation of the sample as low as possible.

Status in January 2003

In January 2003, the status was as follows:

- The primary collimator has been installed in the drum shutter, the secondary shutter inserts are near completion (Fig. 6.6).
- The sample manipulator and control are completed, cabling and programming are in progress (Fig. 6.7).
- The beam size limiter is almost completed, waiting for the BorAl plates to be mounted.
- All shielding walls except for the secondary shutter are completed and are being transported to an assembly hall to be filled with heavy concrete in the fully assembled state.
- The camera system (2048×2048 pixels) for the detector has been delivered and awaits first tests.
- The hydraulic control system is being delivered in parts for assembly with the secondary shutter.

The mechanical mounting of the complete facility will be finished by March 2003, with electrical installations to be completed.

Figure 6.7: The sample manipulator.

[1] B. Schillinger: Estimation and Measurement of L/D on a Cold and Thermal Neutron Guide. World Conf. Neutron Radiography, Osaka 1999, in: Nondestr. Test. Eval., Vol. **16**, pp.141-150

[2] B. Schillinger, E. Calzada, F. Grünauer, E. Steichele: The design of the neutron radiography and tomography facility at the new research reactor FRM-II at Technical University Munich, 4th International Topical Meeting on Neutron Radiography, Pennsylvania 2001, acc. pub Journal of Radiation and Isotopes, 2002.

[3] F. Grünauer, B . Schillinger: Optimization of the Beam Geometry and Radiation Shieldings for the Neutron Tomography Facility at the New Neutron Source in Munich. 4th International Topical Meeting on Neutron Radiography, Pennsylvania 2001, acc. pub Journal of Radiation and Isotopes, 2002.

[4] E. Calzada, F. Grünauer, B. Schilllinger, "Engineering solutions for the new radiography and tomography facility at FRM-II", World Conf. Neutron Radiography, Rome 2002

6.2 Estimation of the Imaging Quality of ANTARES

F. Grünauer(1)
(1)Technische Universität München, Physik-Department E21

The imaging properties of the new neutron radiography and tomography station at Munich´s new neutron source FRM-II were estimated and optimized by simulation of the whole facility by Monte Carlo method.

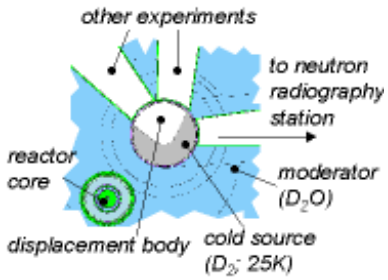

Figure 6.8: horizontal cut through the cold source and its surrounding inside the moderator vessel

Homogeneity of the open beam image

An important question is the influence of the structure of the cold source and its surrounding (fig. 6.8) with regard to homogeneous illumination of our detector.

The cold source itself is not homogeneous. A displacement body without deuterium is included inside the cold source. This is to optimize flux and spectrum, especially for the other two beam tubes, that are connected to the cold source. In addition, the other beam tubes are arranged in an asymmetric way. The result is a flux depression on one side of the cold source, due to missing backscattering from the volumes of the tubes. These influences are estimated by calculation of open beam images in the detector plane for different theoretical arrangements inside the moderator vessel using our 4.3 cm aperture:

- a cold source without displacement body and without other beam tubes. The volumes of the tubes are replaced by heavy water

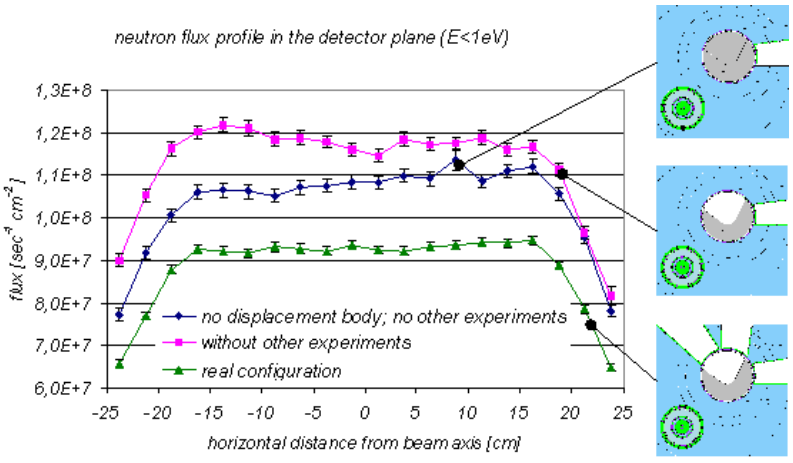

Figure 6.9: Neutron flux profiles (E<1eV) in the detector plane for different theoretical arrangements in the moderator vessel

- a cold source with displacement body but no other beam tubes
- the real arrangement.

Neutron flux profiles in the energy range below 1eV in our detector plane are displayed in fig. 6.9 for different theoretical arrangements in the moderator vessel. Without displacement body a bias in the flux profile occurs, because both sides of the entrance of our beam tube are populated by neutrons that crossed different thicknesses of moderator. The situation is reversed with included displacement body: the total flux increases. The resulting bias is nearly compensated by including the beam tubes for the other experiments. Inhomogeneities are rather low for neutrons in the interesting energy range below 1eV, whereas inhomogeneities in higher energy ranges occur.

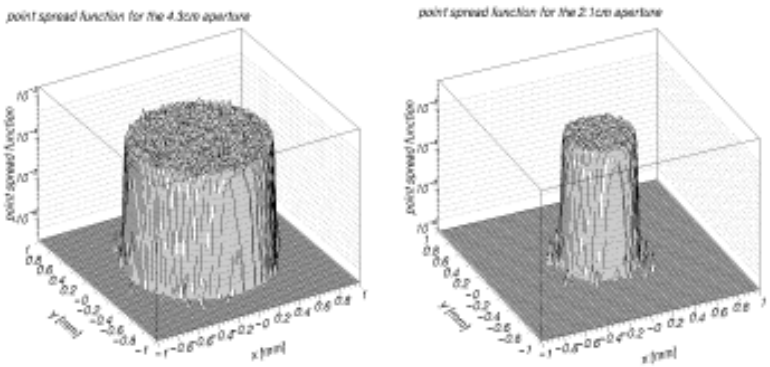

Figure 6.10: Point spread functions for an object plane at a distance of 50cm before the detector plane for the 4.3 cm aperture (left-hand side) and for the 2.1 cm aperture (right- hand side)

Point Spread Function

One of the most important imaging properties for of a neutron radiography station is the point spread function. The point spread function defines the image of a point in the object on the detector plane. It is influenced by several factors: beam geometry, transmission through the collimator material, scattering inside structure material, scattering inside the object, etc. Of course for the last point no predictions can be made as long as the object is not known. The resulting point spread function (PSF) from all other factors was estimated for an object plane at a distance of 50cm before the detector. The results for our two different apertures are displayed in fig. 6.10

Both PSFs have the shape of a pill-box, that can theoretically be expected for the case of a homogeneous and isotropic source, that is observed through a round aperture in ´black´ material. That means our beam geometry, especially our ´beam adjusted´ collimator is very close to the ideal configuration. The PSFs will be used for image deconvolution in the future.

6.3 NECTAR

Neutronen Computer Tomography and Radiography Facility

T. Bücherl[(1)], Ch. Lierse von Gostomski[(1)], E. Kutlar[(1)], E. Calzada[(2)]
[(1)]Technische Universität München, Institut für Radiochemie
[(2)]Technische Universität München, ZWE FRM-II

For the instrumentation of the FRM-II, a radiography and tomography facility utilizing fast (fission) neutrons is designed, implemented and tested by the Institut für Radiochemie (RCM) of the Technische Universität München (TUM). It is set-up at the converter facility (beam tube SR 10) where it will share beam time with the therapy installation. At the measurement position about 10 m away from the converter plates, fast neutron fluxes of $6.4 \times 10^7 cm^{-2}s^{-1}$ and $7.2 \times 10^6 cm^{-2}s^{-1}$ will be available for L/D values of 100 and 300, respectively [1]. NECTAR (NEutron Computer Tomography And Radiography facility) will be used for the non-destructive characterization of samples covering a broad range of scientific and technical questions, e.g. the detection of hydrogen containing materials in large volume metallic samples, the detection of cracks, the determination of the distribution of linear attenuation coefficients etc. Special focus in the layout is set on industrial applicability.

General

The basic components of the facility are the casemate, the collimator systems, the manipulator for sample handling, the two detector systems and the control and data evaluation software package. Here the progress in developing and setting up the latter three is reported.

Manipulator and Control Unit

The manipulator is a three-axes system for lifting, translating and rotating objects of up to 400 kg maximum burden and 80 cm×80 cm×80 cm in dimension (Figure 6.11). The axes are driven by servo motors being connected to programmable controllers. Actually, the cabling of the limit

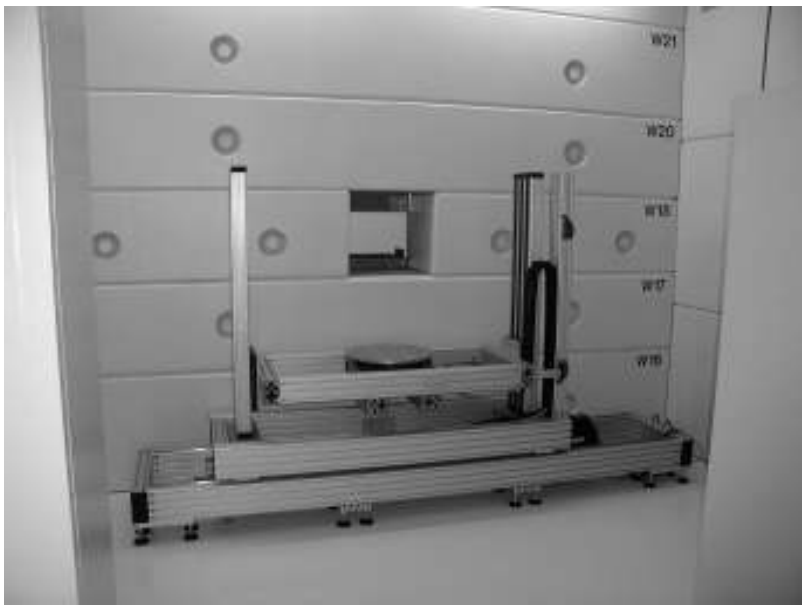

Figure 6.11: Manipulator at measuring position at the converter facility.

switches and the adaptation of the lengths of all cables are performed. For connecting the manipulator with the external control unit an interface box which will be attached to the manipulator frame is under construction.

The control unit is completed and tested, hosting four programmable controllers which take care of the complete measuring procedure in routine operation including control of the detector system.

Detector Systems

Two-dimensional position sensitive detectors are state-of-the-art systems in radiography and tomography. A CCD-based system using an inorganic converter for the conversion of neutrons into visible light was designed and set up. Depending on the composition of the sample, radiographs and tomographs may be blurred due to forward scattering and beam hardening of fast neutrons in the sample. Fore those cases a set of well collimated single beam detectors is under construction.

CCD camera system

The final layout of the CCD detector system is presented in [2]. The actual work is focused on the determination of specific detector parameter as there are efficiency, linearity, gamma sensitivity, spatial resolution and signal-to-noise ratio. Since fission neutrons from FRM-II are not available yet, these investigations are performed at RCM using a ^{244}Cm source emitting ca. 2.110^5 n/s. The detection efficiency is determined to (0.46(0.21)%, being clearly higher than calculated when only the converter material (^{6}LiF) is taken into account, indicating that recoil effects in the organic binder play an important role. The linearity between neutron fluence and the number of events detected by the CCD (usually expressed in greylevels) proofed to be excellent within the experimentally accessible range of about 10 n/pixel to 3.510^4 n/pixel. As the detector system will be used in a gamma field having the same order of magnitude in gamma intensity as in fast neutron intensity, the gamma sensitivity is an extremely important factor for judging the applicability of the system. Being determined to $(4.6(2.9)\times10^{-6}$ it is well suited for the intended applications. The signal-to-noise ratio is about 30 but requires validation measurements at the original measuring position at FRM-II. The intensity of the 244Cm source was not sufficient for determination of the spatial resolution, so only an upper limit by optical measurements is given. For a detection area of 30 cm$\times$30 cm, the spatial resolution will be less than 0.9 mm increasing for smaller detection areas.

With the availability of fast neutrons at FRM-II, studies for selecting an optimised scintillator screen with regard to thickness, composition etc. must be performed. Measurements with the scintillator screen using (moderated) 14 MeV neutrons at Chalmers University, Sweden, showed that it is already suited but still open for further improvements [3].

Set of collimated single beam detectors

At FRM-I fast neutron radiography and tomography was successfully performed in single beam geometry using a NE-213 scintillator in combination with a photomultiplier [4] resulting in a detection efficiency of about 30%. The applied electronics performed an excellent gamma-to-neutron discrimination and provided all information necessary for correction of beam hardening effects. Actually 4 of these single beam detectors are set up. The main challenge is the development of an automatic balancing of the detector electronics to assure that all four systems show the same spectral response function for neutrons and gamma radiation.

Manipulator for detectors

Depending on the sample and the type of investigation one of the two detector systems is selected for measurement. To avoid time consuming recalibration procedures when exchanging the detector systems, a manipulator is designed, moving the selected detector in a predefined, well calibrated position. Thus, in routine operation calibration is only necessary for quality control purposes.

Control and Evaluation System

The NECTAR facility will be controlled by a modular software package being actually under development. The modules for image reconstruction [5] and, in a preliminary version, for control of the manipulator are already existing. In its final state additional modules for control of the different detector systems, for data management and for setting up measurement procedures will complete the package. One basic goal of the development will be the user-friendliness of the program, i.e. routine operation should be performed by non-specialists. On the other hand, specialists should have access to all possibilities given by NECTAR. For the visualisation of three-dimensional data sets (e.g. tomograms) the program VGStudio MAX of Volume Graphics GmbH is available.

[1] T. Bücherl, E. Kutlar, Ch. Lierse von Gostomski, E. Calzada, G. Pfister, D. Koch, *Radiography and Tomography with fast neutrons at FRM-II: A Status Report*, Proceedings of the Fourth International Topical Meeting on Neutron Radiography (ITMNR), State College, Pennsylvania, USA, 3 - 6. June 2001.

[2] T. Bücherl, Ch. Lierse von Gostomski, E. Calzada, *The NECTAR Facility at FRM-II: Status of the Set-Up of the Radiography and Tomography Facility using fast neutrons*, Proceedings of the Seventh World Conference on Neutron Radiography, Rome, Italy, 15 -20. September 2002.

[3] E. Lehmann, G. Frei, A. Nordlund, B. Dahl, *Measurement of 14 MeV neutrons with a CCD based radiography detector system*, PSI-Report, TM-897-01-04, 19.11.2001.

[4] A. Schatz, G. Pfister, *Computer Tomography with Fast and Thermal Neutrons*, Proceedings of the Third World Conference on Neutron Radiography, Osaka, Kluwer Academic Publishers, 1989.

[5] B. Masschaele, *Octopus, a complete tomography reconstruction package*, Proceedings of the Seventh World Conference on Neutron Radiography, Rome, Italy, 15 -20. September 2002.

FRM-II: Sources

7.1 Cold Neutron Source

Erich Gutsmiedl
Technische Universität München, ZWE FRM-II

The FRM-II will be equipped with a cold neutron source (CNS). The centre of the CNS will be located in the D_2O-reflector tank at 400 mm from the reactor core axis, close to the thermal neutron flux maximum. The power of 4500 W developed by the nuclear heating in the 16 litres of liquid deuterium at 25 K, and in the structures, is evacuated by a two phase thermal siphon avoiding film boiling and flooding. The thermal siphon is a single tube with counter current flow. It is inclined by 10° from vertical, and optimised for a deuterium flow rate of 14 g/s.

Those parts of the structure, which are exposed to high thermal neutron flux, are made from Zircaloy 4 and 6061T6 aluminium. Structure failure due to embrittlement of the structure material under high rapid neutron flux is very improbable during the life time of the CNS (30 years). Double, in pile even triple, containment with inert gas liner guarantees lack of explosion risk and of tritium contamination to the environment.

Adding a few percent of hydrogen (H_2) to the deuterium (D_2) will improve the moderating properties of our relatively small moderator volume. Nearly all of the hydrogen is bound in the form of HD molecules. A long term change of the hydrogen content in the deuterium is avoided be storing the mixture not in a gas buffer volume but as a metal hydride at low pressure. The metal hydride storage system contains two getter beds, one with 250 kg of $LaCo_3Ni_2$, the other one with 150 kg of $ZrCo_{0.8}Ni_{0.2}$. Each bed can take the total gas inventory, both beds together can absorb the total gas inventory in less than 6 minutes at a pressure <3 bar.

The mounting of the hardware components of the CNS into the reactor has started in the spring of 2000. The CNS went into trial operation in 2001/2002.

Features of the CNS

The integral cold neutron flux in our CNS will be comparable to that in the vertical one at ILL although the ILL reactor runs at a power nearly three times as high. This is possible because:

- the core of the FRM-II is light water cooled and more compact
- the axis of the CNS is much closer to the core
- the flux depression in the CNS due to voids is less
- the cooling power needs can be kept small by reducing size and wall thickness of the CNS.

The centre of the CNS is so close to the core that the cold moderator volume is partly located in the thermal neutron flux maximum. At this location the epi-thermal and fast neutron flux is considerable, in spite of the light water cooling of the core. The moderator fluid therefore has to absorb a high specific heat load of up to 4 W/g, leading to a high bubble content and a strong internal fluid circulation.

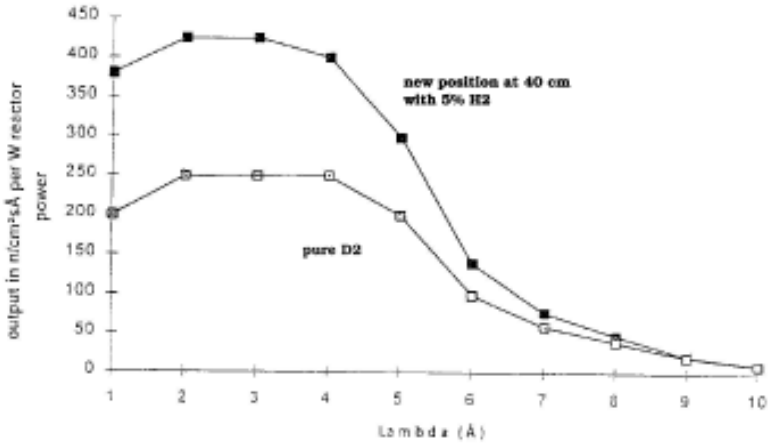

Figure 7.1: Neutron Flux at a Point Detector in the Beam Tube at 4m.

In order to keep the refrigeration needs below 5 kW, the mass of the cold moderator fluid has been limited to 2000 g, of which about 100 g will be hydrogen, the rest deuterium (D2). This is a possible mixture to adapt the mean free path of the neutrons to the vessel dimensions. The optimum concentration of hydrogen will be determined during the first tests with reactor power.

Although the total integral neutron flux in the CNS is about the same as at the ILL vertical CNS, the spectral distribution will be much flatter between 1 and 4 Å, emphasising the thermal part of the spectrum (Fig. 7.1). This can be of some advantage for cold neutron users.

In spite of the fact that nowadays very exact and detailed data for zircaloy are available [1], the lack of knowledge about the hydrogen diffusion into zircaloy under radiation at low temperature, and consequently about the risk of embrittlement in a zircaloy wall of the moderator cell, led to the decision to use the aluminium alloy Al-6061 T6 instead. This strong alloy shows no important embrittlement during the projected life time of our reactor. A mean wall thickness of only 1 mm is sufficient for withstanding a 6 bar overpressure inside the moderator cell.

During a normal operation cycle the maximum overpressure in the deuterium system should not occur when the moderator cell is warm. This will be achieved by chemically storing the warm moderator fluid (gas) as a metal hydride in the two getter beds. The D_2 storage capacity is about 1 to 2% weight, depending on the pressure. Each getter bed can store the total inventory of gas on its own.

Additional advantages of such a metal hydride storage system :

- the total deuterium inventory is only about 60% of a CNS with gas buffer
- during reactor stop the in-pile system is always empty of hazardous gas
- the whole (later tritium-activated) gas inventory can be shipped as compact solid nuclear waste for retreatment or underground storage
- the isotopic mixture does not change its concentration with time due to fractional distillation, because there is no buffer volume.

The vacuum vessel of the in-pile part will be made from zircaloy, the moderator cell and tubing from the aluminium alloy 6061 T6. The insert, which optimises the geometry of the cold moderator volume, will be made from magnesium. The deuterium condenser has a 10 m^2 heat-exchanger area made from aluminium tubing. Bi-metallic junctions (Al/stainless steel) are used at the 25 K level in different places to take advantage for thermal insulation from the low thermal conductivity of the stainless steel. The in-pile part will be connected to the gas handling system via flexible stainless steel tubing

throughout in order to guarantee vibrational decoupling of the in-pile part to the rest of the reactor building in case of an external shock (e.g. earth quake or air craft accident).

The main feature of the gas handling system is the double containment of deuterium throughout. All vessels and tubes, including the metal hydride storage tanks, which do (or could eventually) contain D_2, are surrounded be at least one envelope containing pure nitrogen as an inert gas at a pressure slightly higher than ambient. Such a system allows a continuous leak testing and makes impossible the build-up of an (explosive) D_2-air mixture. Also, the vacuum exhaust pipes are connected to a tritium monitor to detect traces of (later activated) D_2 which could have leaked into the insulation vacuum.

The refrigerator has to move 5 kW of nuclear radiation heating away from the cold source at the 25 K temperature level. It can be upgraded to 8 kW refrigeration power by adding an extra compressor and further expansion turbines, in case of additional needs of refrigeration near the reactor core (e.g. for a second CNS). The actual compressor will need about 500 kW of electrical power to deliver about 300 g/s of helium at 16 bar.

Status of the CNS construction

Monte Carlo simulations with the MCNP-4A codes to optimise the moderator shape and position, and to estimate the heat load, have been completed [2]. The general contractor, Linde AG, Germany, is responsible for the construction of the 4 main components of the CNS, i.e. the in-pile part, the gas handling, the metal hydride storage system, and the refrigerator. Main subcontractors are ACCEL GmbH for the in-pile part, HYCOB GmbH for the metal hydride storage system, and Linde Kryotechnik (CH) for the refrigerator.

Two rooms on the 11.70 m floor of the reactor building are dedicated for the CNS cold box, gas handling and control desk. Additional floor space is foreseen inside and near the compressor building. All the buildings are erected now, and the mounting of the hardware has completed. First test operation started in 2001/2002 and will be finished in early spring 2003.

[1] Scheuer, A., E. Gutsmiedl : *Use of Zircaloy 4 material for the pressure vessels of cold and hot neutron sources and beam tubes for research reactors*, IGORR 7 Meeting, Argentina

[2] Gaubatz, W., K. Gobrecht, *The FRM-II Cold Neutron Source*, Physica B, **276-278**, 104 (2000)

7.2 Hot Neutron Source

Christian Müller, Erich Gutsmiedl
Technische Universität München, ZWE FRM-II

Design of the HNS

The FRM-II will be equipped with a hot neutron source. This secondary source will shift a part of the thermal neutron energy spectrum in the $D-2O$ moderator to energies from 0.1 to 1 eV. The hot neutron source consists of a graphite cylinder (200 mm ∅, 300 mm high) with a density of 1,82 g/cm^3, which is heated by gamma radiation up to a maximum temperature of

about 2400°C. The volume of graphite cylinder is approximately 10 dm^3. Apart from well known behaviour in high irradiation fields, graphite as moderator material was also chosen because of its ability up to 2800°C in inert-atmosphere.

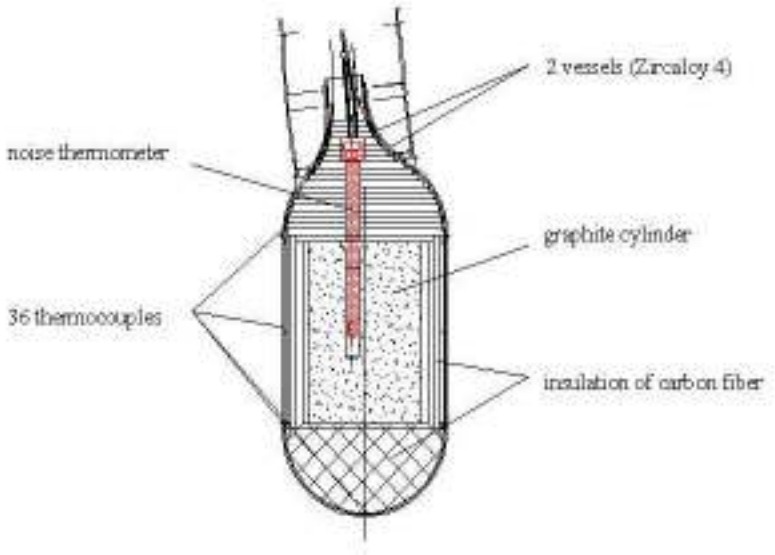

Figure 7.2: Hot neutron source vessels with graphite cylinder and insulation.

The graphite cylinder is surrounded by a high-temperature insulation of carbon fiber, to achieve this high temperature. We have accomplished mock-up tests of the carbon fiber in a high temperature furnace, to investigate the insulation properties of the material. The graphite cylinder and the insulation are covered with two vessels made out of Zircaloy 4. The space between the vessels is filled with helium. The hot neutron source is permanent under control by pressure and temperature measurements. The temperature inside the graphite cylinder will be measured by a purpose-built noise thermometer due to the extremely harsh environment conditions (temperature and nuclear radiation). The hot neutron source is designed and manufactured according to the general specification basic safety and to the German nuclear atomic rules (KTA). The source will be completely installed in early spring of year 2003.

The graphite cylinder will be heated by the nuclear radiation of the reactor core up to high temperatures. Therefore, complex electrical system necessary for heating can be avoided. The temperature of the graphite cylinder depends on the gas filled in the vessel. On a first calculation the temperature can be varied between 2000°C and 2400°C using helium, neon or by evacuating the vessel. There are no problems with helium and neon due to neutron activation.

A schematic cut showing the graphite cylinder, the high thermal insulation and the source vessels is given in Figure 7.2.

There are no problems of incompatibility between insulation and moderator at high temperature because they are the same material. However, graphite reacts at moderately high temperatures with oxygen (in air) and water. Therefore, the graphite cylinder and the insulation are double contained within two independent vessels. Each vessel of 3 mm thickness is manufactured out of Zircaloy 4. The diameter of the outer vessel is about 300 mm. The small space between the vessels will be filled with helium of 3 bar and permanently controlled. Hence there are two barriers which will safely separate the hot graphite cylinder from air and water.

Figure 7.3 shows all parts of the HNS in the reactor pool. The in-pile section is tilted 5° against the vertical axis and is located in the D_2O - reflector tank. The hot moderator in the in-pile section has a distance of 420 mm from the reactor core axis and is close to

the thermal neutron flux maximum.

The external instrument container is also placed in the reactor pool. All necessary valves, pressure gauges and an ion pump are located in the external instrument container. Instrument container and in-pile section are connected by tubes.

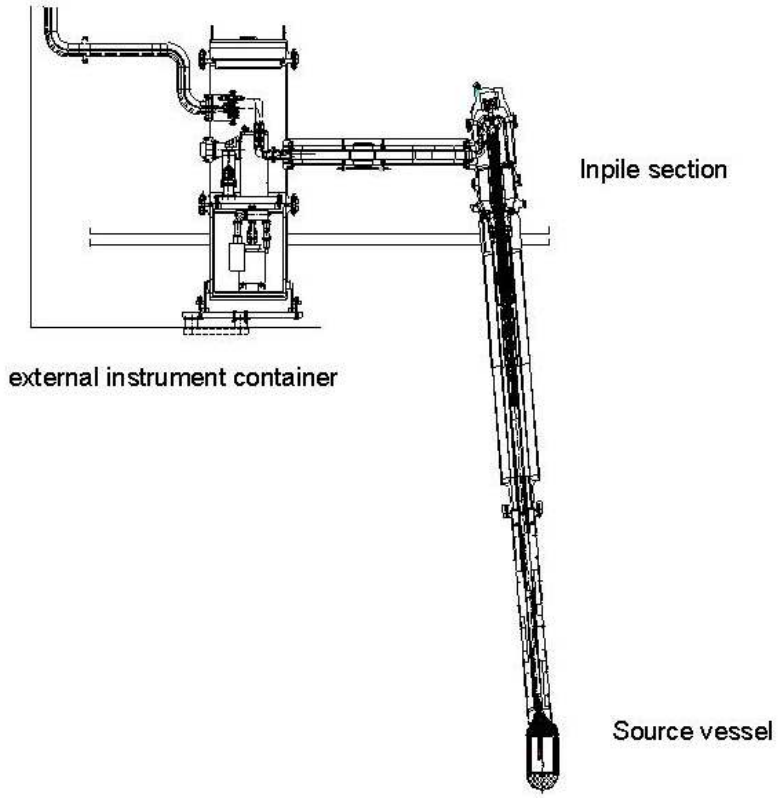

Figure 7.3: In-pile section and the external instrument container of the HNS

The remaining instruments, the gas supply and the control system of the HNS are placed outside of the reactor pool.

Instrumentation

All pressures and temperatures of the HNS are measured and monitored permanently. Differences to normal pressures are registered and reported. If a leakage in one of the vessels occurs, the reactor will be shut down automatically. There are 36 chromel-alumel thermocouples spread over the inner vessel (fig.7.2), which will control the wall temperature. All temperatures above 200°C will lead to a shut down of the reactor.

It is quite difficult to measure the temperature in the graphite cylinder due to the extremely harsh environment conditions e.g. high graphite temperature, chemical reactivity and nuclear radiation. Under these conditions thermocouples and pyrometer are not suitable. Therefore a noise thermometer is installed to measure the temperature in the hot graphite cylinder (fig. 7.2). The noise thermometer is a contact thermometer and is not affected by changes of the sensor. This thermometer measures the white noise of an electrical resistance and determines the absolute temperature [1]. The noise sensor, built of graphite, was developed and tested at the Technischen Universität München. The data acquisition system for the noise thermometer is delivered from the Forschungszentrum Jülich, ZEL - Germany.

Mock-up Tests

Calculation with finite element method were made to get the temperature distribution over the HNS. Also thermal stress analysis was done to find condition for burdening of the source vessels. Apart form theoretical calculation we have accomplished mock-up tests in a high-temperature furnace. The furnace is purpose-built to investigate properties of carbon fiber insulation and the

graphite cylinder. The furnace consists of two vessel of stainless steel. The space between the vessels is water cooled. The inner vessel contains a graphite block and the carbon insulation. The graphite block and the insulation consist of the same materials and have the same sizes as in the real HNS. Hence, the tests are comparable to the HNS. The furnace is heated electrically by a graphite heater and reaches temperature values up to 2300°C.

Both results of the mock-up tests and the finite element calculations are quite good. The agreement between experimental and theoretical results is satisfying.

The mounting of the hardware components of the HNS into the reactor facility will be finished in early spring of 2003. After this the test operation phase will begin.

[1] Brixy, H.: "Noise Thermometers" in: Sensors , Vol.4, VCH Verlag, 1990, Chapter 6

7.3 Experimental Facilities at the Intense Positron Source

C. Hugenschmidt[(1)], G. Kögel[(2)], R. Repper[(1)], K. Schreckenbach[(1)], P. Sperr[(2)], B. Strasser[(1)], W. Triftshäuser[(1)]

[(1)] Physik Department E 21 und FRM-II, Technische Universität München, D-85747 Garching
[(2)] Institut für Nukleare Festkörperphysik, Universität der Bundeswehr München, D-85577 Neubiberg

Positron Source

At the new Munich research reactor FRM-II an in-pile positron source based on neutron capture is installed. After thermal neutron capture in cadmium the absorption of the released high-energy γ-radiation in platinum generates positrons by pair production [1]. The positron source is placed in the tip of the declined beam tube SR11 at FRM-II. The design of the source is schematically shown in figure 7.4. Inside the tip of the beam tube a cap of cadmium (∅=11 cm, l=9.5 cm) is encapsulated in aluminium. Besides the function as γ-source after neutron capture, cadmium is a perfect shielding for thermal neutrons. Consequently, it also protects inner source components from neutron activation. The inner part of the source consists of a honeycomb structure at the tip and rings of platinum acting as converter and positron moderator. Electrical acceleration lenses and magnetic coils are

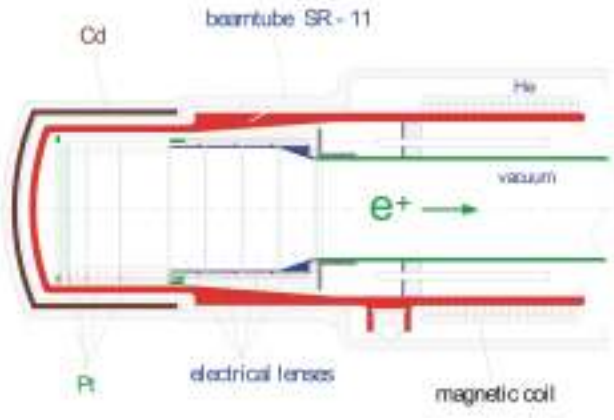

Figure 7.4: Cross-sectional view of the in-pile positron source at FRM-II.

used for beam formation. The source is placed at a position where the calculated unperturbed thermal neutron flux amounts to 2×10^{14} n/cm^{2}s. Taking into account the neutron capture rate, the absorbing mass, the geometry, the moderation efficiency, and a recent test run at an external neutron beam at the ILL high flux reactor in Grenoble [2], an intensity of the order of 10^{10} slow positrons per second in the primary beam is expected.

Experimental Facilities

The beam line guides the positrons to an experimental platform where it will be connected via a beam switch to three experiments: A pulsed low energy positron beam system (PLEPS) [3], a scanning positron microscope [4] and a facility for positron annihilation induced Auger electron spectroscopy (PAES) [5].

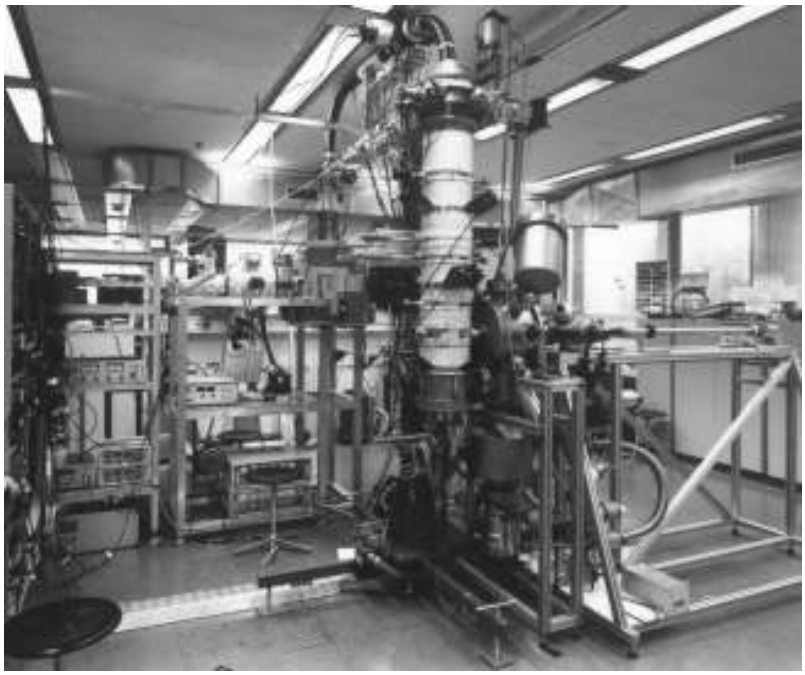

Figure 7.5: Pulsed low energy positron beam system (PLEPS) under operation at the university of the Bundeswehr in Munich.

The PLEPS and the positron microscope were constructed and built at the university of the Bundeswehr in Munich (figs. 7.4 and 7.5). At present, both facilities are under operation with ^{22}Na positron sources with beam intensities up to 10^3 positrons per second. In order to get depth dependent information from the surface to the bulk of the material, the positron energy can be varied from a few 100 eV up to 18 keV. The lateral resolution is about 3 mm at PLEPS and less than $10\mu m$ at the microscope. The PAES facility was built at E21 at TUM and is designed for extremely sensitive studies in surface science [5]. The Auger process is usually initiated by photo- or impact ionisation of core electrons by irradiation with X-rays or keV-electrons. An alternative technique to induce core shell ionisation is the annihilation of core electrons

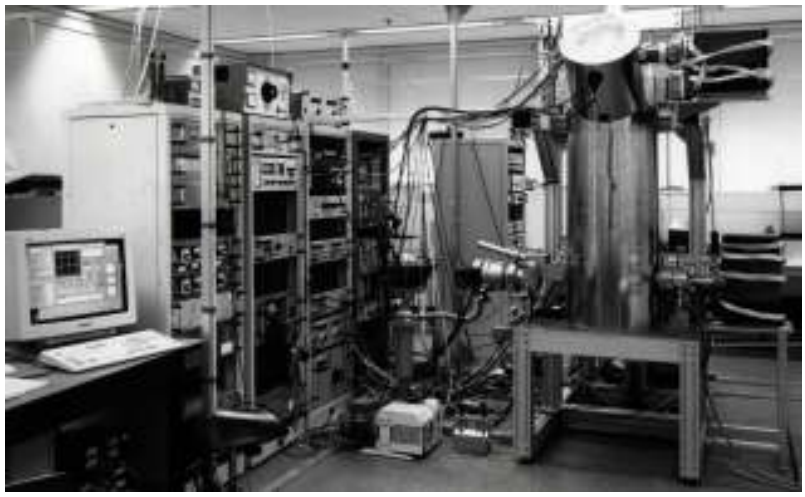

Figure 7.6: The scanning positron microscope under operation at the university of the Bundeswehr in Munich.

electrons with slow positrons. Due to the low positron energy of some 10 eV, no background of secondary electrons is produced in the higher energy range of released Auger electrons. Besides this advantage, PAES is an exceptionally surface sensitive technique since most of the implanted positrons annihilate with electrons of the topmost atomic layer. In first experiments on polycrystalline copper the spectrometer was tested and optimised with a low intense positron beam at TUM.

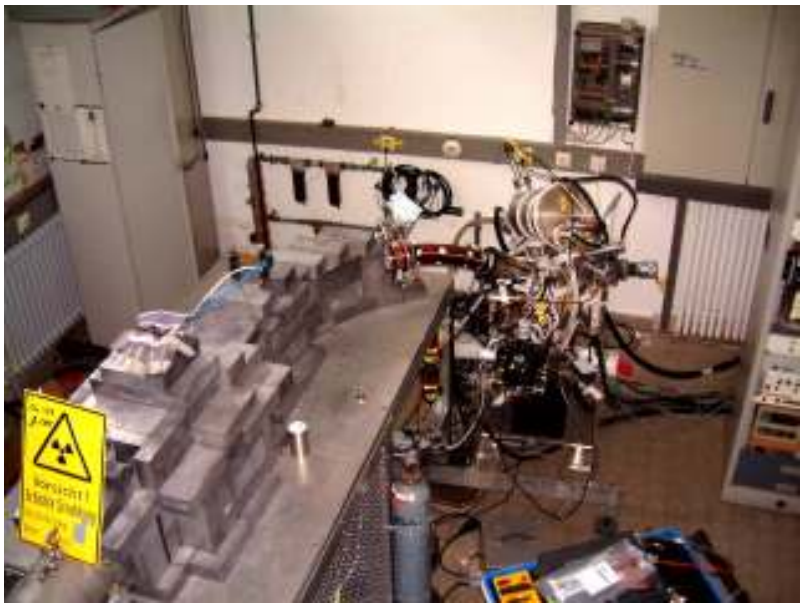

Figure 7.7: Facility for positron annihilation induced Auger electron spectroscopy (PAES) at E 21, TUM.

[1] C. Hugenschmidt, G. Kögel, R. Repper, K. Schreckenbach, P. Sperr, B. Straßer, and W. Triftshäuser; Appl. Phys. A **74**, 295 (2002)

[2] C. Hugenschmidt, G. Kögel, R. Repper, K. Schreckenbach, P. Sperr, and W. Triftshäuser; Nucl. Instr. Meth. B **198**, 220 (2002)

[3] A. David, G. Kögel, P. Sperr, and W. Triftshäuser; Phys. Rev. Lett. **87**, 067402 (2001)

[4] W. Bauer-Kugelmann, P. Sperr, G. Kögel, and W. Triftshäuser; Mat. Sci. For. **363-365**, 529 (2001)

[5] B. Straßer, C. Hugenschmidt, and K. Schreckenbach; Mat. Sci. For. **363-365**, 686 (2001)

7.4 Converter Facility

Wolfgang Waschkowski
Technische Universität München, ZWE FRM-II

At up to date neutron sources the beam tubes pass the fuel element tangentially. That means there are practically no possibilities for experiments in the epithermal (1–100 keV) and the fast (0.8–4 MeV) energy range. This gap can be closed by the converter facility (SKA) at FRM-II. It produces a large (20 cm$\times$30 cm) and intense (1.5×10^9 n/cm^{2}s) beam of reactor fission neutrons for the following applications and experiments:

Medical applications

- Therapy of surface near cancer to support other percutaneous therapy.
- Development of boron capture therapy.

- Research on biological dosimetry and on metabolism processes.

Technical applications

- Radiography and tomography on technical samples.
- Irradiation on samples with fast reactor neutrons.
- Supply of a standard source of a quasi-fission spectrum.
- Source with quasi-monoenergetic neutron spectra at epithermal energies.

Physics

- Determination of strength functions.
- Experiments to examine the optical nucleus model.
- Experiments on p-, d-scattering.

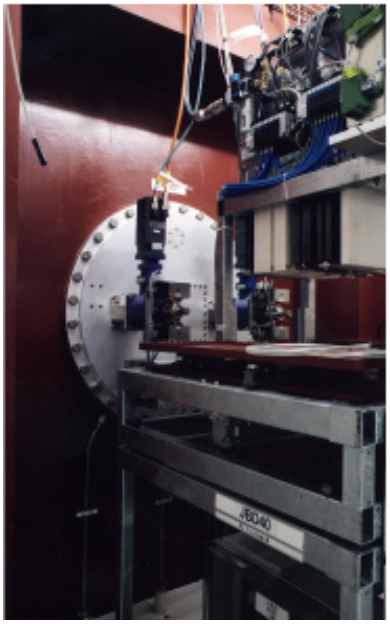

Figure 7.8: Filter bench of the converter facility outside the beam tube.

The converter facility consists of the shaft with cooling system located in the heavy water moderator vessel and the beam tube with an insert and redundant shutter components. The irradiation rooms are located outside the reactor pool (pool wall recess, medical irradiation room (fig. 7.9), room for technical and physical experiments). The control desk is installed in the experimental hall, outside the irradiation shielding. For the medical treatment a filter bench (variation of the spectrum see fig. 7.8), a light sight (for adjustment), a multi-leaves collimator (beam geometry), a patient couch and a beam catcher were installed. All components are manufactured, installed and checked, with the exception of the filling material of the beam catcher. The collimator will ready within the next months.

Similar to other secondary neutron sources the converter facility is subject to examinations by the safety standards authority (TÜV). To obtain the official approval four reports were reworked and in final version submitted.

Two converter plates were produced under special specification by CERCA, France and accepted by safety standard authority. Installations for changing the converter plate arrangements and for storage of burned down plates were manufactured and installed at the storage part of the reactor pool. The container for transportation of new plates was granted from official side. Several tools for handling new and burned converter plates were ordered.

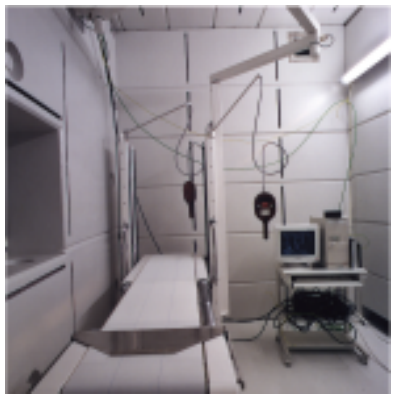

Figure 7.9: Medical application room.

After realisation of the storage programmable control system (SPS) the starting process could be finished in the phase F1 and F2. That means, no open subjects does exist anymore in the permission documents. From safety standards authority the conformation "as build" has been given. At the moment the chapters for returning tests (WKP) are written.

Medical applications

To carry out irradiation on humans the device must be approved concerning the medical product law and must obtain a CE-certification. Also the requirement of industrial safety (Arbeitsschutz) have to bee fulfilled. Therefore six reports had to be written at final version in 2002 which were approved by the safety

standards authority. A special group of authority (TÜV Product Service) has examined all technical components, circuit diagrams, logic systems of the electronic control system (SPS) in the working modes "technique" and "test".

There exist accompanying side rooms as patient entrance, waiting room, lavatory room for handicapped persons, recovery room and changing cubicle. These rooms were completed with installations and furniture.

7.5 Irradiation Facilities

H. Gerstenberg[(1)], X. Li[(1)]
[(1)]ZWE FRM-II, TU München

The FRM-II will be equipped with various irradiation facilities. Due to the different tolerable sample volumina, neutron flux densities and obtainable neutron fluences they allow in their entirety a broad scope of possible applications in basic and applied science.

In particular during the nuclear start-up phase of the FRM-II the following facilities will be available:

- a pneumatic rabbit system,
- a hydraulic rabbit system,
- a test-rig for a silicon doping facility,
- a pneumatic rabbit system for prompt transport of irradiated samples into the neighbouring institute for radiochemistry.

In addition at least a high speed pneumatic rabbit system will be added in the future.

All of the irradiation positions are located within the heavy water moderator tank and can be loaded and unloaded during reactor operation. A major advantage of these irradiation positions is the availability of a very pure thermal neutron field. Thus parasitary threshold reactions by fast neutrons and the production of large clusters of irradiation defects are suppressed effectively.

The **pneumatic rabbit system** serves typically for the activation of samples for neutron activation analysis. The pneumatic devices are operated by carbon dioxide gas in order to avoid the production of radioactive Ar-41 during the irradition of air. The facility is composed of 6 independent irradiation channels being identical except for the vertical position within the moderator tank. Consequently the neutron flux densities in the positions vary between $5 \times 10^{12} cm^{-2} s^{-1}$ and $2 \times 10^{14} cm^{-2} s^{-1}$ and the appropriate irradiation position can be choosen to fit the individual task. For radiation protection reasons the entire handling takes place in a room being exclusively used for this facility. Irradiation times can be choosen between about 20s , i.e a significantly longer times compared to the transport time of the rabbits of a few seconds, and 5 hours. The maximum irradiation time is limited by the use of polyethylene rabbits as outer irradiation package. After irradiation the sample is first transported into a shielded decay position where the induced gamma dose rate is measured. Finally it is transported back into the handling room where it is either removed from the irradiation facility by remote handling tools or alternatively sent directly to the institute for radiochemistry via a connected rabbit system.

In contrast to the penumatic system the **hydraulic rabbit system** will be used for long term exposure or the irradiation of larger sample volumina up to approximately $35 cm^3$. Consequently the samples are contained in

Al rabbits during irradiation, which however are perforated in order to guarantee the cooling of the samples by pool water during irradiation. If necessary the direct contact between sample and pool water is avoided by the use of sealed quartz ampoules or small welded inner Al containers. The facility offers 2 independent identical irradiation channels each of which can be loaded by up to 5 rabbits at the same time. The driving medium of the facility is reactor pool water. The neutron flux densities have been calculated to be about $4 \times 10^{14} cm^{-2} s^{-1}$. Since rather high activities will have to be handled in the hydraulic rabbit system, most of the handling procedures in particular the receipt of irradiated samples and the measurement of the induced gamma dose rate is done remotely under water about 3.5 m below the reactor pool level. In addition also the loading of the samples into lead shielded transport containers takes place under water.

The **silicon doping facility** will serve for the P doping of the semiconductor Si by means of the nuclear reaction Si-30 (n,γ) Si-31 -$\beta^- \rightarrow$ P-31. This so called neutron transmutation doping offers the most homgeneous doping profile being necessary particularly in high power electronic components. In order to fulfil the requirement of homgeneity, however, it is of crucial importance to guarantee a smooth neutron flux density over the entire volume of the Si ingot. Therefore the ingot is rotated during irradiation and the irradiation position has to be equipped with a specially shaped absorber to guarantee a constant neutron flux density along the axis of the ingot. During the nuclear startup phase a simplified setup will be used to determine experimentally the exact shape of this absorber to be made from Ni. Once the absorber profile will be known the final Si doping facility offering a semi automatic operation will be completed. It will be suitable for Si ingots with diameters of up to 200 mm and a capacity of several tons per year.

Facilities

8.1 Detector and Electronics Group

K. Zeitelhack(1), A. Kastenmüller(1), D. Maier(1), M. Panradl(1)
(1)Technische Universität München, ZWE FRM-II

A proper and coherent choice in the design of detector systems as well as measurement & control electronics is essential for the performance and efficient maintenance of the scientific instruments. As both issues are closely related, a joint Detector and Electronics Laboratory (DEL) comprising a staff of 4 members has been established as part of the general scientific infrastructure. It is aimed to assist the instrument scientists in design, purchase and test of detectors, measurement & control electronics and DAQ-hardware. In addition, it developes specific devices adapted to the individual requirements of each instrument.

Laboratory Infrastructure

Since its formation 2 years ago the group's main task was to establish suitable laboratory infrastructure and to provide measurement & test equipment necessary during the installation phase of the instruments. Located within the neutron guide hall 3 different labs dedicated to the specific fields of electro-mechanics, electronics and detectors were installed.

Figure 8.1: View into the clean room area of the detector lab

Lab 1 is equipped with a small workshop and the tools necessary for electromechanic tasks. The scope of duties covers a broad range from cable assembly to the production and test of complete systems for detector and instrument control. In addition, a large stock of electronic components available to all instrument staff has been established.
The second lab is dedicated to the development and test of control and readout electronics. It is equipped with all tools necessary for the design & handling of modern printed circuit boards (e.g. SMD-technology). Mandatory test environments with associated measurement devices (e.g. oscilloscopes, logic analyzer) have been provided. Test setups for FRM-II standard devices (e.g. motion control, cPCI-data acquisition, ^{3}He-detector supply) have been installed. In addition, the lab contains a complete measuring station for neutron detectors including a moderated ^{252}Cf-fission source and a versatile CAMAC-based multiparameter data acquisition system.
Finally, the third lab is dedicated to the maintenance and developement of detectors. Besides a small working area the lab contains a clean room area to assure for the production of detectors under well defined conditions. Fig. 8.1

shows a view of the clean room equipped with laminar flow work benches and a combined fume cabinet. However, completion and commissioning of the lab had to be halted for reasons coupled to the missing operating approval of FRM-II.

Figure 8.2: Remote controlled Bias and HV-power supply system with ratemeter for ^{3}He- and monitor detectors

Detector Equipment

For most of the neutron scattering instruments the detector & electronics group took care of the purchase and test of ^{3}He-detectors and monitors. In close collaboration with Eurisys-Mesures (France) an improved version of squashed series ^{3}He-detectors was developed for the time-of-flight spectrometer ToF-ToF. Several prototype detectors using ^{3}He/CF_4 mixtures as filling gas with total pressure up to p = 10 bar were investigated at FRM-II, HMI-Berlin and FZ-Jülich. At present, the acceptance test of 600 squashed series type 120 NH 40 RTF detectors (^{3}He/CF_4 = 97/3 %; p = 10 bar) already delivered is in progress.

Instrument Control and Readout Electronics

In the meantime several projects have been realized or are in work. Part of the Intense Positron Source beamline slow control (vacuum & dosimetry interlock, magnet power supply control) or the remote controlled bias and HV-power supply system of the ToF-ToF detectors are a few of them to mention. On behalf of DEL an amplifier/w-discriminator unit (MRS 2000) with variable gain and selectable shaping time has been developed by mesytec GbR (Germany). It is used as standard frontend for single ^{3}He-detectors and monitors.

Based on 19”-technology a standard bias and HV-power supply system including a 2-channel ratemeter was developed for those instruments which use only a small number of neutron detectors. Via RS232/RS485 interface the system shown in fig. 8.2 allows the remote control of 2 HV-power supplies (ISEG EHQxxx), readout of the ratemeter and status

Figure 8.3: Multi channel 32-bit counter module (on PCI- and cPCI-carrier) based on M-module technology

control of bias voltage ($\pm$24 V; $\pm$12 V; $\pm$6 V) and crate temperature. System control via FRM-II standard instrument control software TACO or LabView is in progress.
For neutron scattering instruments using CompactPCI bus systems for instrument control and data acquisition a versatile multi-channel counter module for detector and monitor readout had to be designed. For universality reasons the design was based on the M-module technology (men mikro-elektronik, Germany) resulting in a board available as ISA-, PCI-, cPCI- and VME-version (see fig. 8.3). The basic design carries 4 optocoupled 32-bit counters and two I/O channels. Each counter can individually be set as master/slave and operated in absolut, preset, timer or ratemeter mode. The modules are supported by the instrument control software TACO. A special design in progress which carries eight 32-bit counters and an increased number of I/O channels allows for time-resolved multi channel counting at the 3-axis spectrometer Puma.

Summary

The detector and electronics group has established the laboratory infrastructure necessary for maintenance and development in the fields of detectors, measurement & control electronics and DAQ-hardware. First projects - e.g. a multi-channel counter cPCI-board - have been realized successfully. Besides assistance of the instruments during commissioning intensified efforts in the development of detectors and readout electronics are planned in future.

8.2 Sample Environment

J. Peters[(1)], H. Kolb[(1)], A. Schmidt[(1)], A. Pscheidt[(1)], H. Niedermeier[(1)], S. Sedlmair[(1)]
[(1)] Technische Universität München, ZWE FRM-II

The sample environment group at FRM-II was established in July 2000. Starting with two, the sample environment group now comprises six members. The very first activities were the build-up of an adequate laboratory infrastructure, covering both the needs of the group itself and the demands on user service facilities.

Laboratories

In particular the laboratory for low temperature applications, the laboratory for high temperature and high pressure applications and a vacuum laboratory were planned and well equipped. All laboratories are located in the Neutron Guide Hall.

The vacuum laboratory comprises a semi-automatic filling facility for liquid nitrogen. Safety precautions such as automatic filling stop, gas warning system and air extraction system are obeyed. The facility allows parallel filling of two 100 liters LN-storage vessels. To expand storage capacities an intermediate floor was installed. A variety of

Figure 8.4: Cryogen Free Sample Tube Refrigerator

prevalent vacuum components are in stock like flanges, fittings and valves etc. accessible to instrumentalists and users. Other vacuum hardware like pumping and leak detection systems can be lent. Service facilities comprises a laboratory for general sample preparation and a mechanical workshop.

The Sample Preparation Laboratory provides at least chemistry facilities including, precision balance, fridge, purified water supply and an inert gas glovebox with fridge, microscope. For internal reasons, some installation work is put on hold until commissioning the FRM-II.

For any necessary adjustments of smaller mechanical components a fully equipped workshop is available for users and instrumentalists. The workshop is located in the Neutron Guide Hall. Besides prevalent hand tools the workshop is equipped with a CNC- and a manual milling machine, NC-lathe and drilling machine.

Low Temperature Equipment

For low temperature applications, a cryogen free Sample-Tube Cryostat was developed in close cooperation with the companies Vericold (Pulse Tube Coldhead) and CryoVac (Dewar). Low temperatures are achieved by a Pulse Tube Coldhead providing 0.4 W @ 4 K. The diameter of the sample tube is 50 mm. Specific features are easy handling, no use of cryoliquids, rapid sample exchange and the operation of ^{3}He, ^{3}He/^{4}He dilution inserts, respectively.

Figure 8.5: ^{3}He-Insert

The prototype is in operation since August 2001, the performance is in very good agreement with the specifications. A second device with improved compact design and performance comes into operation end of 2002.

Furthermore a ^{3}He-cryostat insert designed for operation in the Sample-Tube Cryostat was developed and constructed at FRM-II as well as the appropriate TACO controlled handling system. The performance tests were successful. In cooperation with the Walther Meissner Institute, Garching, ^{3}He/^{4}He dilution inserts are under construction.

10 T Magnet

Based on specifications developed by the sample environment group an order was placed to ACCEL for a cryogen free superconducting Split Coil Magnet. The magnet provides a guaranteed vertical symmetric magnetic flux of 10 T, a split of 30 mm and a room temperature bore (RTB) of 99 mm. The large diameter of the RTB allows for the operation of other environment variables like high pressure, low temperatures (the sample tube refrigerator fits to the RTB) or chemical reaction cells. The detailed design is now in progress in close cooperation between ACCEL

and the sample environment group.

High Temperature Furnace

For high temperature applications, a furnace with appropriate system control was developed. Based on resistive heating, the Nb heating element combined with 5 Nb radiation shields yields in an upper temperature limit of 2250 K. System Control is accessible via TACO. Three additional similar furnaces are now under construction.

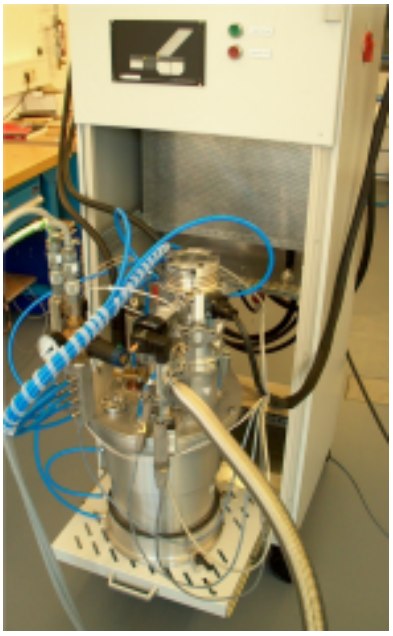

Figure 8.6: High Temperature Furnace.

8.3 Progress Report on the Neutron Guides of FRM II

Ch. Schanzer[(1)], E. Kahle[(2)], G. L. Borchert[(2)], D. Hohl[(3)], S. Semecky[(4)]
[(1)] Physikdepartment E 21, Technische Universität München
[(2)] ZWE FRM-II, Technische Universität München
[(3)] D. Hohl, Technische Dienstleistungen, München
[(4)] S. Semecky, Kommunikationstechnik, München

The realization of modern type neutron guides (NG) at high flux neutron sources gives access to a new kind of high resolution experiments. They offer the unique combination of well-collimated, even highly polarized, high intensity neutron beams in a low background environment. Hence the new research reactor FRM II of the Technische Universität München is being equipped with a large number

Figure 8.7: The 6 NG lines NL1 to NL6 starting at the six-fold shutter system

of such devices.

The final quality of these NG depends both on the performance of the mirrors and the precision of the mechanical adjustment. The former has been adapted to the requirements of the individual experiments at the end of the corresponding beam-line.

For the latter we have realized the following tolerances:

- Maximum displacement of each two consequent NG elements at the joint less than 10 μm, at exceptional complex positions less than 20 μm, in the horizontal and vertical dimension.
- Angular mismatch with respect to the reference direction less than 15 arcsec in the horizontal direction.
- Angular mismatch with respect to the reference direction less than 45 arcsec in the vertical direction.

Figure 8.9: The NG NL6 entering the NG hall. Shown are the supporting construction of the neutron line and the optical elements with their adjustment frames. The final lead cover has not yet been mounted.

In the inferior section 0 all 9 NG have been completed, i.e. installed inside the beam tubes, optically adjusted and leak tested. In section 1 there are 12.5 m of SR8a for SPODI, 9.5 m of SR8b for RESI, SR2 and the 6 NG of the main system, starting at the beam port SR1. These 6 NG including 2 switches have been completed as well in the tunnel area, see fig. 8.7 and fig.8.8.

Figure 8.8: The 6 NG lines NL1 to NL6 passing through the tunnel area. Along the vacuum tubes joints, windows and adjustment elements are visible.

As for the continuation in the NG hall all mechanical supports for the main NG have been mounted and adjusted. Within the casemate area of section 2 about 50% of the optical elements of the beam lines have been installed and adjusted. At the passages through the reactor wall additional mechanical constructions had to be produced and mounted and were certificated

by TÜV. For the SR1 system the following parts of the beam-lines have been installed:

As an example, details of neutron guide NL6 are shown in fig. 8.9 and fig. 8.10. In total, about 100 optical NG elements have been installed, adjusted and leak tested, corresponding to a total length of about 200 m. During the first quarter of 2003 the remaining optical elements will be mounted, so that the final completion can be expected before April 2003 in case no additional requests from the experiments or from TÜV will be raised.

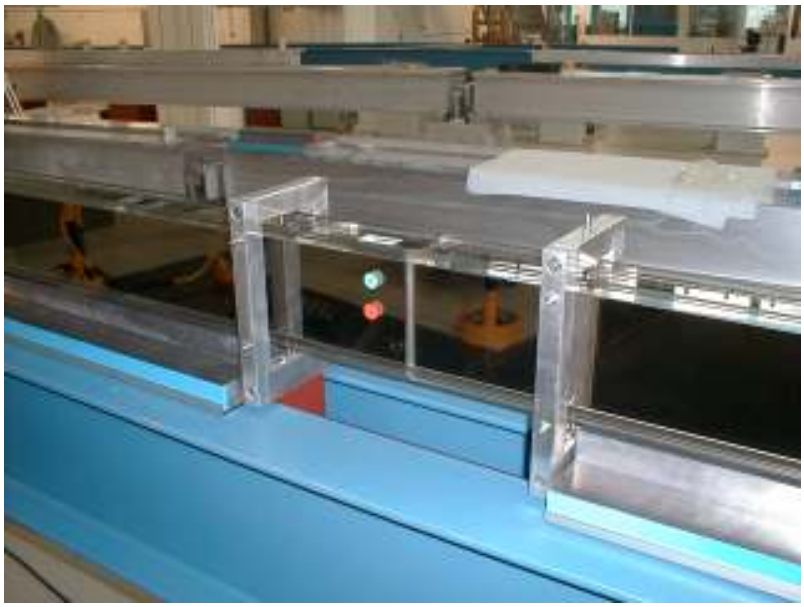

Figure 8.10: Details of the NG NL6. The figure shows the joint of two optical elements with the corresponding adjustment frames. Between optical elements and the mechanical support the bottom lead shields have been introduced.

Neutron guide	**length**	**elements**	**remarks**
NL1, A1	16,5 m	8	
NL2, A1	24,5 m	12	including switch NL2a, NL2b
NL3, A1	20,5 m	10	including switch NL3a, NL3b
NL4, A1	16,5 m	8	
NL5, A1	16,5 m	8	
NL6, A1	16,5 m	8	
NL4, A2	19 m	10	
NL5a, A2	6 m	3	
NL6a, A2	27 m	14	
NL6b	6 m	5 elements	including switch

Table 8.1: Overview of the neutron guide system.

Fabrication of Supermirrors

Ch. Breunig, A. Urban, G. Borchert
ZWE FRM II, Technische Universität München

The research reactor FRM II of the Technische Universität München as a modern high flux neutron source will be equipped with neutron guides which brings collimated and even polarized neutron beams in a low background environment. These neutron guides consist of glass plates the surfaces of which are covered by a multiplayer system for the interference of the neutron waves. The glass plates are arranged to form a rectangular tube which guides the neutrons in horizontal and vertical dimensions.

Production technique

In a first step the glass plates undergo a careful surface preparation procedure. It includes ultrasonic cleaning, tempering, and a glow discharge process before the deposition starts. The multilayers are produced by magnetron sputtering. Deposing several alternating Ti and Ni layers with increasing thickness yields a structure that causes the neutron waves to interfere. This leads to an increased reflection angle range and thus to increased intensity. For example, a mirror with 100 bilayers yields an angular enlargement by a factor 2.5 (m=2.5) of the total reflection angle of Ni. For each mirror reflectivity and adhesion of multilayers are checked.

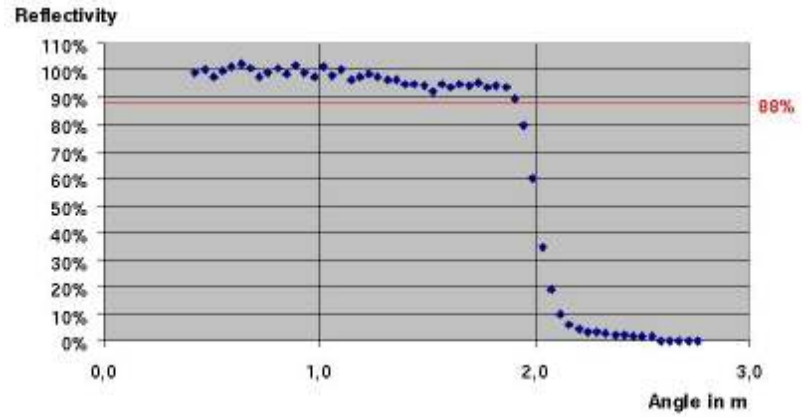

Figure 8.11: Reflectivity of a typical supermirror with m=2.0

The thickness of the deposited layers is in the range from 20 up to 800 Å. In our sputtering machine it is possible to produce supermirrors up to a size of 220mm by 1000mm. Sofar the maximum performance factor of our machine is m=2.5. For a supermirror with a larger m many more bilayers are necessary which imposes more stringent conditions on layer homogeneity and surface roughness. By a modification of our machine in the next future we expect to increase the performance to higher m.

Production Progress

Totally the reactor facility will have 437m of neutron guides. Two companies, Swiss Neutronics and NTK are asked to produce these devices. While Swiss Neutronics delivered the complete components, NTK produces them in cooperation with SDH Heidelberg and the Neutron Optics Group of ZWE FRM II. The Neutron Optics Group produces the multilayer structure on the glass plates which are assembled afterwards by NTK.

For NTK we have to produce neutron guides with a total length of approximately 240m corresponding to a coated surface of approximately 50m2. We started the production of these supermirrors at the end of 2001. After solving a number of small problems successful production

was achieved in spring of 2002. Further interruptions were caused by blocking of the drive screw. Consequently a new driving system was constructed which uses a linkage instead of the drive screw. Since then the production was running continuously.

The major part of the neutron guides was produced in 2002. 130 processes with m=2.0 and 90 processes with m=2.5 were performed, this corresponds a surface of 22.8m^2 and 12.5m^2, respectively. Furthermore 20 processes with various layer systems were performed. By continuous improvements the rate of failure (reflectivity less than 88% for m=2.0 or less than 82% for m=2.5) was reduced below 10%. To check their performance our supermirrors were measured at the neutron beam of BENSC in Berlin. Results of these measurements are shown in fig. 8.11 and fig. 8.12.

The production of the supermirrors, which are needed for the FRM II, will be accomplished in the first quarter of 2003.

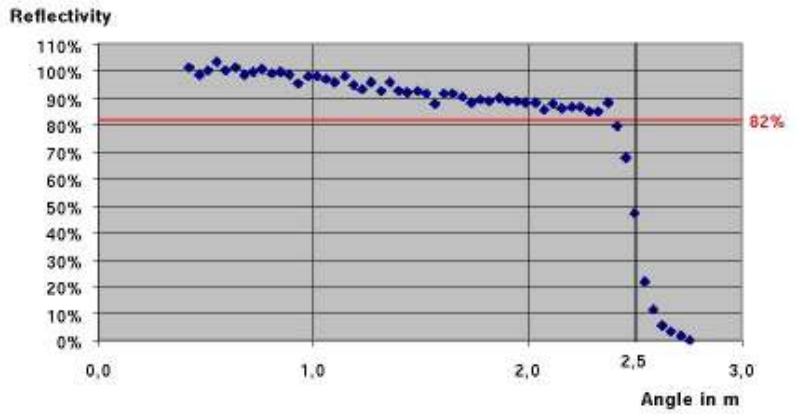

Figure 8.12: Reflectivity of a typical supermirror with m=2.5

8.4 IT–Network Services

Jörn Beckmann, Jörg Pulz, Josef Ertl, Elisabeth Heubl, Felix Zöbisch, Jakob Mittermaier
Technische Universität München, ZWE FRM-II

Nowadays every state of the art scientific institution requires also state of the art computing facilities. This also holds true for FRM-II. The Network Services group is responsible for planning, installation and operation of the FRM-II scientific data network. This includes operation of Mail-, Web-, Name- and Print-Servers, installation and configuration of client computers, assistance with procurement and user support. At the moment the FRM-II network contains about 300 end systems and 190 users.

The policy of the Network Services group is to use Open Source software whenever possible. SuSE Linux is the operation system of choice for desktop machines and instrument control computers, while RedHat Linux or some BSD offspring is used for servers. Unfortunately Windows is still used on most desktop computers. Our goal is to replace windows on all desktop computers by some open Source OS exept on CAD machines, as there is no 3D CAD software available on Linux yet.

Infrastructure

The main design criteria for the FRM-II network was to construct an environment which is fault tolerant and resists hacker attacks on one hand side while being flexible to accommodate the various needs of instrumentation groups on the other side. Security and flexibility exclude each other normally. The solution to this problem is to subdivide the network according to desired function and keep the contact between the different subnets controlled and as minimal as possible. The structure of the FRM-II network is shown in figure 8.13.The whole network is build around a central router. This router subdivides the network. Each subnet is connected to a so called VLAN. Traffic between VLANs is only possible via the router and is controlled by Access Control Lists (ACLs). Each port on a switch belongs to a VLAN and therefore all devices connected to that switchport are within the given subnet. The switches are interconnected by means of a backbone switch. The function of backbone switch and router is provided by a Cisco Catalyst 6500. This Layer 3 switch houses two supervisor engines for fault tolerance. Outlying switches for the connection of office and instrument computers are Cisco Catalyst 2900er, 3500er or HP Procurve 4000M with redundant power supply where necessary.

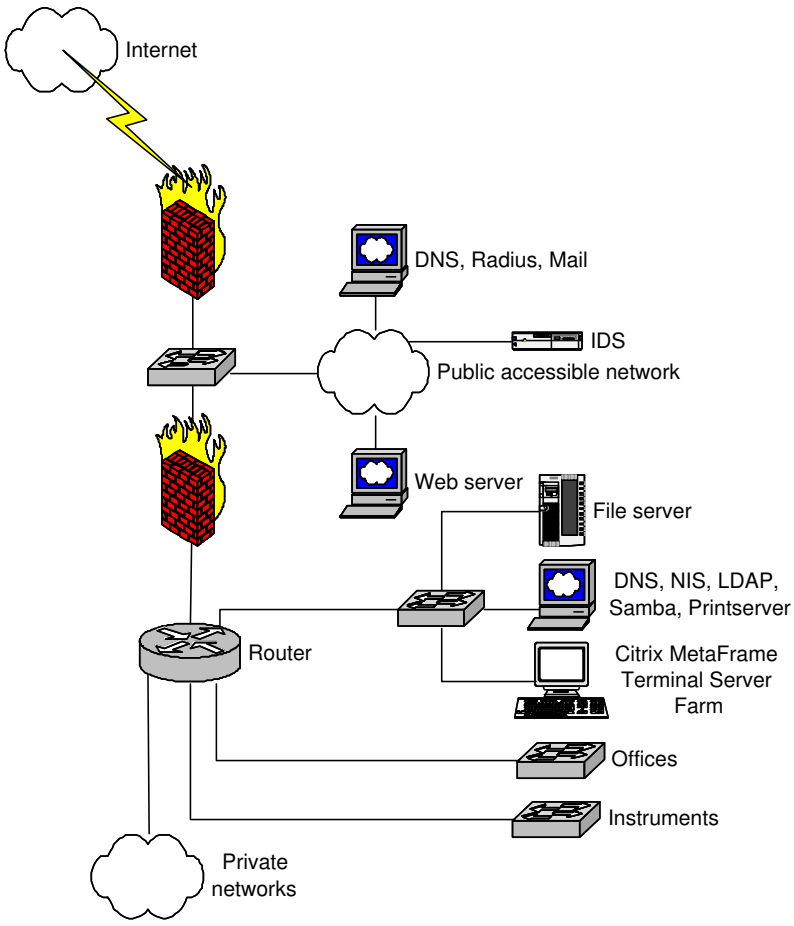

Figure 8.13: Structure of FRM-II IT-network

Connection to and from the internet is secured by a two-stage firewall. The outer stage between the internet and the public accessible network is provided by a packet filter. The public accessible network contains public Web-, Mail- and Name-Servers. Traffic within the public network is under surveillance by the Intrusion Detection System (IDS) Snort running on OpenBSD. This IDS watches for suspicious activities and reports them.

The connection between the public network and the private networks is protected by a second firewall. The first and the second firewall are constructed from different products implementing different algorithms to prevent attacks via bugs in firewall products. The private servers in the internal network are placed in a separated administration network which is protected against attacks by the router ACLs. The central file server

from SGI are part of this administration network. Each user has its home directory on a central file server and can connect this directory to a client machine by means of network file systems like NFS, AFS or CIFS.

Instrument networks

Instrument control is often based on client-server systems like the Taco system of the ESRF. Under all circumstances, even if connection to the central router is lost, the instrument control software must be kept operational. Storage of measured data should be done on the central file server. When this central storage is not accessible temporary storage within the instrument network has to be provided. The same holds true for name resolution services like DNS or NetBIOS for which proxy servers must be included. The third area of concern is, that faulty networking equipment and failure or misuse of software must not affect instruments in the neighborhood.

This is achieved by separating the instrument networks into VLANs and providing each instrument with an own switch. Direct communication between instrument subnets is prevented by the router ACLs again. Where necessary redundant power supply and battery backup will keep instrument networks operational.

Public accessible services

Server in the public network are subject to hacker attacks. The first stage of the firewall filters most of them but is for example not capable to distinguish between regular requests to a web server and illegal requests which might affect server operation. The IDS is able to log and report such attacks but cannot prevent them. The server itself has to be robust enough to sustain hacker attacks and even in case of a successful attack, other systems must not be affected. To guarantee this, servers in the public network use the jail feature [1,2] of FreeBSD.

Normally services run in a so called chroot environment. This chroot environment prevents access to the filesystem outside the assigned area. But full access to the process system is still possible, allowing an successful attacker to manipulate not only the compromised service but the whole system. In a jail environment access to processes outside the jail or to other network resources is prevented. In a jail it is not possible to modify a running kernel, change network parameters, create devices or to reboot the system. As it is possible to run multiple jails on one host system multiple services with different IP addresses could be operated on a single hardware.

The Windows Terminal Server

As already discussed Linux should be installed on as many desktop computers as possible. But unfortunately not all necessary software is available on non-Windows OS. The worst thing to happen is if users would have two computers at their desk, one for Linux and one for Windows. A solution for this is the implementation of a Windows Terminal Server. While it is quite common on Unix-like OS to log on to a remote computer and run specialized software on them, displaying results on the local machine, this is unusual on Windows computers. Microsoft offers the RDP protocol only for Windows clients, therefore third-party software had to be used. We have chosen Citrix MetaFrame, as clients for nearly all OS are available. The Linux user just has to install the client and connects to the Terminal Server Farm. With MetaFrame it is possible to export the whole desktop or just a single application.

The implemented Server Farm is constructed from four computers, three Terminal Servers with Dual Xeon processors and lots of RAM and

a database server for license control. MetaFarme allows load balancing between the three Terminal Servers. The system should support 40 concurrent users and is extendable if accepted by the users. The Terminal Servers have two network cards, a gigabit card to handle requests by the clients and a 100 MBit card for communication with database server, domain controller and file server.

Summary

Network and Server operation in a complex environment like the FRM-II is not possible with only standard products and operation procedures. Research and testing on new concepts and products have to be done as well and the key to success is to put concepts and products from different areas together. While this is already done for networking components and some servers, only half the way is done. Next year we will concentrate on eMail services and file storage. This will require an unified user authentication system which is under investigation in the moment.

[1] P.M. Hausen: A secure hosting environment for Apache/database/PHP applications, presented at BDCon Europe 2001, 9-11. Nov. 2001, Brigton, UK

[2] C. Herrmann: Eingesperrt. iX 3/2002, 138-40

8.5 Software Group

J. Krüger, S. Praßl, T. Unruh, S. Roth, S. Huber, B. Pedersen, Z. Zhang, S. Kreyer, A.Fuchs, M. Salfer, J. Beckmann

Technische Universität München, ZWE FRM-II, http://www.frm2.tu-muenchen.de/software/

The software group developes the software for the instrument control and first analysis of the experimental data of the neutron scattering experiments at the FRM II. The main activities in 2002 were on the following fields:

- Development of the missing hardware device servers (TACO).
- Development of the instrument control software part (NICOS).
- Development of the components for the data analysis (openDaVE).
- Contributions to NeXus, the general data format at FRM-II for experimental data sets.

The instrument control software

The instrument control software at the FRM-II is based on the TACO system [1[developed and widely used the ESRF [2[for the beamline and experiment control.

TACO hardware controller

This year we finished the development of TACO device drivers for the main standard components for the instrument control. At this time we support the following devices:

- Serial line connection over RS232
- ModBus protocol over serial line
- Profibus protocol (provided by the ZEL at FZ Jülich)
- Fieldbus modules (I70xx)
- Motor/Axis control for the stepper motor card, developed at the IPC Göttingen.
- Encoder card, developed at the IPC Göttingen.
- Multi-Channel counter card, developed by the detector group at the FRM-II

- Chopper control for the TOF-TOF
- Temperature controler LakeShore 340
- Aperture, developed by M. Misera(HeiDi)

With the help of the basic servers for line control it is possible to interact with a lot of other hardware which uses serial lines to allow remote access to the hardware.

To simplify the access to the TACO device servers we developed to each exported device type a C++ client class, which hides the details of TACO communication protocol from the user.

Scripting language for instrument control

In cooperation with the ZEL of the FZ Jülich we decided to use Python [3] as the scripting language in our instrument control. There are some reasons for this decision:

- the syntax of Python is well formed and it is easy to learn
- Python is freely available (Open Source)
- Python is widely used (also in the neutron scattering community for instrument control) and well proven.
- Python may be extended by own extensions and embedded in own programs.

To use TACO inside Python we wrote for each device also a Python client class (based on the C++ class).

NICOS experiment control system

The NICOS (see contribution NICOS, T. Unruh) experiment control system may be considered as the glue for the TACO hardware controller. It provides an easy way to setup the instrument and create the instrument specific software part.

NeXus data format

The NeXus data format [4] was choosen as the general data format for the experimental data sets. NeXus will be used by a lot of neutron and X-ray scatterin facilities as their standard data format. Since the NeXus format is only the carrier for the data it is necessary to unify the contents of the data files, i.e. to define the contents, the access pathes and formats of the information in the files. The FRM-II proposed for the TAS and TOF experiments a set of information to be stored for this experiment types. So it will be ensured, that the data file may be read and interpreted by different software without any special conversion routines.

Software for data analysis - openDaVE

For the first data analysis the openDaVE software package was developed at the FRM-II [5]. This modular designed package allowes the user to add its own modules for data treatments. In 2002 we tried to convert parts of the existing data analysis package IDA [6] to openDaVE modules to test the approach of openDaVE, that legacy software may be used in openDaVE as a modules by encapsulation.

It was realized, that it is possible to use some existing code in openDaVE.

[1] http://www.esrf.fr

[2] http://www.esrf.fr/taco

[3] http://www.python.org

[4] http://www.neutron.anl.gov/nexus/

[5] http://www.frm2.tu-muenchen.de/software/openDaVE

[6] http://www.e13.physik.tu-muenchen.de/Wuttke/Ida.html

8.6 Instrument Control with NICOS

T. Unruh[(1)]
[(1)]Technische Universität München, ZWE FRM-II

At the FRM–II, TACO (Telescope and Accelerator Control Objects) is used as a distributed system for the communication with instrument components. The **N**etwork based **I**nstrument **CO**ntrol System NICOS has been developed to serve as a standard frontend for TACO. With NICOS it is possible to control complex actions of instruments remotely by simple commands or graphical applications as well as to setup and configure the software of a complete spectrometer. Thus NICOS is intended to be used by common instrument users, instrument scientists and technical staff.

Although NICOS is best suited to be used as a TACO client it is completely independent from TACO. It includes a modular framework that defines standard interfaces and functionalities for instrument components and by which new hardware can easily be added to a running system. Thus for non–distributed systems NICOS could be used as a standalone instrument control program. It is also possible to extract software components written for NICOS und use them as TACO device servers. NICOS is written in Python, which is also used as general scripting language.

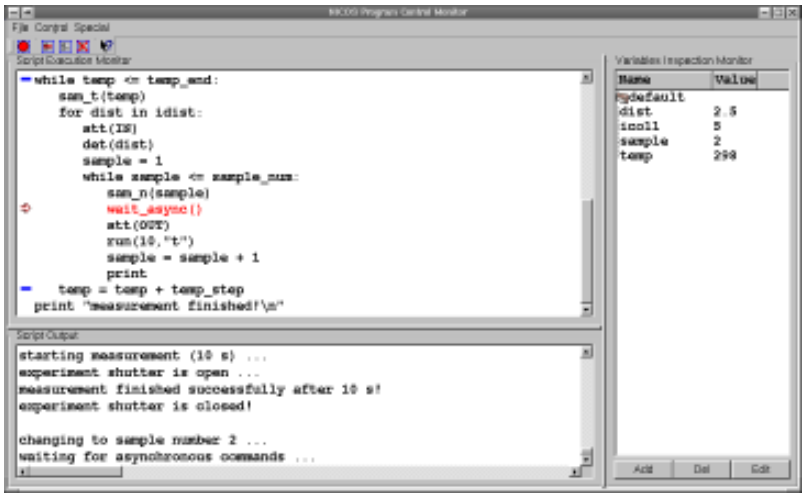

Figure 8.14: The program control monitor window of the NICOS client

In the following two highlights of NICOS will be introduced. A more detailed description of NICOS can be found elsewhere [1].

Interactive Remote Control

After startup of the NICOS client program on any computer in the internet connected to the instrument's network it is possible to establish a connection to the NICOS server via a secure login procedure. A program can be written and started on the server using the user editor of NICOS. During runtime it is possible to update the code of a script which is not yet processed.

Informations about the status of the instrument and the currently executed actions are displayed in the program control monitor, which is shown in Fig. 8.14. By means of three tool buttons the script currently running on the server can be interrupted, continued or stopped by a simple mouse click. The script execution status is indicated by the color of the leftest button: A red color means that a script is currently executed, green means no script is running; yellow means that script execution is interrupted and transparent (grey) means that the client is not connected to a

server.

The window is divided in three subwindows: the script execution monitor, the script output and the variables inspection monitor.

In the **script execution monitor** (upper left subwindow) the source code of the loaded script is displayed. The currently executed line is highlighted and marked with an arrow on the left side. The logical block in which this line is located is marked by blue lines. The update rate of this window can be adjusted.

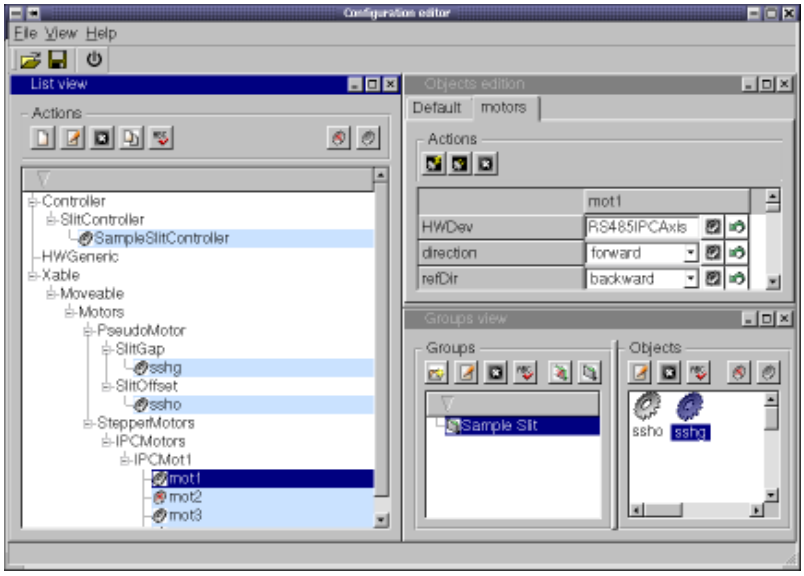

Figure 8.15: The configuration editor of the NICOS client

The output (stdout and stderr) of the script is displayed in the **script output window** (lower left subwindow). Python error messages are displayed here according to the standard Python shell.

In the **variables inspection monitor** (right subwindow) variables and their values can be displayed. It is possible to add and delete values from the script using the "nicd_reg" and "nicd_unreg" commands. Addition, deletion and change of entries are also possible during runtime pressing the "Add", "Del" and "Edit" buttons. Instead of variables it is also allowed to enter any expression. Double clicking on an entry in the variables list causes the pop up of a window in which the value of the selected variable can be changed.

Another possibility to influence the script execution during runtime is to use the command line input window available from the special menu. Here any command can be entered and executed in the context of the current script.

The manipulation of instrument control scripts during runtime is intended to be used e.g. to extend the range of an energy scan at a triple axis spectrometer or to increase the measuring time at a TOF instrument, when the data collected up to this moment indicate that these changes are useful. In this way beam time will be saved because measurements or parts of measurements do not need to be performed twice.

Do Configure Don't Write Code

With NICOS the NICOS-Methods framework is distributed. The basic idea of the framework is to provide standard interfaces for the control of instrument components (devices). The framework allows to implement a new device simply by adding python code to predefined interface functions. The code to add includes only the communication and if necessary some logical operations. A typical device has less than 100 lines of well readable python code.

In order to minimize the code even more NICOS devices should be highly configurable. Thus a device implemented by someone can be used by someone else in another environment just by reconfiguration. For this purpose a configuration editor has been developed at the ESRF in close contact with the FRM–

II.

In Fig. 8.15 the main window of the configuration is displayed. All parameters of all devices of an instrument can be generated and configured using this editor. Of course it is also possible to disable a device, that is e.g. temporarily out of order, and to enable it again later. The configuration editor can only be opened by the administrator and only if the NICOS server is idle. For safety reasons an opened configuration editor blocks all write access to the NICOS server.

NICOS with all its components (client, server, NICOS-Methods, configuration editor) can be used as a powerful frontend for a distributed instrument control system but it may also serve as a standalone control program. Both capabilities can also be mixed. Currently the interface to the TACO system is being extended. It will be possible in the future to convert a NICOS device into a TACO server just by configuration.

[1] T. Unruh, “Instrument Control at the FRM-II using TACO and NICOS”, arXiv: cond–mat/0210433 (2002)

Reactor and Radiation Protection

9.1 Towards the Nuclear Start-up

Klaus Schreckenbach
ZWE FRM-II, Technische Universität München

The FRM-II obtained its first partial licence in April 1996 and the construction started in the same year. With the second partial licence in 1997 all systems could be installed and made operational for the nuclear start-up. The delay due to the very difficult procedure for the licence to operate the FRM-II (third partial nuclear licence) is used for long term tests of the systems and for training programs for the operating staff. Since October 2000 shift operation in the control room of the FRM-II is established in order to run the conventional systems and to test the nuclear operation and safety systems as far as possible without nuclear fuel. The moderator liquid D_2O is analysed and waiting for the transport as well as the fuel elements, of which 4 elements are manufactured till now. Transport and acceptance in the FRM II is only allowed after we have received the licence for operation.

The personal for the reactor division was set-up and all the positions obligatory for the nuclear start up are filled. The entire technical personal is continuously trained by courses and on-site training programs. All together 21 shift operators were licensed for the FRM-II, a part of them were already operators at the FRM. They passed four month external training courses with examinations and had to pass examinations about their specific knowledge of the FRM-II facility under the eyes of the StMLU and TÜV. A typical education for shift operators lasts about one to two years. To maintain the knowledge a training program for the reactor staff is established for the next three years.

The procedure for the nuclear start-up will begin immediately after we have obtained the licence for reactor operation. Since we expect the licence very soon all systems are currently checked for their functioning in a systematic way. With the licence for operation we are then allowed to transport and to bring into the facility the moderator liquid D_2O, the first fuel elements and the converter plates. The following concept for the nuclear start-up is programmed: The first fuel element is inspected in a measurement unit for undercriticality before it is put into the central position of the reactor tank. After several system tests in the nominal position of the fuel element the criticality is carefully approached. Then the shut-down and control rods are calibrated and the power as well as the power density distribution of the reactor core are measured with a first run at low reactor power ($<$200 kW). The reactor power is increased stepwise with check-ups on the reactor control system, the core cooling system, the special experimental facilities and on radiation shielding and protection. As the end of the start-up program a continuos run at 20 MW is foreseen till the first fuel element is burned out. A time of 9 to 10 month is estimated from the third licence to the end of the nuclear start-up program. A report on the practical experience with the

start-up procedure and the first fuel element has to be written and agreed upon before we are allowed to continue with the routine operation of the reactor.

9.2 Nuclear Licensing of the FRM-II

K. Böning
Technische Universität München, ZWE FRM-II

The first draft of the Third Partial Nuclear Licence of the FRM-II, which includes the licence to start up and operate the reactor, had been sent by the Nuclear Licensing Authority, the Bavarian State Ministry of State Development and Environment (StMLU), to the Federal Ministry of Environment and Reactor Safety (BMU) already in August 2000.

After numerous meetings of the representatives of the Technische Universitaet Muenchen (TUM) and its general contractor Framatome-ANP with the technical experts and advisors of the BMU, the Reactor Safety Commission (RSK) and the Commission on Radiation Protection (SSK), the BMU issued its Federal Supervisory Assessment to the StMLU in January 2002. This document listed some 65 questions or conditions - more and including additional topics than contained in the positive assessments of both RSK and SSK - which the BMU wanted to get further discussed in more detail. This represented very hard work for both TUM and Framatome-ANP until we could deliver all the relevant documents to the StMLU and the StMLU could submit an updated draft of the Third Partial Nuclear Permit to the BMU in July 2002.

At the end of October 2002 the BMU sent an updated List of Questions which still contained some 10 items with a focus on Beyond Design Basis Accident scenarios. This again meant hard work for both TUM and Framatome-ANP until we could submit the last documents in mid January 2003. Having answered all these questions we are pretty confident now that the StMLU will receive a positive Federal Supervisory Assessment of the BMU in early 2003. The final, Third Partial Nuclear Licence of the StMLU would probably follow shortly later and the transport of the first fuel elements and the nuclear startup of the FRM-II could be initiated immediately after that.

Fuel Element with Reduced Enrichment

The outstanding performance of the FRM-II to provide a high thermal neutron flux ($8 \times 10^{14} cm^{-2} s^{-1}$ unperturbed) in a large usable volume at a relatively low reactor power (20 MW) is directly related to the design of a single, very compact fuel element in a large tank filled with heavy water moderator. This compact fuel element is cooled by light water and contains uranium-silicide (U_3Si_2) aluminum dispersion fuel with high enrichment (93 % ^{235}U) and with a relatively high uranium density (3.0 gU/cm^3, graded).

After its election in 1998 the red-green Federal Government - following its nonproliferation philosophy - decided to investigate if the FRM-II could be converted to use low-enriched fuel (with 20 % ^{235}U only). The Federal Ministry of Education and Research (BMBF) established an experts' committee which - after many sessions - presented a final report listing a number of alternatives in June 1999.

The position of the TUM was always to maintain the reactor power and the compact dimensions of the fuel element - so that the FRM-II reactor facility would not need to be modified and built once again and that the penalties in reactor performance would be marginal; this means that the enrichment of ^{235}U could be reduced only so far as this could be fully compensated by an increase in the uranium density of new fuels (i.e. without making the fuel element larger). An agreement following this line has been negotiated between the Bavarian State Ministry of Science, Research and Arts (StMWFK) and the BMBF; this agreement was finalized in October 2001 but will be signed by the ministers only once the green light has been given by the Federal Government to start up and operate the FRM-II. This agreement says that the FRM-II will be permitted to operate with fuel elements using highly enriched uranium for about ten years, i.e. until an advanced fuel with a higher uranium density has been developed and tested so that a new fuel element with reduced enrichment can be designed, fabricated, tested and licensed.

The TUM has already established an international working team to develop such an advanced fuel and a modified fuel element for the FRM-II. This work will actually begin once the green light for the FRM-II has been obtained and the agreement has been signed and the necessary budget has been allocated.

9.3 Radiation Protection at FRM and FRM-II

H. Zeising(1)
(1) Technische Universität München, ZWE FRM-II

Research Reactor FRM

On July 28th, 2000, the Munich Research Reactor (FRM) was shutdown and decommissioned for the time being.

In the time period from the end of April 2002 to the middle of June 2002 the last 47 spent fuel elements and a spent converter plate from the medicinal tumor irradiation equipment were loaded into two transport casks (GNS 16), authorized for this purpose. The spent fuel rods along with the converter plate were shipped to Charleston Naval Weapons Station in the USA via Denmark, to be stored at the Savannah River Site. Figure 9.1 shows a loaded transport cask, which is filled with water for shielding purposes.

During the loading procedure, which was carried out by the so-called dry-loading method, extensive radiation protection measures were necessary:

- Monitoring of internal and external personnel using Film- and Albedo-dosemeters for γ- and n-radiation,
- accompanying in-situ γ- and n-dose rate measurements at the workplaces,
- extensive contamination screening through use of wipe tests,
- γ-spectrometric measurements and determination of the tritium concentration in the pool water,
- γ-spectrometric determination of the container water during the leakage test of the fuel elements (Sipping - test),
- γ- and n-dose rate measurements on the outside surface of the loaded 20‘-containers into which the filled GNS-16 casks were transferred.

The loading of the fuel elements proceeded very sucessfully. The collective dose of the circa 30 persons who were involved amounted to only 0.2 mSv. In addition, no

contaminations above the limits according to the StrlSchV were ascertained, neither at the working-places nor in the room-air.

Figure 9.1: Loaded transport cask filled with water for shielding purposes.

Although there are no more spent fuel elements in FRM, the entire radiation protection program was still absolved in the year 2002. In order to concentrate on the new radiation protection program at the new neutron source FRM-II, in November 2002 a request was submitted at the authorising agency, which would provide that the radiation protection tasks, which pertain to the instruments for surveilance as well as the routine radiation protection jobs, be reduced strongly.

Research-Reactor FRM-II

In the years 2001 and 2002 the instruments for monitoring the activity and the radiation protection instrumentation at FRM-II were fully built up, put into operation and commissioned by the authorized expert (TÜV Süddeutschland).

The system for monitoring the activity and the radiation protection instrumentation are comprised of the following parts:

- measuring points which are integrated in the reactor safety system,
- measuring points used for monitoring the reactor systems,
- dose rate monitoring of the rooms (neutron- and gamma-radiation) with permanently installed and mobile instrumentation,
- monitoring of the rooms for tritium, radioactive inert gases and radioactive aerosols,
- monitoring for surface contamination through alpha-, beta- and gammaradiating nuclides as well as specifically for tritium, using mobile measuring systems,
- monitoring of the emissions of the exhaust air and effluents,

∗ exhaust air monitoring: Instruments which continuously monitor tritium activity, the radioiodinening concentration and the activity of the radioactive inert gases in the exhaust air as well as equipment for collecting tritium, carbon-14, radioactive inert gases, radioactive aerosols and radioiodine.

* effluent monitoring:
  In order to control the emission of weakly radioactive effluents, a gamma-sensitive measuring point is installed, which monitors continuously when effluents are given off.
- accident monitoring with instrumentation, which continuously measures the gamma dose rate in the reactor hall as well as the determination of the radioactive inert gas concentrations in the exhaust air. Additionally, equipment for taking samples of radioactive inert gases, iodine and aerosols.
- laboratory measuring equipment for the determination of total-alpha, beta- and gamma-activities as well as special detectors for nuclide-specific determination of alpha-, beta- and gamma-radiating isotopes (spectrometry with high-resolution detectors).
- equipment to monitor for contamination of personnel, such as so-called Hand-Foot- Clothing-Monitors and whole body monitors.

Figure 9.2 shows a contamination control through use of a whole body monitor.

Figure 9.2: Contamination control through use of a whole body monitor.

In addition, in the year 2002 the individual review of requests for the building up of instrumentation and experiments at FRM-II was begun, in order to make an assessment from a safety-related, radiation safety-related and operational point of view. For this purpose a guideline, the specifications of which the experimenters should go by when making their requests, was worked out. The following points are to be followed in the guideline:

Next to the personnel organization the instrumentation is to be described in detail, the safety and risk aspects are to be considered, eventual accidents and their effects should be assessed, radiation protection should be taken into account, and finally plans should be submitted as what should happen with the conventional and radioactive residues and waste materials, which are produced during the operation of the instrumentation and afterwards, when it is no longer in use.

By this means a certain planning reliability can be met and the certainty, that the later operation and also the decommissioning can proceed as safely and as failure-free as humanly possible.

Scientific Highlights

10.1 Phase Contrast Radiography with Thermal Neutrons

N. Kardjilov[(1)], E. Lehmann[(2)], E. Steichele[(1)], P. Vontobel[(2)]
[(1)]Technische Universität München, Physik Department E21, D-85747 Garching, Germany
[(2)]Paul Scherrer Institute, CH-5232 Villigen, Switzerland

An alternative method to the standard radiography is the phase contrast imaging, where the intensity distribution in the radiography picture is proportional to the phase variations induced by the transmission of a coherent radiation through a medium. To achieve a phase contrast in radiography images usually a high spatial and chromatic beam coherence is required. It can be shown that a neutron phase contrast imaging can be performed without monochromatisation of the beam.

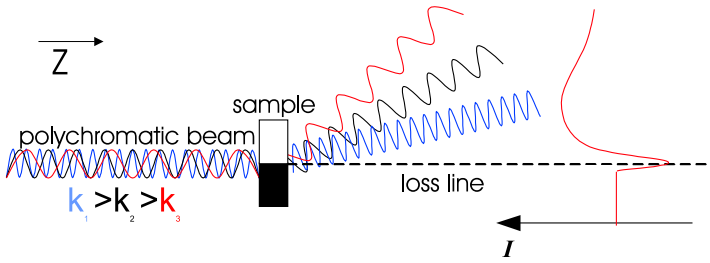

Figure 10.1: Schematic illustration of the energy-dependent deflection of a polychromatic beam from a sample area with a strong variation of the refractive index.

Theory

In case of high transversal spatial coherence all rays emanating from a point source, defined e.g. by a small pinhole, are associated with a single set of spherical waves that have the same phase on any given wavefront. As shown in [1] the variations of the thickness and the neutron refractive index n of the sample cause a change in the shape of a neutron wavefront on passing through the sample. The angular deviation of the normal to the wavefront, $\Delta\alpha$, can be expressed as:

$$\Delta\alpha \approx \frac{1}{k} |\bigtriangledown_{x,y} \varphi(x,y,z)| =$$

$$|\bigtriangledown_{x,y} \int [n(x,y,z)-1]dz|,$$

where the optical axis is parallel to z and φ is the phase change for a ray path through an object relative to vacuum. This means that the deformation of the wavefront after the transmission depends on the gradient of the refractive index n in a plane perpendicular to the direction of the wave propagation, $\vec{k}$.

To show that rapid variations in refractive index can lead to strong phase-contrast effect even with polychromatic radiation, the formal representation shown in Fig. 10.1 can be used [1]. The intensity variations due to the gradient of the refractive index in the sample area can be characterized by a very sharp minimum in the propagation direction (loss line) followed by a broad maximum beside it, Fig. 10.1. Such high values of the refractive index gradient exist mainly on the sample edges. Therefore the phase contrast imaging provides a high edge-enhancement in the resultant images.

Experiment

The experiments were performed at the thermal neutron radiography setup NEUTRA. To produce a high spatial coherence a pinhole with a size of 0.5 mm in a Gd foil (thickness of 0.1 mm) was used. It was placed at a large distance of 7 m from the sample. The sample to detector distance was fixed to 1 m. The exposure time at the used thermal neutron beam was 90 min per image. Steel capillaries with diameters between 0.3 mm and 0.9 mm were investigated with phase contrast and conventional radiography. The obtained profiles through the capillaries are shown in Fig. 10.2 .

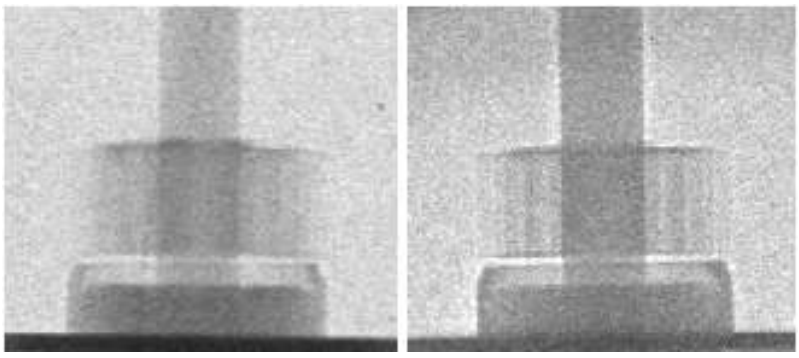

Figure 10.3: Conventional thermal radiography of a toothed wheel (left) and phase-contrast radiography (right).

The edge-enhancement on the needle borders in the case of phase contrast radiography follows the behaviour shown in Fig. 10.1 - a consequence of minimum and maximum in the intensity at rapid variations of the refractive index.

In the case of conventional thermal radiography such an edge enhancement is missing. An example of phase-contrast imaging with thermal neutrons of a small toothed wheel is shown in Fig. 10.3 .

The improved contrast in case of phase-contrast radiography is obvious. The observed edge-enhancement is due to a very sharp change of the intensity on the borders.

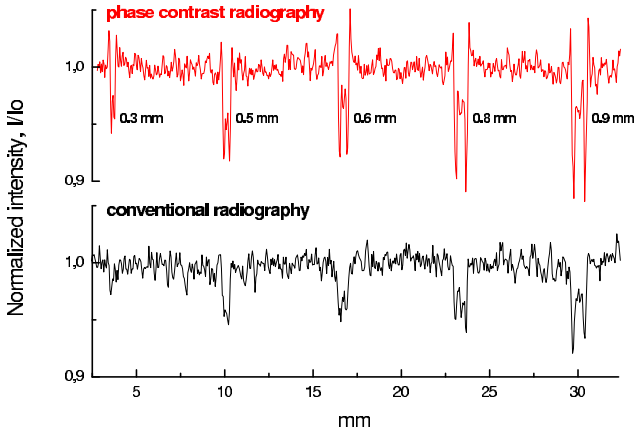

Figure 10.2: Intensity profiles of steel capillaries obtained by phase contrast and conventional radiography.

[1] S.W. Wilkins, T.E. Gureyev, D. Gao, A. Pogany, A.W. Stevenson, Nature, **Vol 384**, 28. November 1996, 335-338 (1996).

10.2 Steps Towards a Dynamic Deutron Radiography of a Combustion Engine

J. Brunner[(1)], H. Abele[(3)], N. Arendt[(3)] , T. Ferger[(3)], G. Frei[(2)], R. Gähler[(4)], A. Gildemeister[(2)], E. Lehmann[(2)], A. Hillenbach[(3)], B. Schillinger[(1)]
[(1)]Technische Universität München, Physik Department E21, 85747 Garching, Germany
[(2)]Paul Scherrer Institut, 5232 Villigen, Switzerland
[(3)]Universität Heidelberg, Physikalisches Institut, 69120 Heidelberg, Germany
[(4)]Institute Laue Langevin, 38042 Grenoble, France

The Dynamic NR is a new technique, which is applied successfully for non-destructive testing for time dependent phenomena with a similar resolution and a similar contrast as in conventional NR. Of special interest is the investigation of the injection process in a running combustion engine under real conditions.

Figure 10.4: A single frame (left) contains only 10 graylevels and 500 summed NR-images contain 3000, image after processing (right), t=4ms.

For obtaining a 16-bit conventional radiography image at a typical flux of 10^6 n/cm^{2}s one has to integrate scintillator light on the CCD chip typically for some seconds. Of course the sample thickness, the sample material as well as the detector efficiency determine the exact time. Additionally the readout time, depending on the dynamic range and the pixel number of the CCD, puts a lower limit to the highest achievable frame rate. The observation of objects in the millisecond time scale is impossible with standard methods. A possible solution for repetitive processes can be stroboscopic imaging. That means a synchronization of the detector with the repetitive process and an integration of 1000 images taken at the same millisecond time window of the cycle. That way a virtual opening time of some seconds can be realized as long as the noise is constant within time (i.e. negligible readout noise) and not determined by the system. With this method a combustion engine towed by a electric motor was observed in the first experiments testing the method with a self constructed detector. The achieved spatial resolution was 1 mm.

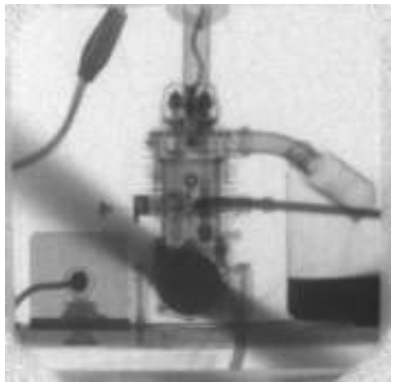

Figure 10.5: 4000 summed frames of the neutron radiography movie of a running model aircraft engine (0.75 kW), one frame = 0.25 ms, running at 4800rpm

This year it was possible to perform dynamic neutron investigations at PSI with an excellent new detector system

and at ILL at a very high flux test beam line with a detector built by the group of the university of Heidelberg. At the NEUTRA facility a dynamic neutron radiography experiment of a running model aircraft engine was performed. The detector consisted of a CCD camera using a multi channel plate as an image intensifier coupled on the CCD-chip with fiber optics. With this equipment and the thermal neutron beam of 10^7 n/cm^{2}s extremely high detection sensitivity was possible. That is hardly reached by any other system. As neutron to light converter a one millimeter thick ^{6}LiF/ZnAg scintillator was used. The achieved spatial resolution was 0.15 mm.

At ILL NR-measurements of an airbrush nozzle with a very high flux of 10^9 n/cm^{2}s were performed. In the false color image Fig. 10.6 the red cloud of injection liquid is clearly visible. Boron water and a Gadolinium emulsion were tested as a contrast liquid. Fig. 10.6 was obtained without synchronizing with the detector.

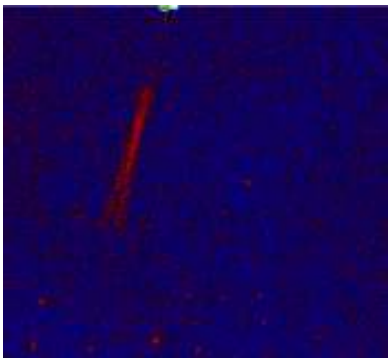

Figure 10.6: A false color NR-image of boron water injection of an air brush nozzle, t=20ms, on the top of the image is the nozzle, the injection is the red strip. The spatial resolution is 0.5 mm.

[1] B. Schilllinger, "Neue Entwicklungen zu Radiographie and Tomographie mit thermischen Neutronen", Ph.D. thesis, Technische Universität München (2001)

[2] M. Balasko, "Neutron radiography visualization of internal processes in refrigerators", Physica B: Condensed Matter, **234-236**, 1033-1034 (1997)

10.3 Polarized SANS Studies from the Weak Itinerant Helimagnet MnSi

R. Georgii[(1)], P. Böni [(2)], H. Eckerlebe[(3)], S. Grigoriev[(4)], N Kardjiloy[(2)], A. Okorokov[(4)], K. Pranzas[(3)], B. Roessli[(5)]
[(1)] Technische Universität München, Germany
[(2)] Technische Universität München, Physik-Department, E21, Germany
[(3)] FRG-1, GKSS, Geestacht, Germany
[(4)] PNPI, St. Petersburg, Russia
[(5)] PSI, Villigen, Switzerland

The intermetallic compound MnSi shows at T_c = 28.5 K a magnetic phase transition from the paramagnetic phase to an ordered phase with a long-period ferromagnetic spiral [1]. The antisymmetric exchange interaction, the so-called Dzyaloshinsky-Moria (DM) interaction, being responsible for this structure, arises from the lack of inversion symmetry in the cubic structure of MnSi. A unique feature of the DM interaction is that the spiral should be either right or left handed depending on the sign of the DM interaction. Polarized SANS is ideal for the investigation of chirality and the critical scattering in such a system. Furthermore in a SANS experiment, where the

MnSi is orientated along its (111) direction, the magnetic peaks should be visible close to the the nuclear diffraction point, which is itself blocked by the beam stop. It also offers the advantage of better q-resolution compared to for example a three axis spectrometer. Another interesting point is how the critical scattering around T_c develops from the ordered to the paramagnetic phase [2]. Here the critical indices can be determined.

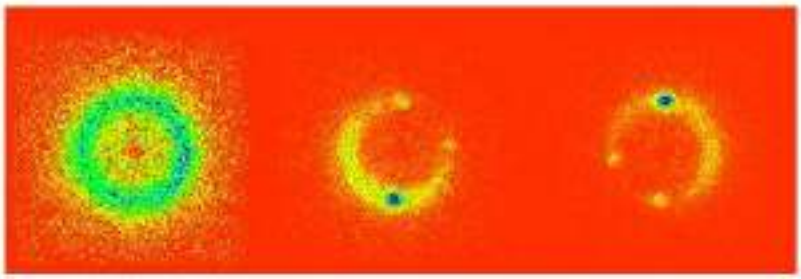

Figure 10.7: The transition from the disordered paramagnetic phase (left) to the spiral ordered phase (middle and right) in MnSi in the critical scattering regime around T_c = 28.5 K. The crystal was oriented along its (111) direction. The two pictures below T_c are shown for both polarisation states of the incoming neutrons.

Therefore we performed a polarised SANS experiment at the SANS-2 of the research reactor FRG-1 of the GKSS in Geestacht. The SANS-2 polarizes the neutrons after they have been monochromatised in a velocity selector with a multilayer supermirror such that only one spin state can pass the mirror unperturbed. A RF spin flipper from PNPI, which has no material in the beam, can then flip this state for all neutrons without being sensitive to the their velocity. Therefore the full wavelength spread of $\Delta\lambda/\lambda$ of $\sim$ 5% at 5 Åcan be used for the experiment. The disk-shaped sample is mounted perpendicular to the beam in a cryomagnet and its temperature is being controlled by a Lake-shore controller. The position sensitive detector (55 cm x 55 cm sensitive area) can be moved from 1 m to 16 m from the sample offering a q-range of 10^{-3} Å^{-1} <q< 0.3 Å^{-1}. For our experiment the magnetic peak is expected to be at 0.035 Å^{-1}, thus the detector was positioned at a distance 1m behind the sample. The data were recorded for each spin state separately allowing for a polarisation sensitive evaluation. This is ongoing, but some preliminary results are given here:

MnSi shows exactly the expected behaviour (see figure 10.7) as described above. At temperatures slightly above the critical temperature a ring around the nuclear peak can be observed, which narrows when approaching T_c. Below the critical temperature two magnetic peaks form, which are sensitive to the incoming neutron polarisation. It should also be noted that the cross sections are huge. We get more then 500000 counts in 100 sec per magnetic peak! The next step will be to evaluate from the 2-dimensional intensity pattern the susceptibility and to determine the critical exponents for the phase transition.

[1] G. Shirane et al., Physical Review B, **28**, 6251 (1983)

[2] B. Roessli et al., Physical Review Letters **88**, 237204-1 (2002)

10.4 In situ Observation of γ′-phase Dissolution in Ni-base Superalloy by SANS

R. Gilles[(1)], P. Strunz[(2)], D. Mukherji[(3)], A. Wiedenmann[(4)], J. Roesler[(3)], H. Fuess[(1)]
[(1)]Technische Universität Darmstadt, Petersenstr. 23, 64287 Darmstadt, Germany
[(2)]Laboratory for Neutron Scattering, Paul Scherrer Institute, 5232 Villigen - PSI, Switzerland
[(3)]Technische Universität Braunschweig, Langer Kamp 8, 38106 Braunschweig, Germany
[(4)]Hahn-Meitner Institut Berlin, Glienickerstr. 100, 14109 Berlin, Germany

Small-Angle Neutron Scattering (SANS) was employed for in situ observation of γ′ precipitate dissolution in a Re-rich Ni-base superalloy. Due to the limited space available for this presentation not all the results can be discussed here: only a few important ones are reported. The complete parts are published elsewhere [1, 2]. The idea was to monitor the γ′ morphological changes at the elevated temperatures up to where incipient melting starts and at the same time to describe the temperature range of the single phase (γ) field above the γ′ solvus but below the solidus temperature to determine the solution heat treatment window. A mixture of several contributions to the scattering intensity complicates the analysis of the SANS data. Nevertheless, on the basis of a microstructural model to represent the various inhomogeneities present in the as cast specimen, the temperature dependence of the relative volume fraction and the size distribution of smaller γ′ precipitates (<5000 Å), the specific surface of larger inhomogeneities as well as some other parameters were determined from the measured scattering curves. The total scattering probability is suggested as the measure of the overall homogeneity distribution in the sample. The temperature dependence of this parameter indicates the optimum temperature at which the alloy can be solution treated to minimize the segregation of heavy elements (e.g. W, Mo, Re) that exist in the as cast condition. Single crystal Ni-base alloys for turbine blades have very complex composition and the modern cast alloys contain high amount of heavy alloying elements like W, Mo, Re, Ta etc. [3, 4]. A segregation of heavy elements is thus common during solidification which influences the mechanical properties of the material. Two harmful effects of the segregation are usually reported: a non-uniform precipitate distribution and a promotion of the harmful secondary phases formation (TCP phases like σ, μ etc.). To eliminate - at least partially - the segregation, a homogenizing (solution) heat treatment has to be carried out in the single phase (γ) region. A "window" of solution-treatment is thus defined by the γ′ solvus and the solidus temperatures. However, the solvus temperature (above 1200°C in modern superalloys) is very close to the melting temperature of the alloy and the solution window is very small (usually $< 30°C$). In some cases, incipient melting region can overlap with the solvus temperature.

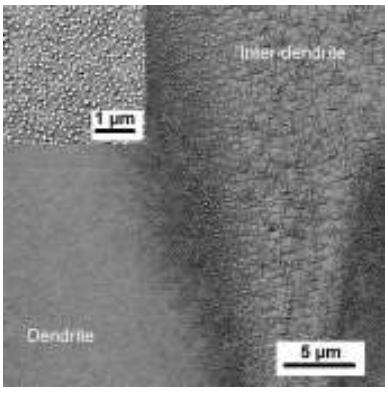

Figure 10.8: The microstructure of Re13 alloy in as cast condition showing inhomogeneous γ′ distribution. Image in inset shows γ′ morphology in dendrite at higher magnification.

A precise knowledge of the

temperature range of this window is an important parameter for new alloy development and for optimizing heat treatment in existing alloys.

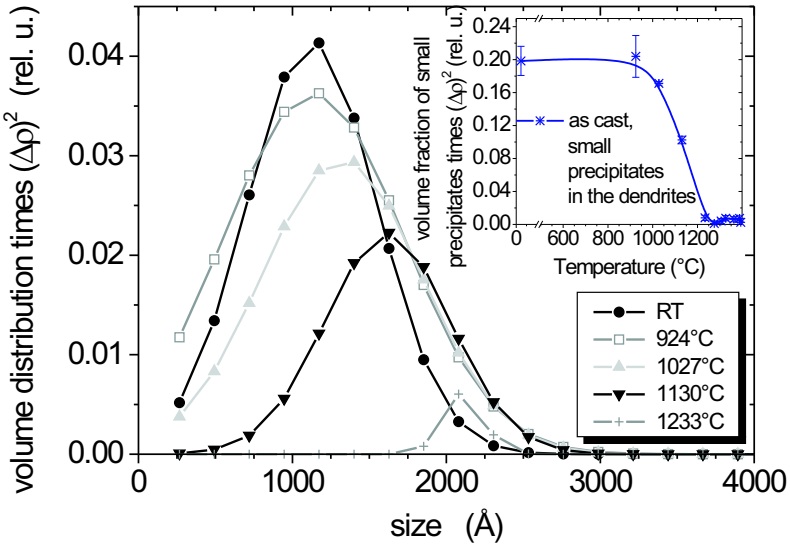

Figure 10.9: Distribution of particle volume in dependence of size for the smaller precipitates in dendrites. The inset displays the decrease of the volume of these precipitates with temperature.

Additionally, the microstructural instability in superalloys during high temperature exposure is an important parameter which determine the service life of turbine components. Small-angle neutron scattering provides an opportunity to monitor the microstructural changes at low and high temperatures. Due to the properties of cold neutrons, SANS can be used for "in situ" tests at extreme conditions [5] and thus also for observation of dissolution of precipitates at high temperatures and the incipient melting. In the past, SANS was very useful in characterization of γ' morphology in single crystal alloys. Our previous experiments as well as literature data show that the γ' precipitates give rise to a strong SANS intensity in many superalloys. The precipitates are - from the point of view of neutron scattering - fluctuations of the so-called scattering length density $\rho(r)$.

The aim of the presented in situ heating experiment during the SANS measurement was to take the two-phase superalloy into the single phase γ' region till incipient melting commences. This procedure allows the determination of the solution window for the alloy and - at the same time - the evolution of the microstructure at high temperatures.

Experimental

The alloy investigated in the present study is a Re-rich Ni-superalloy designated Re13. Specimen in as cast condition was measured by SANS. The alloy has a large amount of heavy element additions (Re and Ta) and therefore exhibits strong segregation tendency, as can be seen from the inhomogeneous γ' distribution in the as cast condition (Fig. 10.8).

Measurement was performed at V4 facility at HMI Berlin employing a standard ILL-type high-temperature furnace equipped with a graphite sample holder. SANS data were collected during increasing temperature of the sample for the sample-to-detector distance of 16 m and $\lambda = 19.4$ Å. This geometry was selected in order to observe preferentially the solution of the largest γ' precipitates. Due to the low flux of the neutron source at such a wavelength, it was possible to measure without the beam stop which usually protects the 2D position sensitive detector (PSD) against overloading by non-scattered neutrons in the primary beam. The bottom limit of the measured Q-range [$Q = |\vec{Q}| = 4\pi sin\theta/\lambda$] is therefore restricted only by resolution of the facility [$\Delta Q = 0.0008$ Å^{-1}] for such a geometry.

Discussion

The first dependencies determined from the fit are the size distributions of small particles in the dendrites (Fig. 10.9) and their relative volume fraction at different temperatures (inset in Fig. 10.9). It should be noted that the absolute volume fraction can not be determined because the scattering contrast ($\Delta\rho$) can change with temperature. The independent estimation of average $\Delta\rho$ can be done usually only with a large uncertainty for Ni-base superalloys even at room temperature; its precise determination at higher temperatures is then practically impossible. Nevertheless, it can be deduced, that the small precipitates are completely dissolved above 1233°C and that their mean size increases from $\approx$ 1200Åup to $\approx$ 2000Åin the temperature region 23 - 1233°C. The important information is carried by the total scattering probability obtained from the fit of the model. This probability is connected with the integral scattered intensity and gives the measure, how homogeneously the elements are distributed in the sample regardless of the size and the type of the inhomogeneity. The evolution of the total scattering probability with temperature can be observed in Fig. 10.10. The probability is lowest at 1275°C.

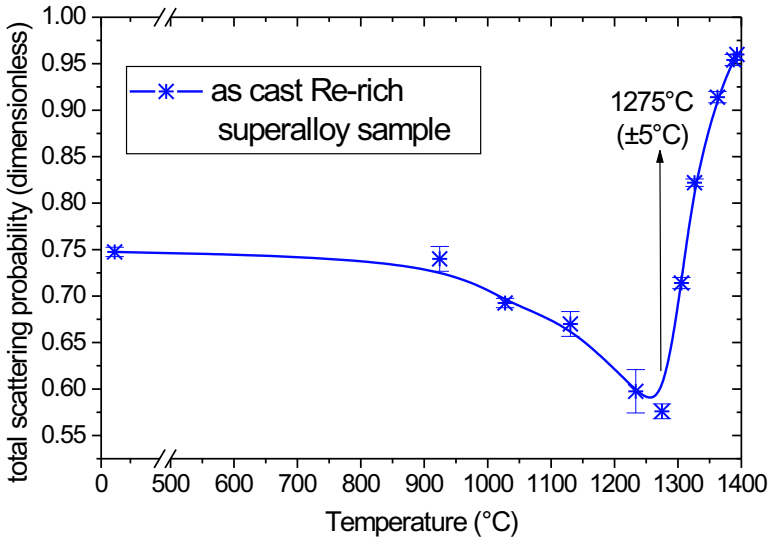

Figure 10.10: The total scattering probability vs. temperature.

Conclusions

The fitted parameters thus contain useful information about dissolution of precipitates and the γ' morphological changes as well as the commencement of melting. The incipient melting starts below 1306°C (large incipient melting islands are detected by SANS at this temperature). The melting temperature (liquidus temperature) of the alloy was determined to be 1403°C by DTA measurements. Strong segregation, of Re and possibly Ta leads to such a broad temperature region where melting commences. Optimum temperature for homogenization of the as cast alloy is suggested by the minimum of the total scattering probability (1275°C). However, a several step procedure with holding at different temperatures could be more advantageous for the homogenization as indicated also by our further results.

[1] P. Strunz, D. Mukherji, R. Gilles, A. Wiedenmann, J. Roesler and H. Fuess, J. Appl. Cryst. **34** (2001), 541-548.

[2] R. Gilles, D. Mukherji, P. Strunz, A. Wiedenmann, J. Roesler, H. Fuess Special Issue: Journal of Materials Processing Technology, Eds. T. Chandra, K. Higashi, C. Suryanarayana & C. Tome, Elsevier Science, UK (October 2001), ISBN 0 08 044026 6.

[3] P. Caron, T. Khan, J. Mater. Sci. and Eng. **61** (1983) 173-184.

[4] R. A. MacKay, M.V: Nathal, Acta Metall. Mater. **38** (1990) 993-1005.

[5] R.J.R. Miller, S. Messoloras, R.J. Stewart & G. Kostorz, J. Appl. Cryst. **11** (1978) 583.

10.5 Valence and Magnetic Transitions in $EuMn_2Si_{2-x}Ge_x$

M. Hofmann[(1)], S.J. Campbell[(2)]
[(1)]ZWE FRM-II, Technische Universität München, 85748 Garching, Germany
[(2)]School of Physics, University College, ADFA, The University of New South Wales, Canberra, ACT 2600, Australia

Rare-earth intermetallic compounds containing europium exhibit a wide range of interesting and unusual physical and magnetic properties [e.g. 1]. This occurs mainly as a result of their mixed valence states (II/III) or changes from one valence state to the other. The $EuMn_2Si_{2-x}Ge_x$ system with the tetragonal $ThCr_2Si_2$ type structure is of particular interest as it exhibits a wide variety of electronic and magnetic properties with evidence for valence instabilities. For example, recent investigations of this series by magnetisation and ^{151}Eu and ^{57}Fe Mössbauer effect measurements reveal that $EuMn_2Ge_2$ contains only divalent Eu whereas $EuMn_2Si_2$ reveals features consistent with the transformation from Eu^{3+} to Eu^{2+} above $\sim$ 350 K [2].

In order to clarify the unresolved issues concerning the magnetic and valence behaviour of those compounds we have carried out neutron diffraction measurements on $^{153}EuMn_2Si_2$ and

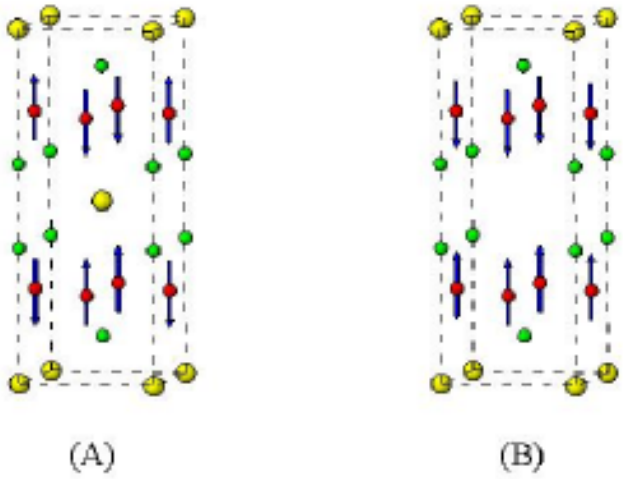

Figure 10.11: Magnetic strcutures of $EuMn_2Ge_2$ (a) and $EuMn_2Si_2$ (b); yellow spheres are Eu, red are Mn and green are Si

$^{153}EuMn_2Ge_2$ over the temperature range $\sim$ 6 - 723 K using the GEM diffractometer at the ISIS Facility, UK. A full account of these experiments, including preparation of these compounds using the low neutron absorption isotope ^{153}Eu, will be given elsewhere [3].

Magnetic Structures

Analysis of the diffraction data reveals that $EuMn_2Ge_2$ exhibits collinear antiferromagnetic order below $T_N \sim 670$ K. $EuMn_2Ge_2$ has the magnetic space group I4'/m'm'm and a Mn moment value of $\sim$ 3.4 μ_B at 6 K (figure 10.11a). The present findings disagree with the earlier magnetisation and Mössbauer results for which ferromagnetic ordering with a Curie temperature of T_C = 302 K was reported [2]. In addition no evidence is found for

ferromagnetic ordering of Eu below the transition temperature range of $T_C \sim$ 9-13 K as reported in [2, 4]. Below 400 K $EuMn_2Si_2$ orders in a collinear antiferromagnetic arrangement with the magnetic space group $I_p4/m'm'm'$ and a Mn moment value of ~ 2.0 μ_B at 6 K (figure 10.11b). No evidence for additional reorientation transitions down to 6 K was observed, in contradiction with earlier magnetisation data [2].

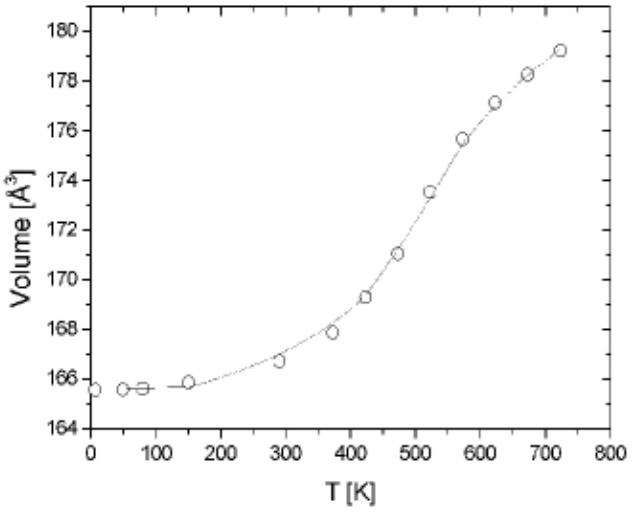

Figure 10.12: ICF-fit (solid line) to the volume data of $EuMn_2Si_2$

Valence Transition

The magnetic structure of $EuMn_2Ge_2$ is found to closely resemble the structure of the corresponding alkaline earth metal compounds $CaMn_2Ge_2$ and $BaMn_2Ge_2$ [5]. The relatively high value for the Mn moment is consistent with the values found for these earth alkaline compounds and has to be correlated to the Mn-Ge distances and the nature of the bond [5]. The lattice parameters determined for $EuMn_2Ge_2$ at ambient temperature in the present experiments (a = 4.24972(3) Å and c = 10.9084(2) Å) are very similar to the lattice parameters values of $SrMn_2Ge_2$ (a=4.30 Å and c=10.91 Å) [6]. Given that the ionic radii of Sr^{2+} and Eu^{2+} are almost identical this agreement in lattice parameter values provides evidence that Eu is in a 2+ valence state in $EuMn_2Ge_2$.

By comparison the Eu ions in $EuMn_2Si_2$ are reported to be almost trivalent at low temperatures with a change in the valence state above $\sim$ 350 K [2]. This finding is supported by the present results with our analysis revealing a significant increase in $EuMn_2Si_2$ lattice parameters (a = 4.08588(6) Å and c = 10.6778(3) Å) above $\sim$ 350 K. As shown in figure 10.12 the thermally driven change in valence state is reflected by the increase in unit cell volume by about 7 % from $\sim$ 300 K to 723 K. The Mössbauer results were successfully considered in terms of the interconfigurational fluctuation (ICF) model [7, 8]. In this model the rare earth ions can be described as fluctuating in time between two configurations, each configuration being characterised by a different integral occupation of the 4f-shell. Assuming that the ground state is Eu^{3+}, the occupation probabilities of Eu^{2+} and Eu^{3+} states (represented by p_2 and p_3 are given by Boltzmann statistics as:

$$\frac{p_2}{p_3} = \frac{8e^{-E_{ex}/kT^*}}{1+3e^{-480/kT^*}+5e^{-1330/kT^*}}$$

where $p_2 + p_3 = 1$ and E_{ex} is the excitation energy required to convert the Eu^{3+} configuration into an Eu^{2+} configuration. The substitution $T^* = \sqrt{T^2 + T_F^2}$ is used to allow for broadening of the various energy levels. However a simple ICF model is insufficient to describe the rapid thermal variation of the mean valence in $EuMn_2Si_2$ [2]. Rather, such a sharp transition is interpreted as evidence for a co-operative phenomenon and has been discussed assuming a dependence of the excitation energy, E_{ex}, on the probability for a valence state p_2 in

the form $E_{ex} = E_0(1 - \alpha p_2)$ [8]. We have adapted this ICF theory to describe the volume changes above $\sim$ 350 K. Firstly, by assuming that the thermal expansion of the lattice can be described by extrapolation of the low temperature data (T < 300 K), the change in volume due to the valence change can then be fitted using $\Delta V_{val} = p_2(V^{2+} - V^{3+}) = p_2 \Delta V_0$, where ΔV_0 is a constant. As shown in figure 10.12 this model describes the change in volume well leading to the derived values: ΔV_0 = 16.8(9) Å^3, E_{ex} = 1690(10) K, T_F = 144(4) K and α = 1.09(2). Comparing the total change of the valence as determined from analysis of the Mössbauer data [2] to the value derived from the present volume analysis, we derive a value for the parameter p_2 $\sim$ 0.6 at 723 K. This value for the occupation probability of the Eu^{2+} state agrees well with the value p_2 = 0.57 at 723 K derived from the Mössbauer data [2]. This good agreement confirms that the volume change associated with the thermally driven valence change can be described well by the interconfigurational fluctuation model.

[1] A Szytula and J Leciejewicz, Handbook of Crystal Structures and Magnetic Properties of Rare Earth Intermetallics (CRC Press, Boca Raton, 1994)

[2] I Nowik, I Felner and E R Bauminger, Phys. Rev. B **55** (1997)

[3] M Hofmann, S J Campbell and AV J Edge (in preparation, 2002)

[4] I Felner and I Nowik, J. Phys. Chem. Solids **39** (1978) 763

[5] B. Malaman, G. Venturini, R. Welter and E. Ressouche, J. Alloys Comp. **210** (1994) 209

[6] W Dorrscheidt, N Niess and H Schafer, Z. Naturf. B **31** (1976) 890

[7] B C Sales and D K Wohlleben, Phys. Rev. Lett. **35** (1975) 1240

[8] M Croft, J A Hodges, E Kemly, A Krishan, V Nurgai and L C Gupta, Phys. Rev. Lett. **48** (1982) 82

10.6 Influence of Gaps in Shieldings against Neutron Radiation

F. Grünauer(1)
(1)Technische Universität München, Physik-Department E21

In most neutron experiments it is neither desirable nor possible to construct radiation shieldings in one piece. There would arise problems with the assembly, the accessibility, and flexibility. Therefore a modular construction has to be preferred. The single modules cannot be shaped to a precision that there will be no gaps between the elements. Gaps of up to some millimeters may occur inside the final shielding construction. For the new neutron radiography station at Munich´s new neutron source (FRM-II), we have the requirement that parts of the shielding can be moved on top of the lateral

walls. Gaps between these parts and the walls are needful therefore. It is necessary to estimate the leakage of radiation through these gaps. The estimation was done by

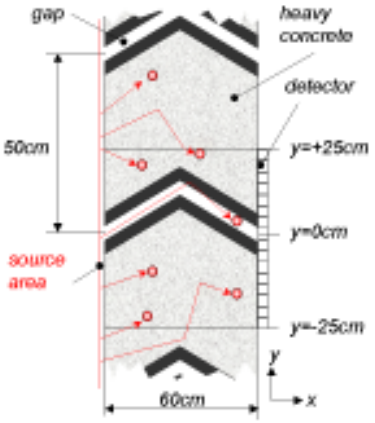

Figure 10.13: Monte Carlo Model for the estimation of neutron radiation transport through gaps

Monte Carlo Method. The neutrons are emitted from an area source on one side of the shielding. The dose on the opposite side of the shielding is calculated with a spatial resolution of 2mm. The shielding is infinite long and high. The gaps are repeated with a period of 50cm. The shielding material is heavy concrete (density: 3.5g/cm^3) with colemanite, hematite, and steel resin as additives.

Three different shapes of gaps were examined (fig. 10.14)

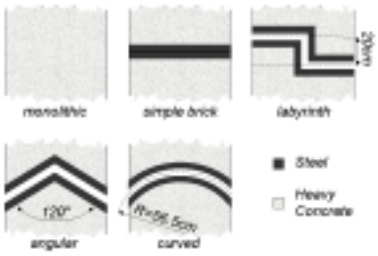

Figure 10.14: Gap configurations in radiation shieldings: A: monolithic, B: simple brick, C: labyrinth (two 90° bends), D: angular (one 120° bend), E: curved gap

- Curved
- Angular: one bend with an angle of 120°
- Labyrinth: two 90° bends, 20cm offset

or all shapes a gap width of 1cm was assumed. The elements are coated by a steel liner of 1cm thickness along the gap. For comparison two additional ´ideal´ configurations were calculated (fig. 10.14):

- Monolithic: homogeneous, no gaps
- Simple brick: coated by 1cm steel, no gaps

Factors of increase of the neutron dose outside the different shielding types compared to the monolithic shielding are shown in fig. 10.15 for an isotropic source. The ´average´ values show the average dose increase in the total detector area, and the peak values the increase at the gap mouth.

The curved structure

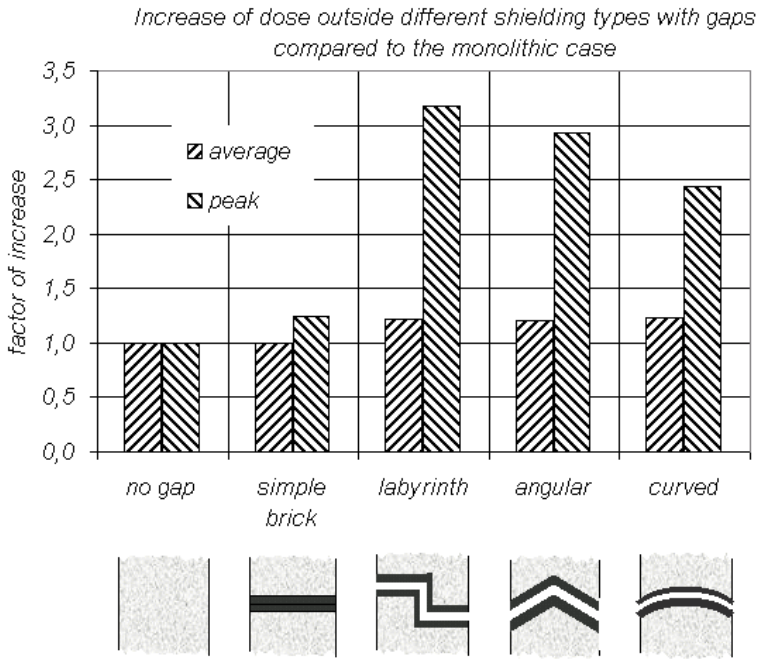

Figure 10.15: Factors of neutron dose increase outside the different shielding types compared to the monolithic shielding for an isotropic source

shows the lowest and the labyrinth shows the highest dose peak at the gap mouth. However, the dose integral in the entire detector area is in all cases 20% above the integral dose without gap. The shielding power does not so much depend on the type of gaps.

The situation changes completely for a parallel beam (neutrons enter the shielding perpendicular). The dose outside of the different gap systems for a parallel beam is shown in fig. 10.16.

The labyrinth with two 90° bends increases the dose considerably more than all other gap systems (78% in the total detector area). Two distinct dose peaks appear at the position of the two parallel gap parts. The bad shielding quality of the labyrinth for a parallel beam is obvious: The transmission through both parallel parts of the gap (gap entrance and gap exit) is enormous. All other gaps show even better results than for the isotropic beam.

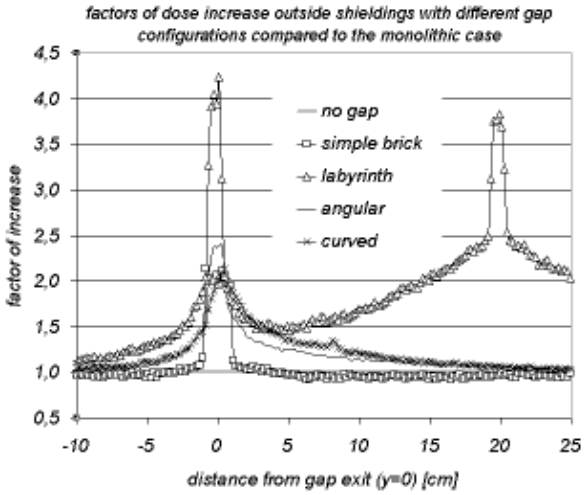

Figure 10.16: Spatial neutron dose distribution outside of shieldings with different gap configurations for a parallel source (gap width=1cm)

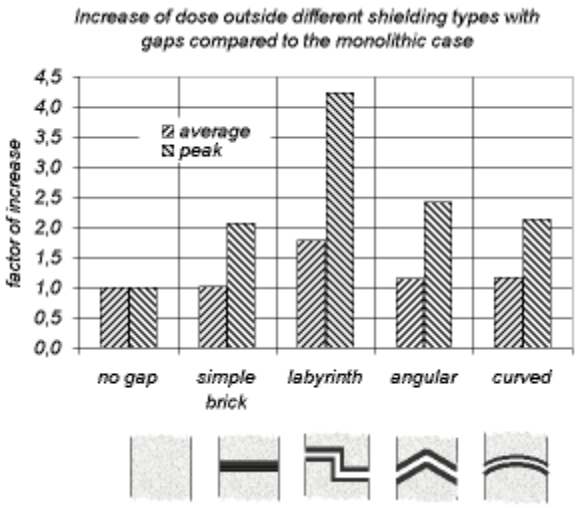

Figure 10.17: Factors of neutron dose increase outside the different shielding types compared to the monolithic shielding for a parallel source. The average values show the average dose increase in the total detector area, and the peak values the increase at the gap mouth

Facts and Figures

11.1 Public Relations

The ongoing public interest of the FRM-II resulted in almost 3500 visitors in 2002. Among them were pupils, students, politicians, clubs and societies, business people, journalists and last but not least scientists from all over the world. Almost every day a visitor group came to Garching. They were guided through the reactor building by a large number of members from our institut. The highlight for our visitor service in 2002 was the open day of the campus on Saturday, 23rd November. Here 550 persons visited the FRM-II, and almost twice as much wanted to use the opportunity. However, due to formal limitations the number of visitors could not be increased that day.

In addition to their activities on site, many scientists gave public talks about research with neutrons and the new neutron source FRM-II. In two editions of the universities' newspaper 'Nachbarschaftszeitung', which is distributed in neighbouring villages, people were informed about research at the Garching campus. Of course, our public relation activities were determined by the current situation of the licencing procedure. We pointed out in press releases, talks with journalists and newspaper articles that the state of stagnancy

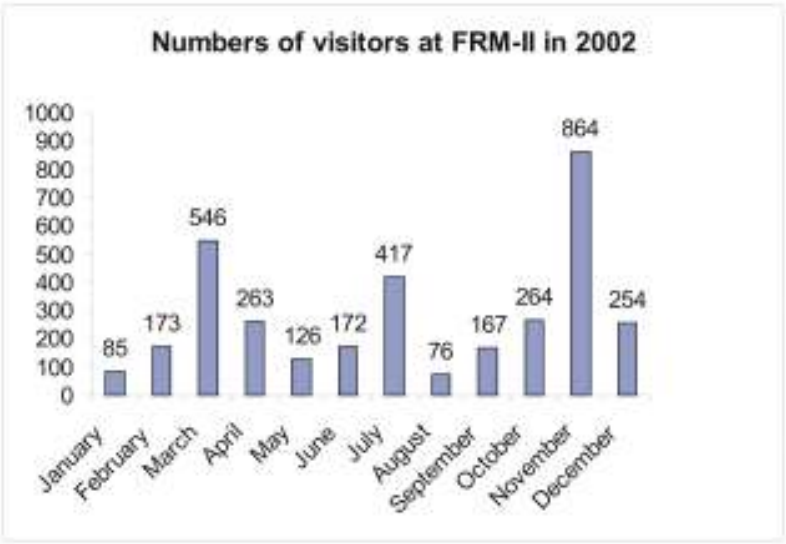

Figure 11.1: Visitors at the FRM-II in 2002

leads to an irreparable loss of scientific know-how. Scientists from Technische Universität München and other universities or science organisations send letters to the chancellor of Germany, to ministers and members of parliament to call their attention to the FRM-II.

The German version of the brochure ‚Experimental facilities at FRM-II' was published in a completely revised edition in December 2002. Primarily it addresses scientists who want to do experiments at the neutron source. The brochure describes all instruments, beam tubes, secondary beam sources and irradiation facilities in detail and overviews planned research projects. Progress in experimental design within the last two years and changes of technical and scientific staff have been considered. A copy as well as former publications from the FRM-II can be ordered at the visitor service (tel. +49 89 289-12147).

Our Internet site has been revised and provides now detailed and well-illustrated up-to-date informations.

11.2 Instrument Groups

ANTARES
Prof. Dr. Peter Böni
TU München
Physik Department E21
James-Frank-Str. 1
D-85747 Garching

HEIDI
Prof. Dr. Gernot Heger
RWTH Aachen
Institut für Kristallographie
Jägerstr. 17-19
D-52056 Aachen

MAFF
Prof. Dr. Dietrich Habs
LMU München
Sektion Physik
Am Coulombwall 1
D-85748 Garching

MatSci-R
Prof. Dr. Helmut Dosch
Max-Planck-Institut für Metallforschung
Heisenbergstr. 1
D-70569 Stuttgart

MEPHISTO
Prof. Dr. Oliver Zimmer
Technische Universität München
Physik Department E18
James-Franck-Str. 1
D-85747 Garching

Dr. Hartmut Abele
Physikalisches Institut
Universität Heidelberg
Philosophenweg 12
D-69120 Heidelberg

MIRA
Prof. Dr. Peter Böni
TU München
Physik Department E21
James-Frank-Str. 1
D-85747 Garching

NECTAR
Prof. Dr. Andreas Türler
Technische Universität München
Institut für Radiochemie
Walter-Meissner-Str. 3
D-85747 Garching

NRSE-TAS
Prof.Dr. Bernhard Keimer
Max-Planck-Institut
für Festkörperforschung
Heisenbergstraße 1
D-70569 Stuttgart

PANDA
Prof. Dr. Michael Loewenhaupt
TU Dresden
Institut für Angewandte Physik
D-01062 Dresden

PGA, Nuclear Spectroscopy
Prof. Dr. Andreas Türler
Technische Universität München
Institut für Radiochemie
Walter-Meissner-Str. 3
D-85747 Garching

Prof. Dr. Jan Jolie
Universität zu Köln
Institut für Kernphysik
Zülpicherstr. 77
D-50937 Köln

Positron Source
Prof. Dr. Werner Triftshäuser
Universität der Bundeswehr München
Institut für Nukleare Festkörperphysik
Werner Heisenberg Weg 39
D-85579 Neubiberg

Prof. Dr. Klaus Schreckenbach
Technische Universität München
ZWE FRM-II
D-85747 Garching

PUMA
Prof. Dr. Götz Eckold
Georg-August-Universität Göttingen
Institut für Physikalische Chemie
Tammannstraße 6
D-37077 Göttingen

Dr. Jürgen Neuhaus
TU München
ZWE FRM-II and Physik Department E13
D-85747 Garching

REFSANS
Prof. Dr. Erich Sackmann
Technische Universität München
Physik Department E22
James-Franck-Str.1
D-85747 Garching

Dipl.-Phys. Reinhard Kampmann
GKSS-Forschungszentrum
Institut für Materialforschung
Max-Planck-Str. 1
D 21502 Geesthacht

RESI
Prof. Dr. Friedrich Frey
LMU München
Institut für Kristallographie
Theresienstr. 41
D-80333 München

Dr. Wolfgang Scherer
Universität Augsburg
Institut für Physik
Lehrstuhl für chemische Physik und Material-wissenschaften
D-86135 Augsburg

Rückstreuspektrometer
Prof. Dr. Dieter Richter
Forschungszentrum Jülich
Institut für Festkörperforschung
D-52425 Jülich

SPODI
Prof. Dr. Hartmut Fueß
Technische Hochschule Darmstadt
Strukturforschung
FB Material- u. Geowissenschaften
Petersenstr. 23
D 64287 Darmstadt

Dr. Hans Boysen
LMU München
Institut für Kristallographie
Am Coulombwall 1
D 85748 Garching

STRESS-SPEC
Dr. Reiner Schneider
Hahn-Meitner Institut
Glienickerstr. 100
D-14100 Berlin

Prof. Dr. W. Reimers
Technische Universität Berlin
Metallphysik BH18
Ernst-Reuter-Platz 1
D 10587 Berlin

Dr. Heinz-Günter Brokmeier
TU Clausthal Institut für Werkstoffkunde
c/o GKSS- Forschungszentrum Abt. WTUC
Max-Planck-Str., Geb. 03
D-21502 Geesthacht

TOFTOF
Prof. Dr. Winfried Petry
Technische Universität München
Physik Department E13 und ZWE FRM-II
James-Frank-Str.1
D 85747 Garching

UCN Source
Prof. Dr. Stephan Paul
Technische Universität München
Physik Department E 18
James-Franck-Str. 1
D-85747 Garching

11.3 Committees

TUM advisory board

Chairman
Prof. Dr. Ewald Werner
Lehrstuhl für Werkstoffkunde und -mechanik
Technische Universität München

Members

Prof. Dr. Peter Böni
Physik Department E21
Technische Universität München

Prof. Dr. Andreas Türler
Institut für Radiochemie
Technische Universität München

Prof. Dr. Markus Schwaiger
Nuklearmedizinische Klinik und Poliklinik
Klinikum rechts der Isar
Technische Universität München

Prof. Dr. Bernhard Wolf
Heinz Nixdorf-Lehrstuhl für medizinische Elektronik
Technische Universität München

Prof. Dr. Arne Skerra
Lehrstuhl für Biologische Chemie
Technische Universität München

Guests

Dr. Markus Busold
University Management
Technische Universität München

Guido Engelke
ZWE FRM-II
Technische Universität München

Prof. Winfried Petry
ZWE FRM-II
Technische Universität München

Prof. Klaus Schreckenbach
ZWE FRM-II
Technische Universität München

Instrumentation advisory board

Chairman
Prof. Dr. Götz Eckold
Institut for Physical Chemistry
Georg-August-Universität Göttingen

Members
Prof. Dr. Dieter Habs
Sektion Physik
Ludwig-Maximilian-Universität München

Prof. Dr. Peter Böni
Physik Department E21
Technische Universität München Prof. Dr.

Dirk Dubbers
Physikalisches Institut
Universität Heidelberg

Dr. Hans Graf
Abteilung NE
Hahn-Meitner-Institut, Berlin

Prof. Dr. Andreas Magerl
Chair for Crystallography and Structural Physics
Friedrich-Alexander-Universität Erlangen-Nürnberg

Prof.Dr. Gottfried Münzenberg
Gesellschaft für Schwerionenforschung mbH, Darmstadt

Prof. Dr. Wolfgang Scherer
Lehrstuhl für Chemische Physik
Universität Augsburg

Dr. habil. Dieter Schwahn
Forschungszentrum Jülich
Institut für Festkörperforschung

Prof. Dr. Markus Schwaiger
Lehrstuhl für Nuklearmedizin
Technische Universität München

Prof. Dr. Andreas Türler
Institut für Radiochemie
Technische Universität München

Dr. habil. Regine Willumeit
GKSS Forschungszentrum, Geesthacht

Guests
Dr. Markus Busold
University Management
Technische Universität München

Dr. Klaus Feldmann
BEO-PFR
Forschungszentrum Jülich

Ministerialdirigent Jürgen Großkreutz
Bayrisches Staatsministerium für Wissenschaft, Forschung und Kunst

Prof. Dr. Gernot Heger
RWTH Aachen Institut für Kristallographie

Dr. Felix Köhl
Bayerisches Staatsministerium für Wissenschaft, Forschung und Kunst

Dr. Maximilian Lang
Bayerisches Staatsministerium für Wissenschaft, Forschung und Kunst

Dr. Jürgen Neuhaus
ZWE-FRM-II
Technische Universität München

Prof. Dr. Winfried Petry
ZWE-FRM-II
Technische Universität München

Prof. Dr. W. Press
Institut Laue Langevin
Grenoble, France

Prof. Dr. Klaus Schreckbach
ZWE FRM-II
Technische Universität München

Prof. Dr. Tasso Springer

11.4 Staff

Board of Directors

Scientific director:
Prof. Dr. W. Petry
Technical director:
Prof. Dr. K. Schreckenbach
Administrative director:
G. Engelke

Experiments

Head:
Prof. Dr. W. Petry
Secretaries:
E. Doll
W. Wittowetz
Coordination:
Dr. J. Neuhaus

Figure 11.2: Experiments staff

Instruments

H. Bamberger
M.Bleuel
J. Brunner
E. Calzada
D. Etzdorf
J. Franke (MPI-Stuttgart)
Dr. R. Georgii
Dr. R. Gilles (TU-Darmstadt)
F. Grünauer
Dr. E. Gutsmiedl
Dr. M. Hofmann
Dr. K. Hradil (Univ. Göttingen)
Dr. C. Hugenschmidt
N. Kardjilov
Dr. T. Keller (MPI-Stuttgart)
B. Krimmer (TU-Darmstadt)
G. Langenstück
Dr. P. Link (Univ. Göttingen)
Dr. M. Meven
M. Misera
A. Müller
C. Müller
J. Neumann (Univ. Göttingen)
Dr. B. Pedersen
Dr. N. Pyka
R. Repper
J. Ringe
Dr. B. Schillinger
H. Schneider (MPI-Stuttgart)
G. Seidl
Dr .T. Unruh
Dr. W. Waschkowski
Dr. U. Wildgruber (MPI-Stuttgart)

Detectors and electronic

Dr. K. Zeitelhack
Dr. A. Kastenmüller
D. Maier
M. Panradl

Sample environment

Dr. J. Peters
H. Kolb
H. Niedermeier
A. Pscheidt
A. Schmidt
S. Sedlmair

Neutron optics

Prof. Dr. G. Borchert
C. Breunig
E. Kahle
Dr. S. Massalovitch
C. Schanzer
A. Urban

Instrument control and software

J. Krüger
S. Praßl
S. Roth

Networking and computers

J. Beckmann
J. Ertl
E. Heubl (until 1. Nov. 02)
J. Mittermaier
J. Pulz
F. Zoebisch

Public relations

Dr. W. Waschkowski
Dr. V. Klamroth (ZV, TUM)
J. Jeske
I. Maier

Guests

Dr. G. Horton, (ANSTO, Australia)

Administration

Head:
G. Engelke
Secretary:
C. Zeller
Members:
B. Bendak
B. Gallenberger
I. Heinath
R. Obermeier

Secretaries:
K. Lüttig
M. Neuberger
S. Rubsch

Management

Dr. H. Gerstenberg (irradiation and sources)
Dr. J. Meier (reactor projects)
Dr. C. Morkel (reactor operation)

Shift members

F. Gründer
A. Bancsov
A. Benke
M. Danner
M. Flieher
H. Groß
L. Herdam

Figure 11.3: Administration staff

Reactor operation

Head:
Prof. Dr. K. Schreckenbach

K. Höglauer
T. Kalk
G. Kaltenegger
U. Kappenberg
F. Kewitz
M. G. Krümpelmann
J. Kund
A. Lochinger
G. Mauermann
A. Meilinger
M. Moser
L. Rottenkolber
G. Schlittenbauer
N. Wiegner

Technical services

N. Waasmaier
J. Aigner
D. Bahmet
F. Doll
H. Gampfer
W. Glashauser
J. Groß
G. Guld
F. Hofstetter
M. Kleidorfer
W. Kluge
H. Kollmannsberger
J.-L. Krauß
R. Maier
K. Otto
A. Schindler
R. Schlecht jun.
J. Schreiner
H. Sedlmeier
C. Strobl
G. Wagner
A. Weber
J. Wetzl
C. Ziller

Electrics and electronics

R. Schätzlein
G. Aigner
W. Buchner
Ü. Sarikaya
H. Schwaighofer

Irradiation and sources

Dr. H. Gerstenberg
J.-M. Favoli
Dr. E. Gutsmiedl
Dr. X. Li
C. Müller
M. Oberndorfer
D. Päthe
M. Schmitt

Figure 11.4: Reactor operation staff

Chemical laboratory

Dr. F. Dienstbach
T. Asam
C. Auer
R. Bertsch

Reactor projects

Dr. J. Meier

Documentation

V. Zill
J. Jung

Safety

R. Lorenz

Technical design

F.-L. Tralmer
J. Fink
H. Fußstetter
J. Jüttner
W. Lange
K. Lichtenstein
P. Mross
M. Ullrich

Workshops

C. Herzog
U. Stiegel
A. Begic
M. Fuß
A. Huber
A. Scharl
R. Schlecht sen.
M. Tessaro

Radiation protection

Dr. H. Zeising
S. Dambeck
W. Dollrieß
Dr. H. Gerstenberg
H. Hottmann
Dr. J. Meier
B. Neugebauer
F. M. Wagner
S. Wolff
H.-J. Werth

Reactor physics

Prof. Dr. K. Böning
Dr. A. Röhrmoser

Security department

L. Stienen
J. Stephani

Nuclear safety

Dr. W. Waschkowski
D. Päthe

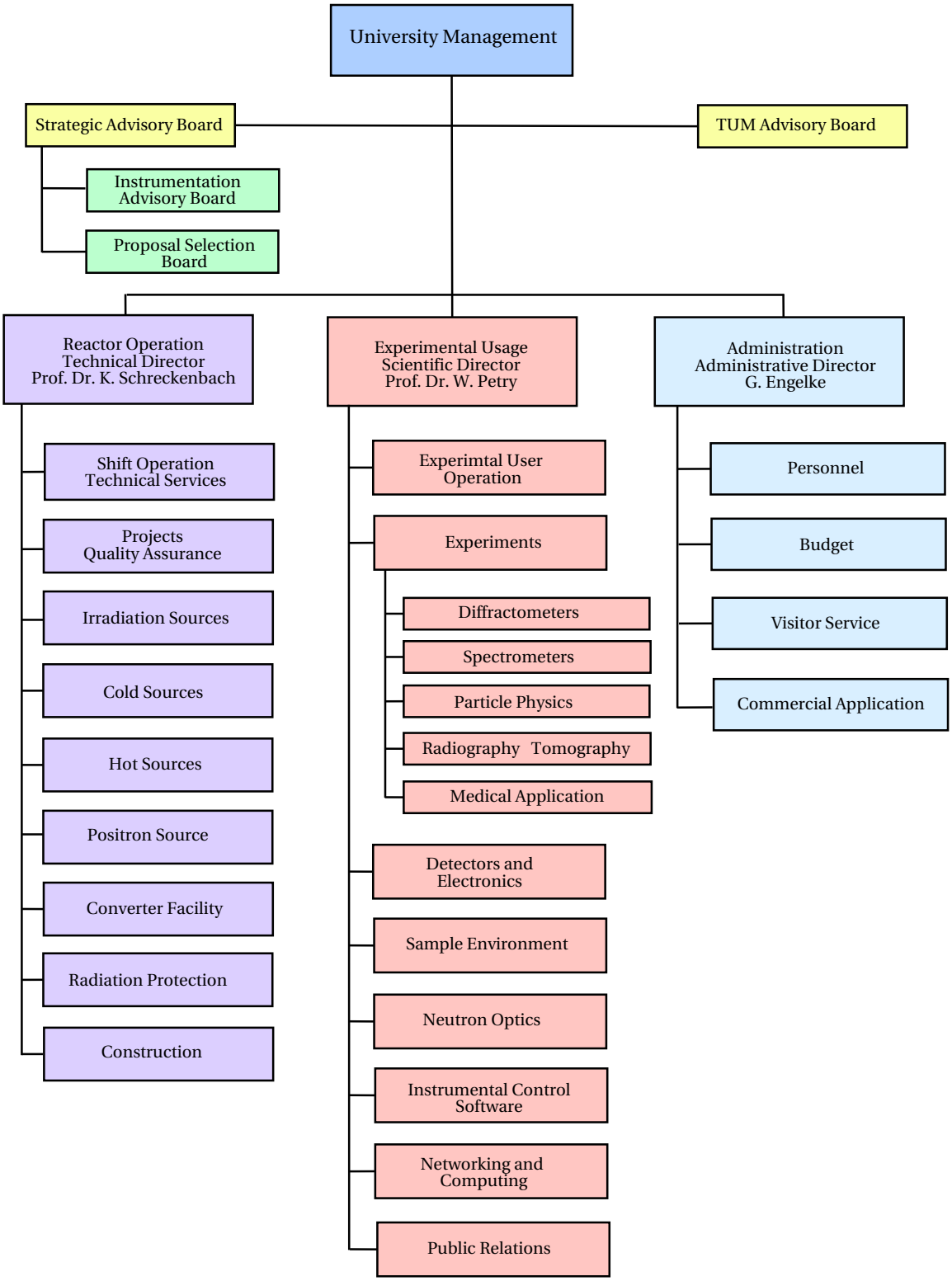
University Management
Strategic Advisory Board
TUM Advisory Board
Instrumentation Advisory Board
Proposal Selection Board
Reactor Operation Technical Director Prof. Dr. K. Schreckenbach
Experimental Usage Scientific Director Prof. Dr. W. Petry
Administration Administrative Director G. Engelke
Shift Operation Technical Services
Projects Quality Assurance
Irradiation Sources
Cold Sources
Hot Sources
Positron Source
Converter Facility
Radiation Protection
Construction
Experimtal User Operation
Experiments
Diffractometers
Spectrometers
Particle Physics
Radiography Tomography
Medical Application
Detectors and Electronics
Sample Environment
Neutron Optics
Instrumental Control Software
Networking and Computing
Public Relations
Personnel
Budget
Visitor Service
Commercial Application

Workshops

12.1 Realization of a ^{3}He facility at the FRM-II

G. L. Borchert, S. Massalovich, W. Petry
ZWE FRM II, Technische Universität München

There was a strong request to build a ^{3}He neutron spin-filter facility (NSF) at the FRM II for neutron polarization and analysis: at least 6 instruments need ^{3}He NSF to achieve the intended performance, namely 3 reflectometers (MatSci-R, RefSans, MIRA), the three axis spectrometer PUMA, the SANS and the particle physics facility, where ^{3}He NSF is the needed tool. Besides them, there is another series of instruments, namely the diffractometers (RESI, HEIDI) and the polarised-neutron-using TAS (PANDA, NRSE-TAS), where polarisation analysis with ^{3}He NSF is seen as future option. Therefore the decision was taken to build a ^{3}He neutron spin-filter facility on the reactor site. To discuss and clarify all the implications of such a project and to bring together the experts who operate such a facility and the instruments' responsibles, we organised a small workshop in Garching on July 4th 2002.

As first speaker Dr. Tasset presented the ILL polarized ^{3}He facility. After a general introduction about the technique and its historical development, he reported about recent challenging progress made at the ILL facility, mainly due to a new generation of Yb-fibre lasers, which allowed to reach ^{3}He polarizations of 70%. The latest installation at ILL will be operational after 2.5years build-time within the next few month. Another important point was his report about the *routine* use of ^{3}He neutron spin-filters at ILL by several instruments. Optimising the cell materials and preparation procedure relaxation times of 100h have been reproducibly reached.

As second speaker Prof. Heil presented the Mainz polarized ^{3}He facility. He gave an insight into the optical pumping technique, explaining requirements to the pump lasers and the recent progress made here. He also pointed out the mechanisms leading to the polarization relaxation in the cells, and to what can be done to come to reasonable relaxation times, suitable also for experiments with longer time-scale. He showed that their preparation methods guarantee to fabricate reproducibly cells with relaxation times around 200h . Inherent contributions arising from field-gradients and unavoidable dipolar interaction dominate now the wall-relaxation process. Also the compression process with a piston compressor has been discussed in detail.

The afternoon session was opened by short reports of four FRM-II instruments demanding for polarized ^{3}He. Thereafter a lively and fruitful round-table discussion followed where the main scientific and administrational implications were reviewed. A possible scenario for a duly realization was developed within the frame of a close collaboration with expert partners. The final conclusion was a clear vote for the envisaged project. There is general agreement about the necessity of a ^{3}He polarisation facility. A way to obtain such a facility at FRM-II is seen in a close

cooperation with partner laboratories at Mainz and Grenoble. This expert meeting stated a clear go ahead for a ^{3}He facility at FRM-II
In line with these recommendations we started an exchange of personnel with the University of Mainz and the ILL in Grenoble. The preparatory investigations on local FRM II infrastructure and laboratory realizations are on the way.

12.2 Workshop on Future Instruments for Nuclear and Particle Physics and Methods at the FRM-II

The Workshop on Future Instruments for Nuclear and Particle Physics and Methods at the FRM-II took place on April 12th, 2002 in Garching. The scope of the workshop was to bring together different groups of interest in the field of nuclear and particle physics as well as nuclear methods in view of the future experimental facilities at the new german neutron source FRM-II. Actually two large projects in these areas are under development at the FRM-II namely the Munich Fission Fragment Accelerator MAFF and the Ultra Cold Neutron Source. The motivation to organise the workshop was to discus new instruments beyond these large projects and possible applications of these sources, respectively.

List of Publications

H. Abele, M. Astruc Hoffmann, S. Baeßler, D. Dubbers, F. Glück, U. Müller, V. Nesvizhevsky, J. Reich, O. Zimmer, *Is the unitarity of the quark-mixing CKM matrix violated in neutron beta decay?*, Phys. Rev. Lett., **88**, 211801 (2002)

P. Allenspach, P. Böni, K. Lefmann, *Loss Mechanism in Supermirror Neutron Guides*, SPIE, **4509**, 157-165 (2001)

A. Axmann, K. Böning, M. Nuding, H.-J. Didier, *FRM-II Status of Construction, Licensing and Fuel Tests*, Proc. of the 5th Int. Topical Meeting on Research Reactor Fuel Management, European Nuclear Society, Bern, Switzerland (ENS RRFM2001), 1 (2001)

J. Beckmann, P. Link, T. Unruh, N. Pyka, D. Etzdorf, *Common Data File Definitions for Neutron Inelastic Scattering Instruments using NeXus*, http://arxiv.org/abs/cond-mat/0210437, (2002)

M. Böhmer, T. Eberl, A. Elhardt, L. Fabbietti, J. Friese, R. Gernhäuser, J. Homolka, A. Kastenmüller, P. Kienle, H.-J. Körner, P. Maier-Komor, M. Münch, B. Sailer, W. Schön, A. Ulrich, J. Wieser, K. Zeitelhack, *Lepton identification with CsI based RICH of HADES*, Nucl. Instr. and Meth., **A471**, 25-29 (2001)

H. Bongers, M. Groß, D. Habs, H.-J. Maier, T. Sieber, P. G. Thirolf, O. Kester, U. Köster, T. Faestermann, T. v. Egidy *Production of Intense Beams of Fission Fragments at MAFF*, Rev. Sci. Inst., **73**, 809 (2002)

P. Böni, B. Roessli, D. Görlitz, J. Kötzler, *Damping of Spin Waves and Singularity of the Longitudinal Modes in the Dipolar Critical Regime of the Heisenberg-Ferromagnet EuS*, Phys. Rev.B, **65**, 144434 (2002)

K. Böning, *IGORR8: Weltkonferenz zu Forschungsreaktoren in München". Internationale Zeitschrift für Kernenergie*, ATW, **46,6**, 411 (2001)

K. Böning, *Uran hoher Anreicherung am FRM-II*, Internationale Zeitschrift für Kernenergie ATW, V, **46,11**, 705 (2001)

Klaus Böning, *Use of Highly Enriched Uranium at the FRM-II*, Proc. of the 6th Int. Topical Meeting on Research Reactor Fuel Management, European Nuclear Society, Bern, Switzerland (ENS RRFM2002), 73 (2002)

K. Böning, W. Petry, C. Schanzer, E. Steichele, *Neutronenleitersysteme am FRM-II jenseits der Totalreflexion*, Jahrestagung Kerntechnik, Deutsches Atomforum e.V., INFORUM Verlags- und Verwaltungsgesellschaft, Bonn, 621 (2001)

G. L. Borchert, B. Manil, D. Anagnosopoulos, M. Augsburger, J. P. Egger, D. Gotta, P. Hauser, M. Hennebach, P. Indelicato, Y. W. Liu, N. Nelms, Th. Siems, L. M. Simon, *Precision Measurement of the Pion Mass by High Resolution X-Ray Spectroscopy*, Hyperfine Interactions, **132**, 195 (2001)

H. Boysen, M. Lerch, R. Gilles, B. Krimmer, D.M. Többen, *Structure and ionic conductivity in doped LaGaO3*, Appl. Phys., A, **74, Suppl.**, 966-968 (2002)

M. Braden, M. Meven, W. Reichardt, L. Pintschovius, M.T. Fernandez-Diaz, G. Heger, F. Nakamura, T. Fujita, *Analysis of the Local Structure by Single-Crystal Neutron Scattering in* $La_{1.85}Sr_{0.15}CuO_4$, Phys. Rev. B,

63, 140510 (2001)

B van den Brandt, E. Fanchon, J. Gaillard, H. Glättli, I. Grillo, M. van der Grinten, P. Hautle, H. Jouve, R. Kahn, J. Kohlbrecher, J. A. Konter, S. Mango, R. May, E. Leymarie, H. B. Stuhrmann, R. Willumeit, O. Zimmer, *Contrast enhancement in polarised neutron scattering by selective proton polarisation in macromolecules*, Proceedings of the ILL millennium symposium, Institut Laue Langevin, Grenoble, France (2001)

B. van den Brandt, H. Glättli, I. Grillo, P. Hautle, H. Jouve, J. Kohlbrecher, J. A. Konter, E. Leymarie, S. Mango, R. May, H. B. Stuhrmann, O. Zimmer, *Neutron scattering from polarized proton domains*, Europhys. Lett., **59**, 62 (2002)

B. van den Brandt, H. Glättli, I. Grillo, P. Hautle, H. Jouve, J. Kohlbrecher, J. A. Konter, E. Leymarie, S. Mango, R. May, H. B. Stuhrmann, O. Zimmer, *Neutron scattering from polarized proton domains*, Proceedings of the International Workshop on Polarized Neutrons in Condensed Matter Investigations, Germany, (2002)
Eurphys. Lett. **59**, 62 (2002)

B. van den Brandt, H. Glättli, I. Grillo, P. Hautle, H. Jouve, J. Kohlbrecher, J. A. Konter, E. Leymarie, S. Mango, R. May, H. B. Stuhrmann, O. Zimmer, *Polarized proton domains in matter*, Proc. of the 9th Int. Workshop on Polarized Sources and Targets, Nashville, Indiana, USA. World Scientific (2002)

A. Braun, K.M. Briggs, P. Böni, *Analytical Solution for Matthews and Blakeslee´s Critical Dislocation Formation Thickness of Expitaxially Grown Thin Film*, J. Crystal Growth, **241, 1-2**, 231 (2002)

J. Byrn, P.G. Dawber, M. G. D. van der Grinten, C.G. Habeck, F. Shaikh, J. A. Spain, R. D. Scott, C. A. Baker, K. Green, O. Zimmer, *Determination of the electron-antineutrino angular correlation coefficient a_0 and the parameter $\lambda = g_A / g_V$ in free neutron β-decay from measurements of the integrated energy spectrum of recoil protons stored in an ion trap*, J. Phys. G: Nucl. Part. Phys., **28**, 1325 (2002)

G. S. Case, M. F. Thomas, C. A. Lucas, D. Mannix, S. Tixier, S. Langridge *Magnetic Anisotropy in Ce/Fe and Ce/FeCoV Multilayers*, J. Phys. Condens. Matter, **13**, 9699-9712 (2001)

E. Collet, M. Buron-Le Cointe, M.H. Lemée-Cailleau, H. Cailleau, L. Toupet, M. Meven, S. Mattauch, G. Heger, N. Karl, *Structural Evidence of Ferrielectric Neutral-Ionic Layered Ordering in 2,6-Dimethyltetrathiafulvalene-p-Chloranil*, Phys. Rev. B, **63**, 054105, (2001)

H. Ehrhardt, S. J. Campbell, M. Hofmann, *Structural evolution of Ball-milled $ZnFe_2O_4$* J. Alloys Comp. **339** 255 (2002)

F. Elf, R. Gilles, G. R. J. Artus, S. Roth, *A new method of Debye-Scherrer pattern integration on two-dimensional detectors, demonstrated for the new structure powder diffractometer (SPODI) at the FRM-II in Garching*, Appl. Phys. A, **74, Suppl.**, 1477-1479 (2002)

R. Georgi, S. Plüschke, R. Diehl, G. G. Lichti, V. Schönfelder, H. Bloemen, W. Hermsen, J. Ryan, K. Bennett, *COMPTEL upper limits for the ^{56}Co γ-Ray Emission from SN1998bu*, Astronomy & Astrophysics A&A, **394**, 517-523 (2002)

R. Gilles, B. Krimmer, H. Boysen, H. Fuess, *Status of the new Structure Powder Diffractometer (SPODI) at the FRM-II in Garching*, Appl. Phys., A **74, Suppl.**, 148-150 (2002)

R. Gilles, B. Krimmer, J. Saroun, H. Boysen, H. Fuess, *The Concept of the New Structure*

Powder Diffractometer (SPODI) at the FRM-II in Garching, Materials Science Forum, **378-381**, 282 (2001)

R. Gilles, D. Mukherji, P. Strunz, D.M. Többens, B. Barbier, J. Rösler, *Neutron-, X-ray- and electron diffraction measurements for the determination of γ/γ' lattice misfits in Ni-base superalloys*, Appl. Phys., A, **74, Suppl.**, 1446-1448 (2002)

R. Gilles, D. Mukherji, P. Strunz, A. Wiedenmann, J. Roesler, H. Fuess, *Small-Angle Neutron Scattering Investigation of γ' phase dissolution in Re-rich Ni-base Superalloy*, THERMEC, eds. T. Chandra, K. Higashi, C. Suryanarayana, C. Tome, Elsevier Science, Ltd., Oxford, J. of Materials Processing Technology, **Sec.D7, Vol 117/3** (2001)

R. Gilles, D. Strunz, D. Mukherji, S. Roth, A. Wiedenmann, J. Rösler, H. Fuess, *Small-Angle Scattering, a Tool to characterize Ni-base Superalloys at High Temperature*, Acta Cryst. A, **58 Suppl.**, C26 (2002)

P. Hautle, W. Heil, D. Hofmann, H. Humblot, T.M. Müller, O. Zimmer, *Opaque spin filters – a new tool for precise neutron polarimetry*, Proc. of the 9th Int. Workshop on Polarized Sources and Targets, Nashville, Indiana, USA, World Scientific, (2002)

M. Hofmann, S. J. Campbell, A. V. J. Edge, *Valence and Magnetic Transitions in* $YbMn_2S_{2i-x}Ge_x$, Appl. Phys. A, **74, Suppl.**, 713 (2002)

M. Hofmann, S. J. Campbell, W. A. Kaczmarek, *Mechanochemical Treatment of* α-Fe_2O_3*-Mircostructural Analysis* Appl. Phys. A, **74, Suppl.**, 1233 (2002)

M. Hofmann, S. J. Campbell, K. Knorr, S. Hull, V. Ksenofontov, *Pressure-Induced Magnetic Transitions in* $LaMn_2Si_2$, J. Appl. Phys., **91**, 8126 (2002)

C. Hugenschmidt, G. Kögel, R. Repper, K. Schreckenbach, P. Sperr, B. Straßer, W. Triftshäuser, *Monoenergetic Positron Beam at the Reactor Based Positron Source at FRM-II*, Nucl. Inst. Meth. B, **192,1-2**, 97-101 (2002)

C. Hugenschmidt, G. Kögel, R. Repper, K. Schreckenbach, P. Sperr, B. Straßer, W. Triftshäuser, *Intense Positron Source at the Munich Research Reactor FRM-II*, Appl. Phys. A, **74**, 283 (2002)

C. Hugenschmidt, G. Kögel, K. Schreckenbach, P. Sperr, B. Straßer, W. Triftshäuser, *Intense Positron Source at the Munich Research Reactor FRM-II*, Mat. Sci. Forum, **363-365**, 425-429 (2001)

C. Hugenschmidt, G. Kögel, R. Repper, K. Schreckenbach, P. Sperr, W. Triftshäuser, *First Platinum Moderated Positron Beam Based on Neutron Capture*, Nucl. Instr. Meth. B, **198**, 220 (2002)

C. Hugenschmidt, G. Kögel, K. Schreckenbach, P. Sperr, B. Straßer, W. Triftshäuser, *Intense Positron Source at the Munich Research Reactor FRM-II*, Proc. of IGORR-8 International Group on Research Reactors, 139-142 (2001)

C. Hugenschmidt, K. Schreckenbach, B. Straßer, *Investigation of Positron Work Function and Moderation Efficiency of Ni, Ta, Pt and W(100)*, Appl. Surf. Sci., **194,1-4**, 283 (2002)

A. Illing, T. Unruh, K. Westesen, M. H. J. Koch, *Structural Characterization of the Self-Assemblies of Suspended Triglyceride Nanocrystals using SAXS*, Arch. Pharm. Pharm. Med. Chem., **334, Suppl. 2**, 1-89 (2001)

A. Illing, T. Unruh, K. Westesen, M. H. J. Koch, *Particle self-assembly in tripalmitin nanosuspensions - a SAXS study*, Proc. 4th World Meeting ADRITELF/APGI/APV,

Florence, (2002)

P. Jesinge, A. Kötzle, F. Gönnenwein, M. Mutterer, J. von Kalben, G. V. Danilyan, G. A. Pavlov, G. A. Petrov, A. M. Gagarski, W. H. Trzaska, S. M. Soloviev, V. V. Nesvizhevsky, O. Zimmer, *Angular correlations in ternary fission induced by polarized neutrons*, Yad. Fiz., **65**, 662 (2002)

M. Kenzelmann, A. Zheludev, S. Raymond, E. Ressouche, T. Masuda, P. Böni, K. Kakurai, I. Tsukada, K. Uchinokura, R. Coldea, *Spin Waves and Magnetic Ordering in the Quasi-one-dimensional S = 1/2 Antiferromagnet $BaCu_2Si_2O_7$*, Phys. Rev. B, **64**, 054422 (2001)

O. Kester, D. Habs, M. Groß, H.-J. Maier, P. G. Thirolf, T. Sieber, T. Faestermann, T. v. Egidy, U. Köster *RNB production with thermal neutrons*, Nucl. Phys., **A 701**, 71 (2002)

B. Krimmer, R. Gilles, K. Zeitelhack, R. Schneider, G. Montermann, H. Boysen, H. Fuess, *A new detector system for the structure powder diffractometer (SPODI) at the FRM-II in Garching*, Applied Physics, A **74, Suppl.**, 154-156 (2002)

P. Link, *PUMA - Ein neues Großforschungsgerät für die Festkörperforschung*, Spektrum Universität Göttingen (ISSN 0945-3512), **1**, 18 (2001)

H.-J. Maier, D. Habs, M. Groß, R. Großmann, O. Kester, P. Thirolf *Target Development for the Munich Fission Fragment Accelerator*, NiMA, **480**, 1 (2002)

P. Maier-Komor, J. Friese, R. Gernhäuser, J. Homolka, A. Kastenmüller, H.-J. Körner, A. Ulrich, K. Zeitelhack, *VUV reflective coatings on thin concave float glass substrates with a perimeter of 86cm to be used as provisional HADES RICH mirror segments*, Nucl. Instr. and Meth., **A480**, 65-70 (2002)

J.-M. Mignot, A. Gusasov, C. Yang, P. Link, T. Matsumara, T. Suzuki, *Antiferroquadrupolar Order in the Magnetic Semiconductor TmTe*, J. Phys. Soc. Jpn. Suppl., **71**, 39-44 (2002)

Yu. A. Mostovoi, I. A. Kuznetsov, V. A. Solovei, A. P. Serebrov, I. V. Stepanenko, T. K. Baranova, A. V. Vasiliev, Yu. P. Rudnev, B.G. Yerozolimsky, M. S. Dewey, F. Wietfeldt, O. Zimmer, V. V. Nesvizhevsky, *Experimental value of g_A/g_V from a measurement of both P-odd correlations in free-neutron decay*, Yad. Fiz. **64**, 2040 (2001); Physics of Atomic Nuclei **64**, 1955 (2001)

D. Mukherji, P. Strunz, R. Gilles, J. Rösler, A. Wiedenmann, H. Fuess, *In situ SANS investigation of precipitate microstructure at elevated temperatures in Re-rich Ni-base superalloy*, Appl. Phys. A, **74, Suppl.**, 1074-1076 (2002)

N. Nelms, D. Anagnostopoulos, O. Ayranov, G. L. Borchert, J. P. Egger, D. Gotta, M. Hennebach, P. Indelicato, B. Leoni, Y. W. Liu, B. Manil, L. M. Simons, A. Wells, *A Large Area CCD X-Ray Detector for Exotic Atom Spectroscopy*, Nucl. Inst. Meth. A, **484**, 419 (2002)

J. Neuhaus, *Concept and Research Program of the New Research Neutron Source FRM-II*, Transactions of the American Nuclear Society, TANSAO 86, **86**, 9 (2002)

K. Nikolaus, J. Neuhaus, W. Petry, J. Bossy, *Phonon dispersion of bcc cerium*, Eur. Phys. J. B., **21**, 357 (2001)

R. Nirmala, A.V. Morozkin, M. Hofmann, V. Sankraharayanan, K. Sethupathi, Y. Yamamoto, H. Hori, *Magnetic Structure of $Tb_2Mn_3Si_5$*, J. Alloys Comp., **335**, 47 (2002)

M. Nuding, K. Böning, *Bestrahlungstests an U_3Si_2-Al Brennstoffen bis zu sehr hohen*

Spaltungsdichten, Internationale Zeitschrift für Kernenergie ATW, **46,6**, 417-419 (2001)

M. Nuding, K. Böning, *Irradiation Testing of U3Si2-Al Fuels up to Very High Fission Densities*, Proc. of the 8th Meeting of the Int. Group on Research Reactors (IGORR8), München, Germany, 273 (2001)

M. Pissas, G. Kallias, M. Hofmann, D. M. Többen, *Crystal and Magnetic Structure of* $La_{1-x}Ca_xMnO_3$ *Compounds (x=0.8, 0.85)*, Phys. Rev. B, **65**, 1 (2002)

Yu. V. Petrov, M. S. Onegin, K. Böning, M. Nuding, *Heterogeneous Effects at FRM-II*, Proc. of the 8th Meeting of the Int. Group on Research Reactors (IGORR8), München, Germany, 259 (2001)

Yu. V. Petrov, M. S. Onegin, K. Böning, M. Nuding, *Heterogeneous Calculations of FRM-II*, Russian Academy of Sciences, Petersburg Nuclear Physics Institute (PNPI), Gatchina, Russia (2001)

W. Petry, *High resolution Spectroscopy at FRM-II, Neutron Reource Spin Echo, Back Scattering and Time-of-Flight Instrumentation*, J. Phys. Soc. Jpn., **70 Suppl. A**, 423-427 (2001)

W. Petry, *Neutronen bringen Licht ins Dunkel* in *"Unter jedem Stein liegt ein Diamant, Struktur-Dynamik Evolution"*, Gesellschaft Deutscher Naturforscher und Ärzte, ed. Ernst-Ludwig Winnacker, Hirzel Verlag, Stuttgart, **121**, 55-61 (2001)

W. Petry, *Neutronen bringen Licht ins Dunkel* in *"...und Er würfelt doch! von der Erforschung des ganz Großen, des ganz Kleinen und der ganz vielen Dinge"*, eds. H. Müller-Krumbhaar, H.-F. Wagner, Wiley-Vch, Weinheim, 482-493 (2002)

W. Petry, *FRM-II, ein einzigartiges Mikroskop für Naturwissenschaft, Technik und Medizin*, TUM Mitteilungen, **3-01/02**, 22 (2002)

N. Pyka, K. Noack, A. Rogov, *Optimization of a partially non magnetic primary radiation shielding for the triple axis spectrometer PANDA at the Munich high flux reactor FRM-II*, J. Appl. Phys. A, **74**, 277 (2002)

H. Rauch, W. Waschkowski, *Neutron Scattering Lengths*, Neutron Data Booklet, Institut Laue Langevin, eds. A. J. Dianoux, G. Lander, (2002)

B. Roessli, P. Böni, *Polarized Neutron Scattering*, Scattering and Inverse Scattering in Pure and Applied Science, eds. E. R. Pike and P. Sabatier, Academic Press, 1242-1263 (2002)

B. Roessli, P. Böni, W. Fischer, Y. Endoh, *Charal Fluctuations in MnSi above the Curie Temperature*, Phys. Rev. Lett., **88**, 237204 (2002)

S. V. Roth, A. Zirkel, J. Bossy, J. Neuhaus, J. Peters, H. Schober, W. Petry, *Measurement and simulation of the inelastic resolution function of a time-of-flight spectrometer*, Appl. Phys. A, **74, Suppl.**, 1449-1451 (2002)

M. Rotter, S. Kramp, M. Loewenhaupt, E. Gratz, W. Schmidt, N. Pyka, B. Hennion, *Magnetic excitations in the antiferromagnetic phase of* $NdCu_2$, J. Appl. Phys., **A 74**, 751 (2002)

C. Schanzer, E. Steichele, K. Böning, W. Petry, *Neutronenleitersysteme am FRM-II jenseits der Totalreflexion*, Jahrestagung Kerntechnik 2001, Dresden, 15 - 17 May 2001, ISSN 0720-9207, 621 - 624 (2001)

R. Schedler, M. Rotter, M. Loewenhaupt, N. Pyka, *Monte Carlo simulation of the cold triple axis spectrometer PANDA*, J. Appl. Phys. A, **74**, 1468 (2002)

W. Schweika, P. Böni, *The Instrument DNS: Polarization Analysis for Diffuse Neutron Scattering*, Physica B, **297**, 155-159 (2001)

F. Semadeni, A. Amato, B. Roessli, P. Böni, C. Baines, T. Masuda, K. Uchinokura, G. Shirane, *Macroscopic and local magnetic moments in Si-doped CuGeO3 as determined by neutron and μSR studies*, Eur. Phys. J. B, **21**, 307-311 (2001)

F. Semadeni, B. Roessli, P. Böni, *Three-axis Spectroscopy with Remanent Benders*, Physica B, **297**, 152 (2001)

M. Senthil, P. Böni, *Influence of Interstitial Nitrogen on the Structural and Magnetic Properties of FeCoV/TiNx Multilayers*, J. Appl. Phys., **91**, 3750 (2002)

T. Soldner, L. Beck, C. Plonka, K. Schreckenbach, O. Zimmer, *Test of time reversal invariance in neutron decay*, Proc. of the ILL millennium symposium, Institut Laue Langevin, Grenoble, France (2001)

T. Soldner, L. Beck, C. Plonka, K. Schreckenbach, O. Zimmer, *Test of time reversal invariance in free neutron decay with TRINE*, Proceedings of the 11th International Symposium on Capture Gamma-ray Spectroscopy and Related Topics, Prague, Czech Republic, (2002)

T. Soldner, L. Beck, C. Plonka, K. Schreckenbach, O. Zimmer, *Trine – a new limit on time reversal invariance violation in neutron beta decay*, Proceedings of the CKM workshop, Heidelberg, Germany, (2002)

T. Soldner, C. Plonka, L. Beck, K. Schreckenbach, O. Zimmer, P. Liaud, A. Bussière, R. Kossakowski, I. Kuznetsov, *: Test of time reversal invariance in free neutron decay with TRINE*, Proceedings of the IX International Seminar on Interaction of Neutrons with Nuclei, Dubna (2001)

M. Stampanoni, G. L. Borchert, R. Abela, B. Patterson, D. Vermeulen, P. Rüegsegger, P. Wyss, *An X-Ray Tomographic Microscope with Submicron Resolution*, Acta Phys. Pol. B, **33**, 463 (2002)

M. Stampanoni, G.L. Borchert, R. Abela, P. Rüegsegger, *Bragg Magnifier: A Novel Detector for Submicrometer X-Ray Computer Tomography*, J. Appl. Phys., **92**, 7630 (2002)

M. Stampanoni, G.L. Borchert, P. Wyss, R. Abela, B. Patterson, S. Hunt, D. Vermeulen, P. Rüegsegger, *High Resolution X-Ray Detector for Synchrotron-Based Microtomography*, Nucl. Inst. Meth. A, **491**, 291 (2002)

B. Straßer, C. Hugenschmidt, K. Schreckenbach, *Set-Up of a Slow Positron Beam for Auger Spectroscopy*, Mat. Sci. Forum, **363-365**, 686-688 (2001)

P. Strunz, D. Mukherji, R. Gilles, A. Wiedenmann, J. Roesler, H. Fueß, *Determination of γ' Solution Temperature in Re-rich Ni-base Superalloy by small-angle neutron scattering*, J. Appl.Cryst., **34**, 541 - 548 (2001)

P. Strunz, G. Schuhmacher, W. Chen, D. Mukherji, R. Gilles, A. Wiedenmann, *SANS examination of precipitate microstructure in creep-exposed single-crystal Ni-base superalloy SC16*, Appl. Phys. A **74, Suppl.**, 1083-1085 (2002)

N. Stüsser, M. Hofmann *An Adjustable In-pile Fan Collimator for Focusing at a Neutron Diffractometer*, Nucl. Inst. Meth. A, **482**, 744 (2002)

M. Tafipolski, W. Scherer, K. Ofele, G. Artus, B. Pedersen, W. A. Herrmann, G. S. McGrady, *Electron delocalization in acyclic and n-heterocyclic carbenes and their complexes: A combined experimental and theoretical charge-density study.*, J. Am. Chem. Soc., **124,20**, 5865- 5880 (2002)

V.A. Ul'yanov, P. Böni, V.N. Khamov, S.P. Orlov, B.G. Peskov, N.K. Pleshanov, V.M. Pusenkov, A.F. Schebetov, A.P. Serebrov, P.A. Sushkov, V.G. Syromyatnikov, *The Effect of*

Large Irradiation Doses on Polarizing and Non-polarizing Supermirrors, Physica B, **297**, 155-159 (2001)

T. Unruh, *Instrument Control at the FRM-II using TACO and NICOS*, http://arxiv.org/abs/cond-mat/0210433, (2002)

T. Unruh, H. Bunjes, K. Westesen, M. H. J. Koch, *Investigations on the Melting Behaviour of Triglyceride Nanoparticles*, Colloid and Polymer Science, **279(4)**, 398 (2001)

T. Unruh, K. Westesen, P. Boesecke, P. Lindner, M. H. J. Koch, *Self-Assembly of Triglyceride Nanocrystals in Suspension*, Langmuir, **18**, 1796-1800 (2002)

G. Wagner, R. Herrmann, B. Pedersen, W. Scherer, *Synthesis and structure of chiral silatranes derived from terpenes*, Zeitschrift f. Naturforschung, **B 56(1)**, 25-38 (2001)

R. Willumeit, G. Diedrich, S. Forthmann, J. Beckmann, R.P. May, H.B. Stuhrmann, K.H. Nierhaus, *Mapping proteins of the 50S subunit from Escherichia coli ribosomes*, Biochim. Biophys. Acta, **1520**, 7-20 (2001)

R. Willumeit, S. Forthmann, J. Beckmann, G. Diedrich, R. Ratering, Stuhrmann, K.H. Nierhaus, 0, *Localization of the protein L2 in the 50S subunit and 70S E. coli ribosome*, J. Mol. Biol., **305**, 167-177 (2001)

A. Zheludev, T. Mazuda, J. Isukada, Y. Uchiyama, K. Uchinokura, P. Böni, S.-H. Lee, *Magnetic Excitations in Coupled Haladane Spin Chains near the Quantum Critical Point*, Phys. Rev. B, **62**, 8921 (2001)

O. Zimmer, *Experimental challenges in neutron decay*, Proc. of the ILL millennium symposium, Institut Laue Langevin, Grenoble, France (2001)

O. Zimmer, G. Ehlers, B. Farago, H. Homblot, W. Ketter, W. Scherm, *A precise measurement of the spin-dependent neutron scattering length of ^{3}He*, Eur. Phys. J. A, **1**, 1 (2002)

O. Zimmer, J. Felber, O. Schärpf, *Stern-Gerlach effect without magnetic field gradients*, Europhys. Lett., **53**, 183 (2001)

Ph.D. thesis

M. Meven, *Entwicklung eines hochauflösenden Röntgen-Einkristalldiffraktometers und Strukturuntersuchungen an La2-xSr xCuO4-Einkristallen*, Dissertation, RWTH Aachen (2001)

Imprint

. . . . . .

Publisher:
Technische Universität München
Neue Forschungsneutronenquelle
ZWE-FRM-II
Lichtenbergstr. 1
85747 Garching
Germany
Phone: +49 89-289-14965
Fax: +49 89-289-14995
Internet: http://www.frm2.tum.de
email: userinfo@frm2.tum.de

. . . . . .

Editors:
J. Neuhaus
E. Doll
P. Link
B. Pedersen

. . . . . .

Photographic credits:
Max Prugger: page 3
All others: TUM

. . . . . .

Design:
J. Neuhaus, TUM

. . . . . .

Typesetting (LaTeX 2ε):
B. Pedersen, TUM

. . . . . .